



*Republic of Iraq  
Ministry of Higher  
Education and Scientific  
Research  
University of Baghdad  
College of Education for  
Pure Science Ibn-AL-  
Haitham*



# **Estimation and Reduction of the Total Activity for the Liquid Waste Pool in Radiochemistry Laboratories in Al-Tuwaitha Site**

*A Thesis*

*Submitted to University of Baghdad \College of Education for Pure  
Science (Ibn-AL-Haitham) in partial Fulfillment of the Requirements for  
the Degree of Master of Science in Physics*

*By*

**Zaidoon Hafudh Ibrahim**

**B.Sc Physics 1997**

*Supervised by*

*Assistant Professor  
Dr.Ahmed Fadhil Mkhaimer*

*Chief of Engineers  
Dr. Salam Kudhair Al-nasri*

*September 2018*

*Muharram 1440*

بِسْمِ اللّٰهِ الرَّحْمٰنِ الرَّحِیْمِ

رَفَعُ دَرَجَاتٍ مِّنْ نَّشَأٍ

وَفَوْقَ كُلِّ ذِي عِلْمٍ

عَلِیْمٍ

صدق الله العظيم

سورة يوسف - الآية 76

## **Supervisors Certification**

I certify that this thesis was prepared by **Zaidoon Hafudh Ibrahim** under my supervision at the Physics Department, College of Education for pure Science Ibn-Al-Haitham, University of Baghdad in partial fulfillment requirements for the Degree of Master of Science in Physics.

**Signature:** 

**Name:** *Dr. Ahmed Fadhl Mkhaimer*

**Title:** *Assistant Professor*

**Address:** *College of Education for pure Science Ibn-Al-Haitham, University of Baghdad*

**Date:** 2018 / /

**Signature:** 

**Name:** *Dr. Salam Kudhair Al-nasri*

**Title:** *Chief of Engineers*

**Address:** *Central Laboratories Directorate/Iraqi Ministry of Science and Technology*

**Date:** 2018 / 9 / 24

In view of the available recommendations, I forward this thesis for debate by the Examination Committee.

**Signature:** S. A. MAKI

**Name:** *Dr. Samir Ata Maki*

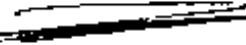
**Title:** *Professor*

**Address:** *Chairman Department of Physics College of Education for pure Science Ibn-Al-Haitham, University of Baghdad*


**Date:** 2018 / 9 / 25

## Committee Certification


We certify that we have read this thesis titled " Estimation and Reduction of the Total Activity for the Liquid Waste Pool in Radiochemistry Laboratories in Al-Tuwaitha Site " submitted by (Zaidoon Hafudh Ibrahim) and as examining committee examined the student in its content and that in our opinion it is adequate with standard as thesis for the Degree of Master of Science in Physics.

Signature:   
Name: *Prof. Dr. Bashair M. Saied*  
Address: *University of Baghdad*  
**(Chairman)**

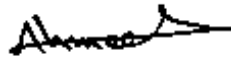
Date: 7/4/2018

Signature:   
Name: *Assistant Prof. Dr. Ahmed Aziz Ahmed*  
Address: *University of Al-Mustansiriyah*  
**(Member)**


Date: / / 2018

Signature:   
Name: *Dr. Rawnaq Qays Gadhiban*  
Address: *University of Baghdad*  
**(Member)**

Date: / / 2018

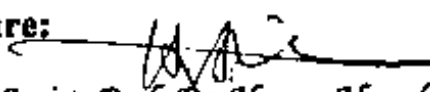
Signature:   
Name: *Assistant Prof. Dr. Ahmed Fadhil Mkhiaiber*  
Address: *University of Baghdad*  
**(Member-Supervisor)**

Date: 24/9/2018

Signature:   
Name: *Chief of Engineers Dr. Salam Kudhair Al-nasri*  
Address: *Iraqi Ministry of Science and Technology*  
**(Member-Supervisor)**

Date: 27/9/2018

**Approved by the Council of the College of Education for Pure Sciences Ibn-Al-Haitham / University of Baghdad**

Signature:   
Name: *Assist. Prof. Dr. Hasan Ahmed Hasan*

Address: *Behalf / The Dean of college of Education for pure science/ Ibn al-Haitham*

*Dedication*

*For My loving family...*

*May Allah protect them*

*My father,  
Brothers,  
My wife,  
And my daughters and son..*

*I Dedicate the Product of My Effort*

*Zaidoon*

## *Acknowledgments*

Praise and thanks to ALLAH, who gave me the health, strength, faith, and patience to get along completing this work and peace be upon the messenger of ALLAH, Mohammad.

I would like to express my sincere thanks and deep gratitude to my supervisors, Dr. Ahmed Fadhil Mkhaimer and Dr. Salam Kudhair Al-nasri, for suggesting this project, their valuable guidance and for their support and encouragement throughout the research.

I am most grateful to the Dean of College of Education for Pure Science Ibn-AL-Haitham, and I wish to thank the head of Physics Department and the staff of this Department.

My special thanks to my first teacher in my career the expert Mr. Assim A. Mahdi, who always supports and helps me.

I would like to thank Mr. Jomaa R. Mahmood in Research Material Directorate and all my colleges in Field Measurements Department/Iraqi Decommissioning Directorate at Ministry of Science and Technology, especially Mr. Salman A. Ali, Mr. Radi M. Jabor, Mr. Al-Sadek Al-Amen N., Mr. Fouad S. Nory, Mr. Ahmmmed Ibrahim and to everyone who helped me throughout the fulfillment of this study.

I wish to acknowledge the Radiation Measurements and Radiation Chemistry Department / Central Laboratories Directorate at Ministry of Science and Technology specially Mr. Zuheir Wuhaib, Mr. Fadhil Hussein, Mr. Amer A. Sakran, Mr. Mohammad Jabbar, Mrs. Marrwa K. Mohammad, Mrs. Najlla, , Mr. Mohammad Shuhab, Mr. Taiseer Kudhair Mr. Mohammad Adel and the chemist Dr. Suhaylla, Mr. Yasser Abdulluh and Mrs. Zainab.

*Zaidoon*

## **Abstract**

The aim of work is estimating and reducing the total activity for the radioactive liquid waste pools (RLWPs) in the radiochemistry laboratories (RCL) in Al-Tuwaittha site. The collected samples from these pools analyzed by using two techniques, the first is the gamma spectroscopy system with a high purity germanium detector (HPGe) with a relative efficiency 65% to measure the radioactivity concentration of radionuclides for gamma-ray emitters and determine the types of radionuclides. The results show that the average radioactivity concentration of cesium ( $^{137}\text{Cs}$ ) is  $2.688 \text{ MBq.L}^{-1}$  and  $850.61 \text{ Bq.L}^{-1}$  for high and low level liquid waste pools (HLLWP and LLLWP) respectively. The second technique is gross alpha, beta, gamma system type S5XLB with proportional gas flow detector to measure the radioactivity concentrations of the pure beta emitters radionuclides for the same samples which cannot detect in the first technique.

Cesium-137 and strontium-90 are the main two radioactive isotopes of nuclear fission products of Uranium-235 ( $^{235}\text{U}$ ) isotope with half-lives about 30 and 29 years respectively. Cesium-137 was separated from these samples by developing a new method (novelty) called evaporation process because it emit beta particles associated with gamma photons, therefore the average remaining activity of HLLWP samples is  $2.606 \text{ MBq.L}^{-1}$  and for LLLWP samples is  $0.0017 \text{ MBq.L}^{-1}$ . According to work history of the radiochemistry laboratories, this liquid waste is belong to the nuclear fission products for  $^{235}\text{U}$  isotope, therefore the remaining activity refers to strontium-90 radionuclide due to its long half-life.

The treatment of these liquid wastes which contained cesium and strontium was performed using ion-exchange technique by using natural zeolite (clinoptilolite) material, it has already found wide-ranging

applications to the remediation. The weight of clinoptilolite and solution acidity (pH) effects on removal efficiency for cesium and strontium were studied.

The results revealed that the clinoptilolite was highly efficient in removing cesium ions from liquid waste at all range of clinoptilolite weight and the solution acidity that used, while the removal efficiency of strontium ions varies with these factors.



## *List of Contents*

<i>Abstract</i> .....	I
<i>List of Contents</i> .....	III
<i>List of figures</i> .....	VI
<i>List of tables</i> .....	VIII
<i>List of Abbreviations</i> .....	X
<b>CHAPTER ONE (Introduction and Literature Review)</b>	
1.1 Preface .....	1
1.2 Importance of Radioactive Waste Removal .....	2
1.3 Radioactive Wastes Treatment .....	3
1.4 Zeolite and Adsorbent for Ion Exchange.....	3
1.5 Area of the Study .....	4
1.5.1 Al-Tuwaitha Site Description .....	4
1.5.2 Radiochemistry Laboratories.....	4
1.6 The Previous Studies .....	6
1.6.1 Al-Tuwaitha Nuclear Research Center.....	7
1.6.2 Determination the Radioactivity Concentration .....	7
1.6.3 The Radioactive Liquid Waste Treatment.....	9
1.7 The Aim of Study .....	11
<b>CHAPTER TWO (Theoretical Considerations)</b>	
2.1 Radioactivity.....	13
2.2 Radiation sources.....	13
2.2.1 Natural sources .....	13
2.2.2 Man-made sources .....	15
2.3 Nuclear Fission .....	15
2.3.1 Fission Products.....	16
2.3.2 Fission Product Inventory.....	17
2.4 Activity .....	19
2.5 Specific Activity .....	21
2.6 Radiation Detection .....	22
2.6.1 The Semiconductor Hyper-pure Germanium Detector .....	22
2.6.2 Proportional Counters.....	24
2.7 Radioactive Waste .....	26
2.7.1 Sources of Radioactive Waste .....	26
2.7.2 Classification of Nuclear Waste .....	27
2.7.3 Radioactive Liquid Waste .....	29

2.7.4	Classification of Radioactive Liquid Waste .....	29
2.7.5	Cesium-137 and Strontium-90 as Nuclear Waste .....	30
2.7.5.1	Cesium .....	30
2.7.5.2	Strontium .....	31
2.8	Separation Techniques for Radioactive Wastes .....	32
2.9	The Zeolites .....	33
2.9.1	Definition of Zeolites.....	33
2.9.2	General Properties of Zeolites and Structure.....	33
2.9.3	Applications of Zeolites.....	35
2.9.4	Clinoptilolite .....	35
2.9.5	Ion Exchange Properties of Clinoptilolite .....	36

### ***CHAPTER THREE (Experimental Technique)***

3.1	Introduction.....	38
3.2	Description of Radioactive Liquid Waste System.....	38
3.3	Radiological Characterization of Radioactive Liquid Waste Hall ....	40
3.3.1	Dose rate measurement.....	40
3.4	The Sampling.....	42
3.4.1	Samples collection .....	42
3.4.2	Preparation of Samples .....	45
3.4.3	Samples Preparing Tools and Equipment.....	45
3.4.4	Samples Preparing for Gamma Analyzing .....	45
3.4.5	Samples Preparing for Gross Alpha Beta Gamma counting .....	46
3.4.6	Preparing Samples for Treatment .....	47
3.4.7	Preparing Samples for Acidity Solution Run-1 Test.....	50
3.4.8	Preparing Samples Run-2 Test for Improving removal efficiency ....	50
3.5	Gamma-ray Spectroscopy System.....	51
3.5.1	Computer and software.....	54
3.5.2	Dead Time Mode .....	54
3.5.3	Calibration .....	54
3.5.3.1	<i>Energy calibration</i> .....	55
3.5.3.2	<i>Efficiency calibration</i> .....	57
3.5.4	Interpolative Fit .....	58
3.5.5	Energy Resolution .....	59
3.5.6	Determination of Detection Limits and Minimum Detection activity	59
3.5.7	Calculation of radioactivity Concentration.....	61
3.6	Gross Alpha Beta Gamma System .....	61
3.6.1	Gas Regulation and Control .....	63

3.6.2	Determining Operating Voltages .....	63
3.6.3	Beta Counting .....	65
3.6.4	Efficiency Calibration.....	65
3.6.5	Gross beta activity .....	67
3.7	The X-Ray Fluorescent (XRF) .....	67
3.7.1	Zeolite Sample Preparing for Analyzing .....	68
3.7.2	Liquid Sample Preparing for Analyzing.....	68
<b>CHAPTER FOUR (Results, Discussion, and Conclusions)</b>		
4.1	Introduction.....	71
4.2	Gamma Spectroscopy Measurements.....	71
4.2.1	The Radioactivity Concentration of HLLW Pool Samples.....	72
4.2.2	The Radioactivity Concentration of LLLW Pool Samples .....	76
4.3	Gross Alpha Beta Gamma System Measurements .....	78
4.3.1	The Count Rate of HLLW Pool Samples .....	78
4.3.1.1	Calculation of Strontium Radioactivity Concentration for HLLWP..	81
4.3.1.2	Developing a New Method to Separating <sup>90</sup> Sr from <sup>137</sup> Cs .....	83
4.3.1.3	The Radioactivity Concentration of Strontium for LLLWP .....	87
4.4	The Reduction of Total Radioactivity for HLLW Pool.....	92
4.4.1	Effecting of Clinoptilolite Weight on Removal Efficiency for <sup>137</sup> Cs..	93
4.4.2	Effecting of Clinoptilolite Weight on Removal Efficiency for <sup>90</sup> Sr...	96
4.4.3	The Effect of the Acidic Solution on Removal Efficiency for <sup>137</sup> Cs..	98
4.4.4	The Acidic Effect on Removal Efficiency for <sup>90</sup> Sr.....	99
4.4.5	Improving Removal Efficiency for <sup>137</sup> Cs and <sup>90</sup> Sr .....	100
4.5	XRF Results.....	105
4.6	Conclusion .....	107
4.6.1	The Results Related to the radiation measurements.....	107
4.6.2	The results related to the treatment of liquid waste.....	108
4.7	Future Work.....	109
<b>References</b>	.....	110

## **List of figures**

Figure 1-1: a- Iraq map and b- Al-Tuwaitha site .....	5
Figure 1-2: a- The building in Al-Tuwaitha site, b- Radiochemistry laboratories RCL building .....	6
Figure 2-1: The fission process .....	16
Figure 2-2: Fission product yield from thermal fission of $^{235}\text{U}$ .....	17
Figure 2-3: Block diagram of a basic gamma spectrometry system .....	23
Figure 2-4: Schematic of a P-N semiconductor detector .....	24
Figure 2-5: The different regions of operation of gas-filled detectors. ....	25
Figure 2-6: Diagram of a gas flow proportional counter .....	26
Figure 2-7: Nuclear fuel cycle. ....	27
Figure 2-8: Conceptual illustration of the waste classification scheme. ....	28
Figure 2-9: Relative volume of radioactive waste type nuclear cycle .....	29
Figure 2-10: The decay scheme of $^{137}\text{Cs}$ .....	31
Figure 2-11: The strontium-90 decay diagram displays two main features. First, it happens to be a cascade decay. ....	32
Figure 2-12: Natural zeolite .....	33
Figure 2-13: Synthetic zeolite .....	33
Figure 2-14: (a-) Tetrahedral units ( $\text{SiO}_4$ or $\text{AlO}_4$ ) are the basic structural component of zeolite networks and (b-) $\text{TO}_4$ tetrahedral where $\alpha$ is the O- T-O bond angle and $\beta$ is the T-O-T bond angle (T= Si or Al) .....	34
Figure 2-15: (a) two-dimensional channel system of clinoptilolite. (b) the ten and eight-membered channels of Clinoptilolite with their size. ....	35
Figure 2-16: Natural clinoptilolite: (a) Clinoptilolite–K, (b) Clinoptilolite- Na, and (c) Clinoptilolite–Ca .....	36
Figure 3-1: The scheme of waste hall (WH) in the RCL .....	39
Figure 3-2: a, b are the radioactive liquid waste hall, and c, d are the radioactive liquid waste pool and tanks. ....	40
Figure 3-3: The LUDLUM dose rate meter device. ....	42
Figure 3-4: a, b samples collecting from WH and c, d samples preservation. ..	44
Figure 3-5: a- The fume hood, b- The prepared samples, c- The 2 in. planchets, d- The hot plate, e- The burn oven MUFFLE FURNACE, f- samples preparation for treatment, g- The sensitive scale with zeolite and h-The shaker .....	49
Figure 3-6: Gamma-ray spectroscopy system which used in the current study.	53
Figure 3-7: The HPGe detector .....	54
Figure 3-8: The multichannel analyzer .....	54
Figure 3-9: Gamma-ray spectrum of mixed radionuclides which used as a calibration source. ....	56
Figure 3-10: The relationship between gamma energy and channel numbers. .	56
Figure 3-11: The efficiency calibration curve. ....	58

Figure 3-12: The gross alpha beta gamma system.....	63
Figure 3-13: Alpha plateau graph .....	64
Figure 3-14: Beta plateau graph.....	64
Figure 3-15: Figure (3-14): Changing the Operating Voltage.....	65
Figure 3-16: a- XRF system, b- zeolite sample and c- filter paper sample. ....	68
Figure 4-1: Gamma-ray spectrum of HLLW-P-S liquid sample. ....	75
Figure 4-2: Gamma-ray spectrum of HLLW-M (C) liquid sample.....	76
Figure 4-3: Gamma-ray spectrum of liquid sample LLLW-P-B. ....	77
Figure 4-4: Gamma-ray spectrum of liquid sample LLLW-P-M. ....	78
Figure 4-5: Gross beta radioactivity CPM of HLLW-P samples as a function of samples volume at 300 C° . ....	81
Figure 4-6: Gross beta radioactivity CPM for different HLLW samples as a function temperature.....	81
Figure 4-7: <sup>137</sup> Cs spectrum of C-7 sample (planchet) at 300 °C.....	86
Figure 4-8: <sup>137</sup> Cs spectrum of C-7 sample (planchet) at 500 °C.....	86
Figure 4-9: <sup>137</sup> Cs spectrum of C-7 sample (planchet) at 700 °C.....	87
Figure 4-10: Gross beta radioactivity (CPM) of LLLW pool samples (L-2,4,7) with temperature degree C° . ....	90
Figure 4-11: <sup>137</sup> Cs spectrum for L-7 planchet sample at 300 °C. ....	91
Figure 4-12: <sup>137</sup> Cs spectrum for L-7 planchet sample at 700 °C. ....	92
Figure 4-13: Removal Efficiency of <sup>137</sup> Cs for five samples. ....	94
Figure 4-14: <sup>137</sup> Cs spectrum of C-ST (10ml) sample.....	95
Figure 4-15: <sup>137</sup> Cs spectrum of C-A1 (10ml) sample. ....	95
Figure 4-16: <sup>137</sup> Cs spectrum of C-A5 (10ml) sample. ....	96
Figure 4-17: The count rate of <sup>90</sup> Sr for five samples. ....	97
Figure 4-18: Removal Efficiency of <sup>90</sup> Sr for five samples. ....	98
Figure 4-19: Removal Efficiency of <sup>137</sup> Cs for four samples at different pH. ....	99
Figure 4-20: <sup>137</sup> Cs spectrum of CA2-ph(3) (10ml) sample.....	102
Figure 4-21: <sup>137</sup> Cs spectrum of CA2-ph(6) (10ml) sample.....	103
Figure 4-22: <sup>137</sup> Cs spectrum of CA2-ph(9) (10ml) sample.....	103
Figure 4-23: <sup>137</sup> Cs spectrum of CA2-ph(12) (10ml) sample.....	104

## **List of tables**

Table 2-1: Fission products of $^{235}\text{U}$ with half-lives greater than one year .....	19
Table 3-1: Dose rate Measurements inside and outside the waste hall. ....	41
Table 3-2: The location of samples in the waste hall. ....	43
Table 3-3: Dose rate measurements of samples the waste hall.....	43
Table 3-4: The mixture of radioactive source data and the absolute detection efficiency for each radionuclide. ....	55
Table 3-5: The values of MDA for some isotopes in the liquid samples have been obtained from the measurements system. ....	60
Table 3-6: The counting efficiency of beta for $^{90}\text{Sr}$ and $^{137}\text{Cs}$ . ....	66
Table 4-1: The radioactivity concentration results in liquid samples at different dilution percent for HLLW-P-B liquid samples.....	73
Table 4-2: The radioactivity concentration results in liquid samples at dilution percent 0.2% for HLLW pool. ....	74
Table 4-3: The radioactivity concentration results of liquid samples at dilution percent 100% for HLLW pool. ....	75
Table 4-4: The radioactivity concentration of LLLW pool liquid samples. ....	77
Table 4-5: The radioactivity of alpha, beta and gamma at 300°C for HLLWP. ....	80
Table 4-6: The radioactivity of alpha, beta samples at 500°C for HLLWP. ....	80
Table 4-7: The alpha and beta radioactivity of samples at 700°C to HLLWP. .	80
Table 4-8: The radioactivity of $^{137}\text{Cs}$ for HLLW pool by gamma spectrometry system and the derived RAF for $^{137}\text{Cs}$ . ....	85
Table 4-9: The calculated radioactivity concentration of $^{90}\text{Sr}$ to HLLW-M sample in HLLW pool. ....	85
Table 4-10: The total activity of high level liquid waste pool. ....	85
Table 4-11: The radioactivity of alpha, beta, and gamma for the deposit samples at 100°C to LLLW pool. ....	89
Table 4-12: The radioactivity of alpha, beta, and gamma for the deposit samples at 300°C to LLLW pool. ....	89
Table 4-13: The radioactivity of alpha, beta, and gamma for the deposit samples at 500°C to LLLW pool. ....	89
Table 4-14: The radioactivity of alpha, beta, and gamma for the deposit samples at 700°C to LLLW pool. ....	90
Table 4-15: The $^{137}\text{Cs}$ radioactivity of the deposit samples at a different temperature to LLLW pool by gamma spectrometry system and the derived RAF for $^{137}\text{Cs}$ . ....	90
Table 4-16: The radioactivity concentration of $^{90}\text{Sr}$ for LLLW pool. ....	91
Table 4-17: The total activity of low level liquid waste pool. ....	91
Table 4-18: Removal efficiency of $^{137}\text{Cs}$ by gamma spectroscopy system. ....	94
Table 4-19: Removal efficiency of $^{90}\text{Sr}$ with clinoptilolite zeolite weight by gross alpha beta gamma system. ....	97

Table 4-20: Removal efficiency for $^{137}\text{Cs}$ by gamma spectroscopy system at different pH. ....	99
Table 4-21: Removal efficiency of $^{90}\text{Sr}$ at different pH. ....	100
Table 4-22: Removal efficiency of $^{137}\text{Cs}$ by gamma spectroscopy system by run-2 for the solution. ....	102
Table 4-23: Removal efficiency for $^{90}\text{Sr}$ by gross alpha beta gamma system by run-2 for the solution. ....	104
Table 4-24: The remain radioactivity of $^{137}\text{Cs}$ and $^{90}\text{Sr}$ in HLLWP-M sample and their removal efficiencies at pH(6). ....	104
Table 4-25: The major concentration elements of HLLWP sample (F-sample). ....	105
Table 4-26: The concentration elements of clean liquid sample (F-BG sample). ....	106
Table 4-27: The concentration elements of clinoptilolite (Z-sample). ....	106

### **List of abbreviations**

Abbreviation	Description
ATNRC	Al-Tuwaittha Nuclear Research Center
B.G	Background
$CF_{\text{eff}}$	Correction efficiency factor
$CF_{^{137}\text{Cs}}$	Correction factor of the remain radioactivity for $^{137}\text{Cs}$
CLD	Central Laboratory Directorate
CPM	Count per minute
DPM	Disintegration per minute
EW	Exempt Wastes
HLW	High-Level Wastes
HPGe	High Purity Germanium
IAEA	International Atomic Energy Agency
IAEC	Iraqi Atomic Energy Commission
IDD	Iraq Decommissioning Directorate
ILW	Intermediate Level Waste
LILW	Low and Intermediate-Level Wastes
LILW-LL	Low and Intermediate-Level Long-Lived Wastes
LILW-SL	Low and Intermediate-Level Wastes Short-Lived Wastes
LLLWP	Low-Level Liquid Waste Pool
LLW	Low-level waste
MoST	Ministry of Science and Technology
NORM	Naturally Occurring Radioactive Material
OLWP	Organic Liquid Waste Pool
RCL	Radiochemistry Laboratories
$RAF_{^{137}\text{Cs}}$	The remain radioactivity factor of $^{137}\text{Cs}$
RLW	Radioactive Liquid Waste
VLLW	Very Low-Level Waste
WH	Waste Hall
WNF	Waste Nuclear Fuel
WHO	World Health Organization



# **CHAPTER ONE**

## **Introduction and Literature Review**

**CHAPTER ONE****Introduction and Literature Review****1.1 Preface**

The radiation and radioactivity has been discovered for more than 100 years ago, by a German physicist (Wilhelm Conrad Roentgen) in 1895, who discovered the X-rays which could be used to look into the human body. After one year of Roentgen's discover (1896), a French scientist, Henri Becquerel discovered the penetrating of radiations by putting some photographic plates in a drawer with fragments of mineral containing uranium, it was found that they became fogged, because of their exposure to radiation. This phenomenon is called radioactivity, due to it occurs when energy is released from an atom spontaneously. Today the radioactivity is measured in units called Becquerel (Bq). After this discovery, the science of radioactivity has been extensively studied [1]. In 1898, a young chemist (Marie Skłodowska Curie) and Pierre Curie discovered uranium (U) that gave radiation, and it turned into other elements, one of which, it is called polonium (Po), which belongs to homeland, and another it is called radium (Ra), the (shining) element [2]. In 1899, Ernest Rutherford discovered the compounds of uranium which produce three different types of radiation, he separated and named them alpha( $\alpha$ ), beta( $\beta$ ), and gamma radiation according to their penetrating abilities [3].

The radiation was widely used around the world in medical treatments as well as the application in thousands of usage throughout developed societies. The major sources of radiological dose to the public are natural and medical sources of radiation. Any source of radiation, as with most hospital radiation sources and some industrial processes can be

entirely shielded to protect workers and the public. All uses of radiation and some industrial processes produce radioactive wastes. These radioactive wastes are securely and safely managed. The radioactivity is a continuously decreasing quantity which is a function of the half-life of the responsible radionuclides [4].

After the development of nuclear technology, the number of reactors in the world increases, hence the production of radioactive waste increases as well. The accumulation of this waste without management may expose human and the environment to risks. Thus, researchers focused on the preparation of regulations for the management of these wastes for cleaning up the environment [5]. The contamination separation occurred following planned activities such as weapons testing and from past activities that require decommissioning for example in Iraq or from accidental that releases of radioactive materials such as Chernobyl (1988) and Fukushima in (2011).

## **1.2 Importance of Radioactive Waste Removal**

In some of the nuclear applications, industrial activities, including the generation of electricity and nuclear accidents there are generations of radioactive waste despite of all precautions. These wastes have to be stored and disposed in ways that protect human health and the environment. It has always been recognized that radioactive wastes are potentially hazardous, so both industry and government ensure that they are managed properly. Therefore, one of the most important problems that face us is the pollution that must be dealt with urgently to protect the environment and public health [6].

**1.3 Radioactive Wastes Treatment**

The radioactive wastes treatment is an important phase in the waste management. It is the reduction of the wastes volume to ensure the safety and/or reduction of the costs for further management phases [7]. The conventional treatment options of liquid wastes are usually used to treat them after the consideration of their chemical and biological characteristics [8]. There are different methods to treat these radioactive liquid wastes, such as, evaporation, dialysis, electro-dialysis, ion exchange, reverse osmosis and zeolites and adsorbents for ion exchange [9]. The last method was used in the present study.

**1.4 Zeolite and Adsorbent for Ion Exchange**

The main common types of adsorbents are: silica gel, activated alumina, activated carbon, polymeric adsorbents and molecular sieve zeolites. The adsorption materials can be assessed in term of the quality of pore structure, total surface area, particle size, and the void space between particles [9]. There are many types of ion exchange media available now with different cost, from low cost naturally occurring such as natural zeolite materials to expensive cost synthetic zeolite which made for removing specific ions [10]. Pore sizes of adsorbents may be generally classified into three ranges; macropores have diameters in excess of ( $> 50$ ) nm, mesoporous have diameters in the range (2 – 50) nm, and micropores have diameters which are ( $< 2$ ) nm. Zeolites are microporous materials that have proved its efficiency in environmental remediation due to their ion exchange properties. The ion exchange properties and the existence in large quantities in the world, zeolites have a great attention, especially for their application in low and intermediate level liquid radioactive treatment [11].

The natural zeolite with ion exchange method and batch operation has been used in this study to remove radioactive isotopes ( $^{137}\text{Cs}$  and  $^{90}\text{Sr}$ ). It is preferred over other methods by as the simplicity of operations in equipment modules, the high concentrations of waste can be used, a well understood operating principles and an accepted form of solid waste [12,13].

## **1.5 Area of the Study**

### **1.5.1 Al-Tuwaitha Site Description**

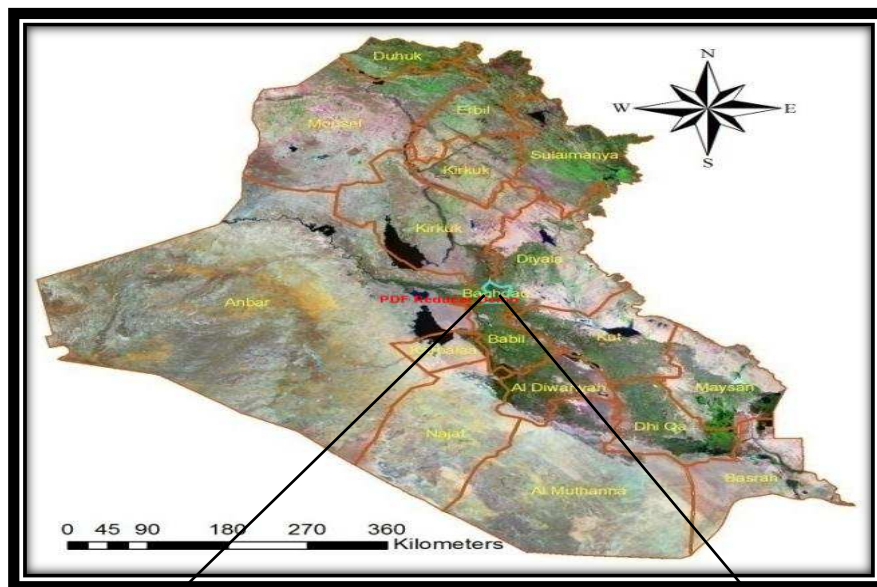
Al-Tuwaitha Nuclear Research Center (ATNRC) was established in about 1960. It lies in Baghdad province, the capital of Iraq at  $33^{\circ} 12.57$  north and  $44^{\circ} 31.822$  east. It covers an area about  $1.3 \text{ km}^2$ . It is located approximately 1 km east of the Tigris river 20 km south of Baghdad. This site was the previous Iraqi Atomic Energy Commission (IAEC), it is surrounded by earthen berms with 30 m height around the facilities. This site currently undergoes the decommissioning project for the nuclear destroyed facilities by the Ministry of Science and Technology of Iraq. Al-Tuwaitha comprised 90 buildings, the radiochemistry laboratories one of them [14].

### **1.5.2 Radiochemistry Laboratories**

Radiochemistry Laboratories (RCL) were established in 1978 by the SNIA TECHINT–Italy company, as a part of the Chemical Research Centre in the previous Iraqi Atomic Energy Commission (IAEC) in Al-Tuwaitha nuclear site. These laboratories were destroyed in the second Gulf war in 1991, the building is covers an area of about  $1000 \text{ m}^2$ . The purposes of the RCL were reprocessing of spent fuel that received from IRT-5000 (Tammuz-14) Reactor in laboratory scale (dissolution, separating, purification and for other chemical research and analysis) to extract the plutonium isotope ( $^{239}\text{Pu}$ ). The spent fuel which was used in

this facility was stored since 1973. From these processes, there are large amounts of radioactive liquid waste with different radionuclides as a result of fission products of Uranium-235 ( $^{235}\text{U}$ ) isotope which belong to fuel rod that used in these processes.

The produced radioactive liquid wastes were stored underground in the waste hall (WH) which divides into three pools (high-level liquid waste pool (HLLWP), organic liquid waste pool (OLWP) and low-level liquid waste pool (LLWP) [14]. Figures (1-1 and 1-2) show Iraq map and Al-Tuwaitha site location with the building layout within this site.

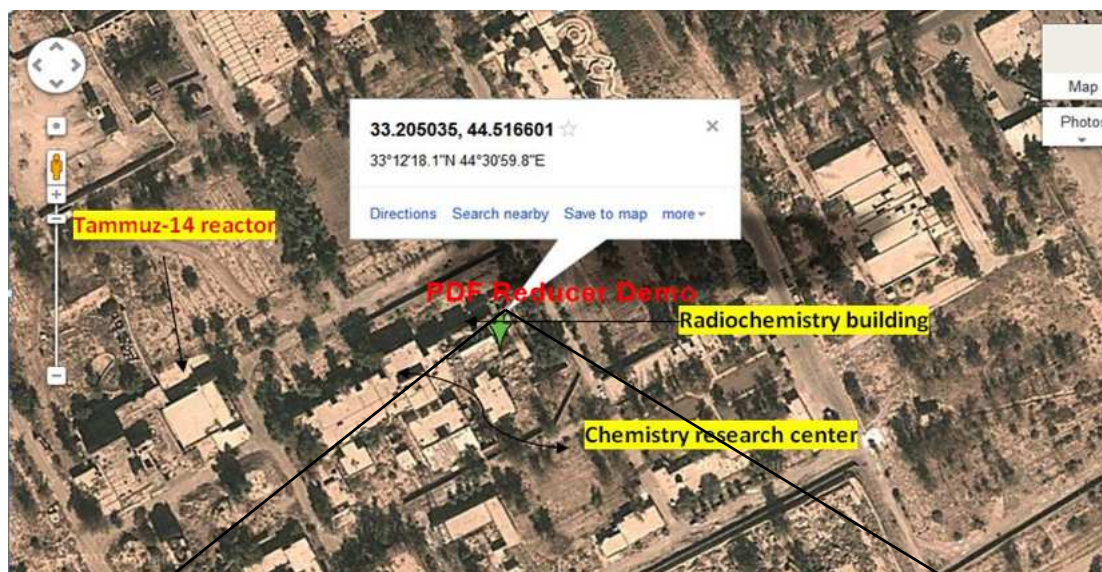


(a)



(b)

**Figure 1-1: a- Iraq map and b- Al-Tuwaitha site**



(a)



(b)

**Figure 1-2: a- The building in Al-Tuwaitha site, b- Radiochemistry laboratories RCL building.**

## 1.6 The Previous Studies

This section is divided into three parts; the first part relates to studies at the Al-Tuwaitha site, while the second part relates to determination of the radioactivity concentration of fission products

radionuclides especially  $^{137}\text{Cs}$  and  $^{90}\text{Sr}$ , and the third part relates to treatment of radioactive liquid waste by using ion-exchange technique especially with clinoptilolite (natural zeolite) adsorbent material.

### **1.6.1 Al-Tuwaitha Nuclear Research Center**

John R. Copland, et al /Sandia National Laboratories (2013), prepared a report which concerns the radiological characterization and quality of the groundwater at Al-Tuwaitha site. Six wells were drilled in the area at a different depth near the main destroyed nuclear facilities. The results found that groundwater exists in two aquifers. The analyses of water samples, using gamma-ray spectroscopy analyzer, showed no significant radioactive contaminations in the groundwater except Bi-214 with maximum contamination equal to  $(12\pm 2)$  Bq/L and Pb-214 with maximum contamination values  $(11\pm 2)$  Bq/L [15].

Auday Al Bayati (2017) studied the natural and artificial radioactivity levels in the soil, water, and plant that had been collected from various locations surrounding the nuclear research center at Al-Tuwaitha. Gamma ray spectroscopy measurements for natural radionuclides ( $^{238}\text{U}$ ,  $^{232}\text{Th}$ , and  $^{40}\text{K}$ ) and artificial radionuclide ( $^{137}\text{Cs}$ ) showed, the average of specific activity in water samples is  $(2.06 \pm 1.435 \text{ Bq.l}^{-1})$ ,  $(1.84 \pm 1.356 \text{ Bq.l}^{-1})$ ,  $(33.11 \pm 5.754 \text{ Bq.l}^{-1})$  and  $(1.37 \pm 1.171 \text{ Bq.l}^{-1})$  respectively. The results obtained for the natural radioactivity and concentration of uranium are almost same compared with a large number of Iraqi, arabic and international researchers [16].

### **1.6.2 Determine the Radioactivity Concentration**

V. L. Petukhov, et al (2003), studied the effect of contamination on the area of highest contaminated Byelorussia republic after the Chernobyl disaster by collecting 408 milk samples from 1995 to 2000.  $^{137}\text{Cs}$  and  $^{90}\text{Sr}$



were detected in these samples by using scintillation gamma spectrometer, their levels were exceeded republic upper limits in 10 and 50 % of milk samples respectively [17].

Milko K. and Sonja A. (2005) studied the contamination from atmospheric past nuclear weapon tests of  $^{90}\text{Sr}$  and  $^{137}\text{Cs}$  in the period of 1951-1980 and also from Chernobyl (1986), in Slovenian territory, typical values of 1.5-2 kBq m<sup>-3</sup> for  $^{90}\text{Sr}$  and 3-4 kBq.m<sup>-3</sup> for  $^{137}\text{Cs}$ . The Chernobyl accident raised the contamination with  $^{137}\text{Cs}$  mostly in northwest part, with an average value of 20-25kBq.m<sup>-3</sup> for the country [18].

N. Casacuberta, P. Masque, et al (2013), studied the radioactivity concentrations of  $^{90}\text{Sr}$  and  $^{89}\text{Sr}$  in both surface water and at depth after the Fukushima accident in March 2011, ranged from 0.8±0.2 to 85±3 Bq.m<sup>-3</sup> and from 19±6 to 265±74 Bq.m<sup>-3</sup>, respectively. The  $^{90}\text{Sr}/^{137}\text{Cs}$  ratio has been calculated to be 0.0265±0.0006. This ratio is significantly different than the global fallout produced by nuclear weapon tests, which was 0.63 [19].

Sousa Silva L. and Pecequilo B.R.S. (2011) determined the levels of gross alpha and beta radioactivity for water in a surface, underground and drinking to the urban living in the real uranium province of Brazil. The preliminary results showed natural radiation levels varying from 0.02 ± 0.001Bq.L<sup>-1</sup> to 0.80 ± 0.04Bq.L<sup>-1</sup> for gross alpha activity and from 0.010 ± 0.006 to 3.0 ± 0.2Bq.l<sup>-1</sup> for gross beta activity. Some values exceeded the 2004 WHO recommendation levels except the drinking water [20].

Ferdous J. et al. (2012) determined the gross alpha and gross beta radioactivity for twenty tap water samples which collected from different

locations in Dhaka city. By using the ZnS(Ag) scintillation detector and gas proportional counter, respectively [21]. The alpha and beta radioactivity concentrations ranging from 1.88 to 8.16 mBq.L<sup>-1</sup> with an average 3.76 mBq.L<sup>-1</sup> and from 29.305 to 115.74 mBq.L<sup>-1</sup> with an average 60.41 mBq.L<sup>-1</sup>, respectively.

### **1.6.3 The Radioactive Liquid Waste Treatment**

N.F., Chelishchev (1993) used the natural clinoptilolite zeolite for Chernobyl various nuclear disasters, where <sup>137</sup>Cs and <sup>90</sup>Sr were removed from the environment to the final discharge in the Irish Sea previously [22].

Ahmet E. Osmanlioglu (2006), investigated the effectiveness of zeolite treatment at the laboratory tests to the waste treatment plant of low-level liquid waste (LLLW), and studied natural zeolites (clinoptilolite) for the removal of the several radionuclides from liquid radioactive waste such as (<sup>137</sup>Cs, <sup>60</sup>Co, <sup>90</sup>Sr and <sup>110m</sup>Ag) of different zeolite formations in Turkey. Batch tests were applied on the sample at temperature, 30°C, solid concentration 10 g/L with stirrer rate 200 rpm. It was found that ion-exchange capacity of the natural zeolite is very good for <sup>137</sup>Cs at pH is about 10. He proved that Gordes clinoptilolite is the most suitable natural sorbent [23].

I. Smičiklas et al (2007), studied the adsorption properties of local clinoptilolite (Serbia) for Cs<sup>+</sup>, Co<sup>+2</sup>, and Sr<sup>+2</sup> by batch equilibration technique and the conditioning effect of equilibration time, initial metal cation concentration and solution pH. Cs<sup>+</sup> is preferably adsorbed by the natural clinoptilolite, followed by Sr<sup>+2</sup> and Co<sup>+2</sup>. The results were; at pH range of 3–12 the adsorption of Cs<sup>+</sup> remains approximately constant and pH range of 2–10 adsorption of Sr<sup>+2</sup> remains almost stable [24].

E.H. Borai et al (2009), used four various zeolite minerals three natural types including clinoptilolite and synthetic mordenite (NaSM). The effective parameters on the sorption behavior of cesium ( $^{134}\text{Cs}$ ) were investigated by using batch equilibrium technique with respect solution pH, contacting time, waste solution volume, sorbent weight, and Cs ion concentration. The obtained results revealed that natural chabazite (NaNCh) has the higher capacity towards Cs ion rather than the other investigated zeolite materials for LLLW [12].

R. O. Abdel Rahman et al (2011), highlighted to the scientific important problems that affect at the different treatment processes, by the directed review to the recently published researches that are concerned with testing and application of different treatment of radioactive waste management practice. His review is divided into advances in conventional treatment of aqueous and organic liquid wastes radioactive wastes, and emerged technological options [7].

Al-Nasri S. K. (2013) was composite new adsorbents, he used diatomite and carbon to prepare the composite by incorporating them with three types of zeolites A, Y, and clinoptilolite. He studies two types of ions Cobalt ( $^{59}\text{Co}$ ) and Strontium ( $^{89}\text{Sr}$ ) content in wastewater. The study investigated some factors which affected to uptake the isotopes, such as pH which range of 5-6 for  $\text{Co}^{2+}$  while for strontium it was at pH 10, the contact time was 120-180 minutes and the temperature was (45-50) °C that gave the highest adsorption [9].

Parthiv Chetan Kavi (2016) studied how to reduce the volume of high-level radioactive waste. Along with the separation of uranium and plutonium, there has been a significant interest in the extraction of fission products such as  $^{137}\text{Cs}$  and  $^{90}\text{Sr}$ , The uptake of fission products from slightly acid solutions (pH value ~5) was more encouraging but not specific to any single ion [26].

Firas Mohammed Radhi (2017) studied the treatment of liquid as a result of processing soil samples from Al- Tuwaitha site of waste contained with cesium ( $^{137}\text{Cs}$ ) by using natural zeolite clinoptilolite. The weight of clinoptilolite and contact time were studied as factors affecting of the removal efficiency of cesium from liquid. The results revealed that the clinoptilolite was highly efficient in removing cesium ions from liquid waste, at all range of weight used. The results also demonstrate that removal efficiency of 96% was obtained of 2 hours contact time and an equilibrium state was achieved after 1 hr. [27].

### **1.7 The Aim of Study**

The primary object of radioactive wastes management is the radiological characterization of the waste in order to know the nature of the radionuclides which found in the waste from the chemical, and the physical properties such as their emitting and half-lives, radioactivity concentration, and the volume of waste. After all information of waste completed, the next step is the waste treatment, to minimize the volume of waste to be ready for disposal. Therefore, the aim of this study is:

- 1- The radiological characterization of the radioactive liquid waste in the waste hall (WH) which includes the radioactive liquid waste pools (RCL). The radiological characterization includes determining the radioactivity concentration of each radionuclide in this liquid waste, determining both the volume of liquid waste and the total activity for each pool in this hall.
- 2- Using suitable radiological devices to detect all expected radionuclides.
- 3- Studying the conventional treatment technology for the liquid wastes by studying suitable conditions to improve the removal efficiency of  $^{137}\text{Cs}$  and  $^{90}\text{Sr}$  which are the main radionuclides in these liquid wastes.

**CHAPTER TWO**  
**Theoretical Considerations**

---

## CHAPTER TWO

### Theoretical Considerations

#### 2.1 Radioactivity

Radioactivity defined as a spontaneous nuclear transformation in an unstable nucleus that leads to formation a new element. This transformation is characterized by one of many different ways, such as alpha-particle emission, beta-particle emission, and orbital electron capture. Each of these transformations may be accompanied by a gamma radiation emission [28]. The available energy of transformations depends on the particular type of nuclear instability which is whether the neutron-to-proton ratio ( $n/p$  too high or too low) for the particular nuclide and on the mass-energy relationship among the parent and daughter nucleus [29]. The radioactivity units in the System International of units (SI) are Curies (Ci) and Becquerels (Bq), one Bq equal to one disintegration per second (dis/s), where 1 Curie (Ci) is equal to  $3.7 \times 10^{10}$  Bq [30].

#### 2.2 Radiation sources

The main origin of radioactivity in the environment belongs to two sources; natural and man-made sources. The natural source of radiation came from terrestrial radionuclides which are widely distributed in the earth's crust and sources arising from cosmic ray. Other sources arise from human activities concerned with the use of radiation and radioactive materials from which releases of radionuclides into the environment may occur [29].

##### 2.2.1 Natural sources

The natural radiation sources consist from extraterrestrial and terrestrial radiation sources [31]. The extraterrestrial radiation sources included two types of radiation sources which are cosmic ray and

cosmogenic radionuclides. Cosmic rays incident on the top of the atmosphere consists of a nucleonic component which in aggregate accounts for 98% of the total, and 2% electrons. The nucleonic component is primarily protons (88%) and alpha particles (11%), with the remainder heavier nuclei. When they enter the upper layer atmosphere of earth, they undergo interactions that may produce charged particles, gamma rays, and neutrons.

The cosmogenic radionuclides are produced by the collision of the highly energetic cosmic-ray particles with stable elements in the atmosphere and the ground. Many different cosmogenic radionuclides are produced, such as  $^{14}\text{C}$ . It is the most important, and other less significant cosmogenic radionuclides such as  $^3\text{H}$ ,  $^7\text{Be}$ , and  $^{22}\text{Na}$ . The cosmic radiation intensity depends upon the degree of shielding provided by the atmosphere, altitude and barometric pressure [32].

The other natural source is terrestrial (primordial) source. The primordial radionuclides have very long half-lives, as a comparable to the age of the earth, they are classified into:

- Series radionuclides groups of radionuclides that are headed by parent radionuclides which decay in sequence to other radionuclides with different half-lives and decay modes, and finally end up as stable isotopes. There are three natural series headed by  $^{238}\text{U}$ ,  $^{235}\text{U}$ , and  $^{232}\text{Th}$  [33].
- Non-series radionuclides; they decay directly to stable nuclide. The most important of non-series radionuclides are the isotopes  $^{40}\text{K}$ ,  $^{87}\text{Rb}$ ,  $^{113}\text{Cd}$  and  $^{115}\text{In}$ . In term of population radiation dose,  $^{40}\text{K}$  and  $^{87}\text{Rb}$  are the most significant radionuclides. The radioactive isotope of  $^{40}\text{K}$  can

decay by beta followed by the emission of a 1460.8 keV gamma ray whereas  $^{87}\text{Rb}$  is a pure beta emitter [34, 35].

### 2.2.2 Man-made sources

Some of the radionuclides have been released into the environment by human due to various purposes. The man-made sources of radiation may result from physical processes involving the nuclear fission and fusion, nuclear explosions, neutron activation and by nuclear accelerators. In the middle of the 20th century, linear accelerators were developed for producing artificially radionuclides. The application of nuclear fission in 1940, presented the ability of humans to produce large quantities of artificial radionuclides by neutron-induced nuclear reactors which are the most important source of artificially created radionuclides [36].

The fission process causes a high neutron flux density which achieved in nuclear weapons explosions and fission reactors, it led to the production of large quantities of fission and activation products. Fission products are the isotopes with a mass number in the range of 70-170, formed by  $^{235}\text{U}$  thermal fission and other heavy fissile nuclei (e.g.,  $^{239}\text{Pu}$ ). High-yield fission products include “ $^{89}\text{Sr}$ ,  $^{90}\text{Sr}$ ,  $^{91}\text{Y}$ ,  $^{95}\text{Zr}$ ,  $^{95}\text{Nb}$ ,  $^{99}\text{Mo}$ ,  $^{103}\text{Ru}$ ,  $^{131}\text{I}$ ,  $^{133}\text{Xe}$ ,  $^{137}\text{Cs}$ ,  $^{140}\text{Ba}$ ,  $^{140}\text{La}$ ,  $^{141}\text{Ce}$ ,  $^{144}\text{Ce}$ ,  $^{143}\text{Pr}$  and  $^{147}\text{Nd}$ ” [36].

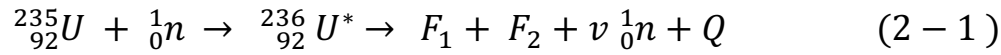
However, in most situations, the most radiologically important fission products are  $^{89}\text{Sr}$ ,  $^{90}\text{Sr}$ ,  $^{131}\text{I}$  and  $^{137}\text{Cs}$  because of their high yields, long half-lives and chemical properties [37].

## 2.3 Nuclear Fission

Nuclear fission is the process of splitting a heavy nucleus into two parts called fission fragments, and several neutrons. The fission process produces high energy of neutrons, photons, nuclear particles (alpha and beta) and generates large amounts of heat and radiation, as shown in



figure (2-1). An important fissionable nuclear material that is widely used in atomic reactors is uranium-235 ( $^{235}\text{U}$ ) and plutonium-239 ( $^{239}\text{Pu}$ ), which are the nuclear fuel. The fission process of  $^{235}\text{U}$  has been clarified below according to the conservation equation [29]:



Where:

$F_1, F_2$  : The fission fragments.

$\nu$  : The mean number of neutrons per fission of  $^{235}\text{U}$ , which about (2.5).

$Q$ : The energy value for any particular pair of fission fragments, which about 200 MeV.

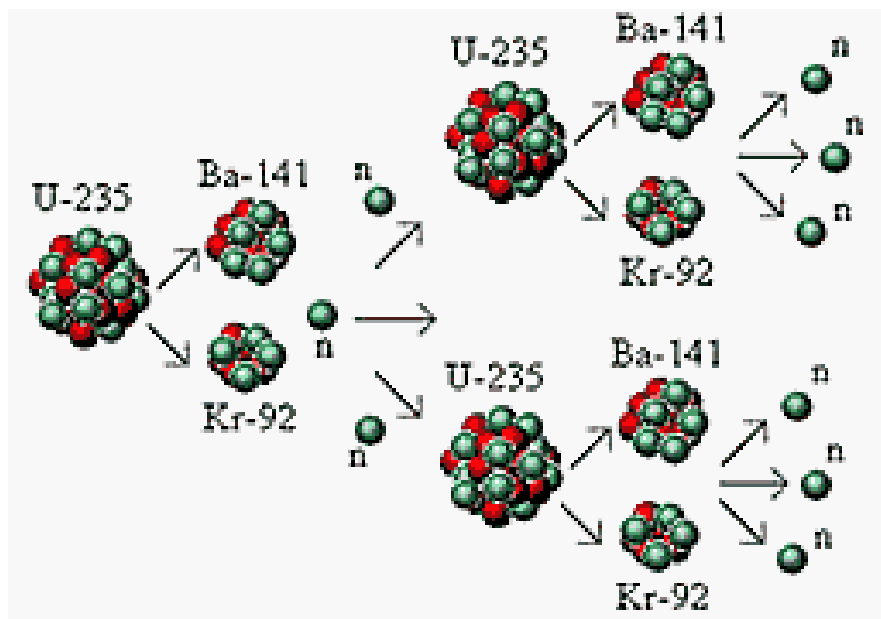


Figure 2-1: The fission process [29].

### 2.3.1 Fission Products

There are a large number of nuclei producing in the fission process and their atomic numbers range from 30 ( $^{72}\text{Zn}$ ) to 64 ( $^{158}\text{Gd}$ ), as shown in figure (2-2). All the fission fragments are radioactive, and they decay, usually in chains to form fission products. After production, each species

of fission product decays according to its unique disintegration rate [36].

There are two main chains of fission products:

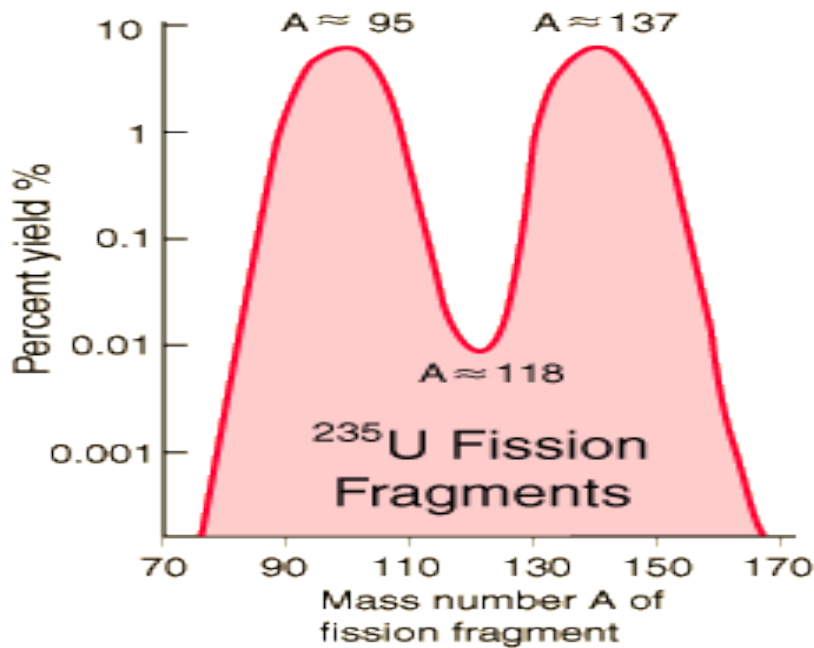
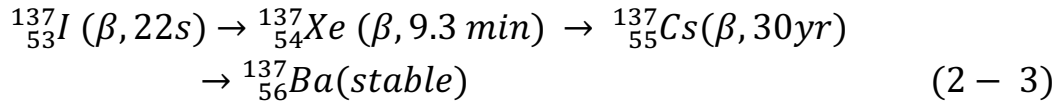
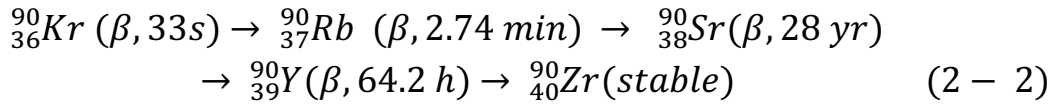


**Figure 2-2: Fission product yield from thermal fission of  ${}^{235}\text{U}$  [29].**

### 2.3.2 Fission Product Inventory

Fission products are produced at a rate proportional to the power level of a reactor when it continues to operate. Fission products vary significantly with the physical states and chemical forms [38]. The fission products are typically divided into five classes as below [39]:

- 1- Noble gases: The noble gases products such as Kr and Xe.
- 2- Volatiles: The volatiles products such as Br, Rb, Te, I and Cs elements, which exist as gases at high temperatures.

- 3- Metals: The metals products such as Mo, Ru, Pd, and Tc elements which form a metallic precipitate and insoluble metallic alloys.
- 4- Insoluble oxides: The elements such as Zr, Ba, and Sr that form oxides and are insoluble in the fluorite lattice.
- 5- Soluble oxides: The elements such as Y, La.

Table (2-1) lists the fission products with half-lives longer than one year with their fission yields for  $^{235}\text{U}$  fuel [40]. The radionuclides with a half-life less than one year have a very small percent of the original activity which remaining after 45 years that have elapsed and radioactivity is usually considered to be insignificant since it is the period of the spent fuel that used as a mentioned in chapter one till the time of this study. The fission yield is the portion of fissions resulting of the specific isotope as shown in percentages in the table (2-1). Since the decay of a radionuclide decrease exponentially, the relative activity of each fission product is the products of the fission yield. These products showed in this table as the relative activity yield which is the relative amount of each fission product radionuclide from the total activity. The relative activity yield of each fission product radionuclide has been corrected for 45 years. The results of the activity percent at 45 years are shown in the table which illustrates a part of the fission yield disappeared and apart are not significant from the total remain activity [41]. The  $^{85}\text{Kr}$  has dissipated into the atmosphere because it is a noble gas [38]. From the table, it can be seen that greater than 98% of the remaining activity is composed of  $^{90}\text{Sr}$  and  $^{137}\text{Cs}$ , and other most of the remaining percentage are from  $^{147}\text{Pm}$  and  $^{155}\text{Eu}$ .

**Table 2-1: Fission products of  $^{235}\text{U}$  with half-lives greater than one year [40].**

Isotopes	$T_{1/2}$ (years) half-life	Fission Yield (%)	Relative Activity Yield at t=0	Activity yield % at t=0	Activity at 29 years%	Activity at 45 years%
Kr-85	10.73	1.317	8.51E-02	6.8337	0.0000	<b>0</b>
Sr-90	29.1	5.8	1.38E-01	11.097	47.959	<b>48.48</b>
Zr-93	1.5E+06	6.37	2.94E-06	0.0002	0.0016	<b>0.0023</b>
Tc-99	2.13E+05	6.1	1.99E-05	0.0016	0.0111	<b>0.016</b>
Ru-106	1.02	0.401	2.73E-01	21.888	0.0002	<b>1.1E-08</b>
Pd-107	6.5E+06	0.145	1.55E-08	0.0000	0.0000	<b>0</b>
Cd-113	9E+15	0.015	1.16E-18	0.0000	0.0000	<b>0</b>
Sb-125	2.76E+00	0.031	7.79E-03	0.6258	0.0280	<b>0.0009</b>
Sn-126	1.0E+5	0.059	4.09E-07	0.0000	0.0002	<b>0.00028</b>
I-129	1.57E+07	0.75	3.31E-08	0.0000	0.0000	<b>0</b>
Cs-134	2.07E+00	7.6E-06	2.57E-06	0.0002	0.0000	<b>0</b>
Cs-135	2.30E+06	6.54	1.97E-06	0.0002	0.0011	<b>0.0015</b>
Cs-137	3.02E+01	6.19	1.42E-01	11.423	50.214	<b>51.428</b>
Sm-146	1.03E+08	3	2.02E-08	0.0000	0.0000	<b>0</b>
Pm-147	2.62E+00	2.25	5.94E-01	47.751	1.6461	<b>0.045</b>
Eu-152	1.35E+01	0.25	9.20E-12	0.0000	0.0000	<b>0</b>
Eu-154	8.59E+00	0.072	1.54E-08	0.0000	0.0000	<b>0</b>
Eu-155	4.71E+00	0.032	4.71E-03	0.3783	0.1371	<b>0.0217</b>

## 2.4 Activity

The activity defines as the rate of nuclei number decaying or disintegrating with time. In a sample where there are  $N_t$  nuclei present, the number of nuclei decaying in time  $dt$  is given by [42]:

$$- dN/dt \propto N_t \quad (2 - 4)$$

$$- \frac{dN}{dt} = \lambda \cdot N_t \quad (2 - 5)$$

Where:

$dN$ : The number of radio-nuclei in the sample in the time  $dt$ .

$\lambda$ : The constant of proportionality known as the disintegration or decay constant ( $\text{s}^{-1}$ ).

The negative sign is an indication of the number of nuclei in the sample decreases along time. The previous equation when solved for the number  $N$  of the radio-nuclei which found in a sample at time  $t$ , that gives.

$$N_t = N_o e^{-\lambda t} \quad (2 - 6)$$

Where:

$N_t$  : The number of radioactive nuclei at time  $t$ .

$N_o$  : The number of radio-nuclei in the sample at  $t = 0$ .

Equation (2-6) is the radioactive decay law, which expresses the exponential decay of every kind of radioactive nucleus with time. The activity of a radioactive source ( $A$ ), i.e. the number of disintegrations per second (Becquerel), is given as:

$$A = - \frac{dN}{dt} = \lambda \cdot N_t \quad (2 - 7)$$

According to eq (2-6) the radioactivity  $A_t$  can be expressed in terms of the initial activity  $A_o$  by using the definition of activity as:

$$A_t = A_o e^{-\lambda t} \quad (2 - 8)$$

Where:

$A_t$  : The activity at time  $t$

$A_o = \lambda N_o$  is the initial activity of the sample.

$T_{1/2}$ : The half-life, which defines as the time needed for one-half of a certain number of radio-nuclei to disintegrate.

The relationship between the half-life ( $T_{1/2}$ ) and the decay constant ( $\lambda$ ) can be found it from equation (2-6) by setting  $N = 1/2 N_o$  this gives [43]:

$$T_{1/2} = \frac{\ln(2)}{\lambda} \quad (2 - 9)$$

From the definition of the half-life, it follows that the fraction of a radionuclide remaining after  $n$  half-lives is given by the relationship [29]:

$$\frac{A_t}{A_0} = \frac{1}{2^n} \quad (2 - 10)$$

Where:

$A_t$  : The remain activity after  $n$  half-lives.

## 2.5 Specific Activity

The specific activity is the concentration of radioactivity or is the relationship between the mass of the radioactive material and its activity. The specific activity is the unit activity (Bq or Ci) per unit mass or volume [44]. The specific activity of a pure radioisotope that is not mixed with any other isotopes of the same element that can be calculated as follows:

If the mass of the radio-nuclei in the sample is known, the number of radio-nuclei ( $N$ ) can be calculated from [44]:

$$N = \frac{N_A}{W} \cdot m \quad (2 - 11)$$

Where:

$N_A$ : Avogadro number, it is  $6.02 \times 10^{23}$  (atom/mol).

$W$ : The atomic weight of the radionuclide (g/mol).

$m$ : The mass of the radio-nuclei (g).

If the radionuclide under consideration weighs 1 g, then, according to the previous equation, the specific activity (activity per unit weight) is:

$$\begin{aligned}
 S.A(Bq. g^{-1}) &= \lambda N = \lambda \cdot \frac{N_A}{W} \cdot m = \frac{\ln 2}{T_{1/2}} \cdot \frac{N_A \cdot m}{W} = \frac{0.693}{T_{1/2}} \cdot \frac{6.02 \times 10^{23}}{W} \\
 &= \frac{4.18 \times 10^{23}}{T_{1/2} \cdot W} \quad (2 - 12)
 \end{aligned}$$

The previous equation valid only if  $\lambda$  and  $T_{1/2}$  are given in seconds (time units) [29].

## 2.6 Radiation Detection

The radiation detection depends on the nature of the radiation interaction with the sensitive medium of a detector, therefore the radiation instruments basically involve generating electrical signals which result from this interaction. The radiation detection methods are based on the process of excitation or ionization of atoms in the detector medium by the passage of a charged particle inside the sensitive medium. Electromagnetic radiation (gamma-ray or X-ray) gives a rise to energetic electrons by one of the three types of processes, namely photoelectric effect, Compton scattering and pair production. There are many kinds of radiation detectors such as passive and active detectors, the active contains many kinds of medium materials such as gas, liquid, and solid (which contain scintillation or semiconductor) detectors. All of them may provide information about radiation, such as its energy, intensity, and/or the type of radiation [29].

### 2.6.1 The Semiconductor Hyper-pure Germanium Detector

The mainly scintillation detectors have been used for gamma spectra analysis. Another type of detectors is almost semiconductor, the main advantage of them are their high energetic resolution, which is about 10 to 20 times better than the scintillator detectors, because the energy needed to produce a pair of charge carriers is very low (only about

2.96 eV) with the consequence that for a certain amount of absorbed energy [45].

There are the older Ge(Li)-semiconductor detectors and the increasingly used high-purity germanium detectors (HPGe). Germanium detector is semiconductor diode having a P-I-N structure, the Intrinsic (I) region is sensitive to ionizing radiation, especially gamma rays. Under reverse bias voltage, the electric field extends across the intrinsic (depleted) region. When photons enter the depleted region of a detector, holes, and electrons (charge carriers) are produced and are moved forward to the P and N electrodes by the electric field. These charges, which are in proportion to the energy deposited in the detector by the incoming photons, they are converted into voltage pulses by an integral charge sensitive preamplifier [46]. Figure (2-3) shows a diagram of a basic gamma spectrometry system.

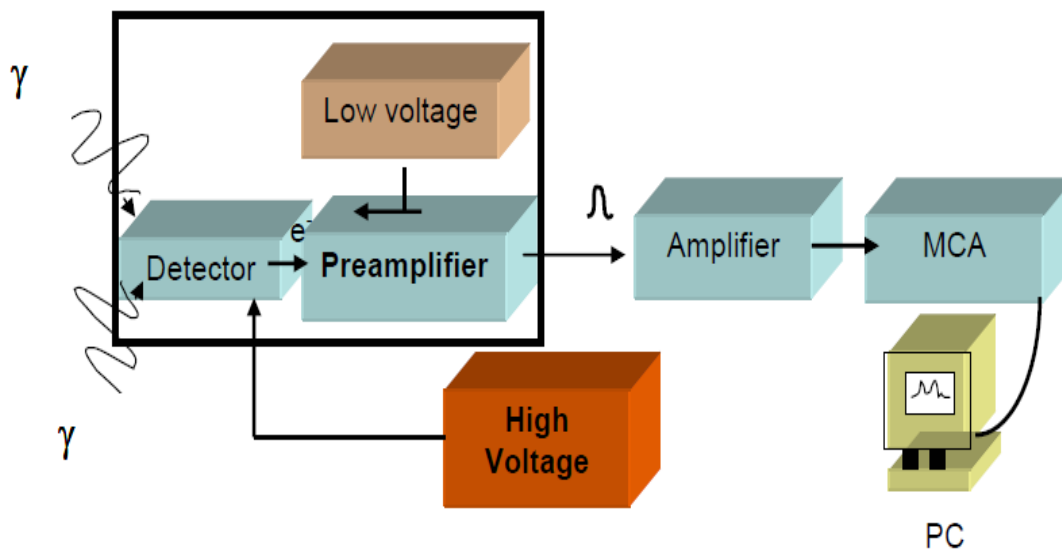


**Figure 2-3: Block diagram of a basic gamma spectrometry system [46].**

The band gap in germanium is 0.7eV, that means a small amount of energy is required to excite an electron into the conduction band whereas in the valance band a hole is created. The electrical conductivity of a



semiconductor is therefore changed when a semiconductor is exposed to radiation. The HPGe detector is cooled to 77 K with liquid nitrogen, in order to reduce dark current and detector noise [46]. A coaxial HPGe detector p-type geometry was used in this study, as shown in the figure (2-4).

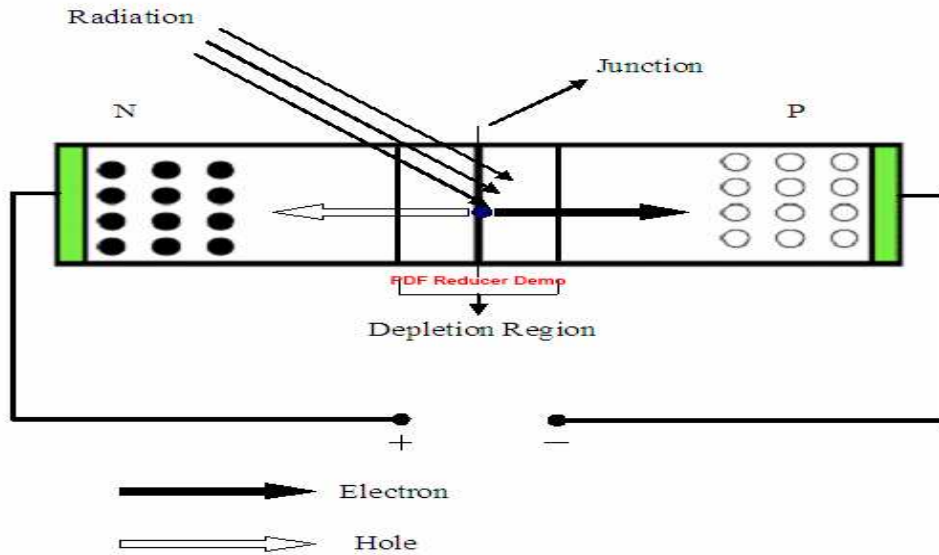


**Figure 2-4: Schematic of a P-N semiconductor detector [46].**

### 2.6.2 Proportional Counters

The proportional counter is a type of gas medium detectors, the most common of these detectors are Geiger-Mueller tubes and ion chamber which depend on the regions of operation voltage. Figure (2-5) shows the different regions of operation of gas-filled detectors. The proportional tubes rely on the gas multiplication phenomenon to amplify the charge represented by the original ion pairs created within the gas. Therefore, the pulses are considerably larger than those form in ion chambers that used under the same conditions [45].

When a fast charged particle passes through a gas, it will create both excited and ionized atoms along its path. The resulting positive ion

and free electron are called an ion pair. Ions can be formed either by direct interaction or through a secondary process in which some of the particle energy is first transferred to an energetic electron or "delta ray".

The practical quantity of interest is the total number of ion pairs created along the track of the radiation. A minimum amount of particle energy is equal to the ionization energy of gas molecule and must be transfer to permit the ionization process to occur [47].

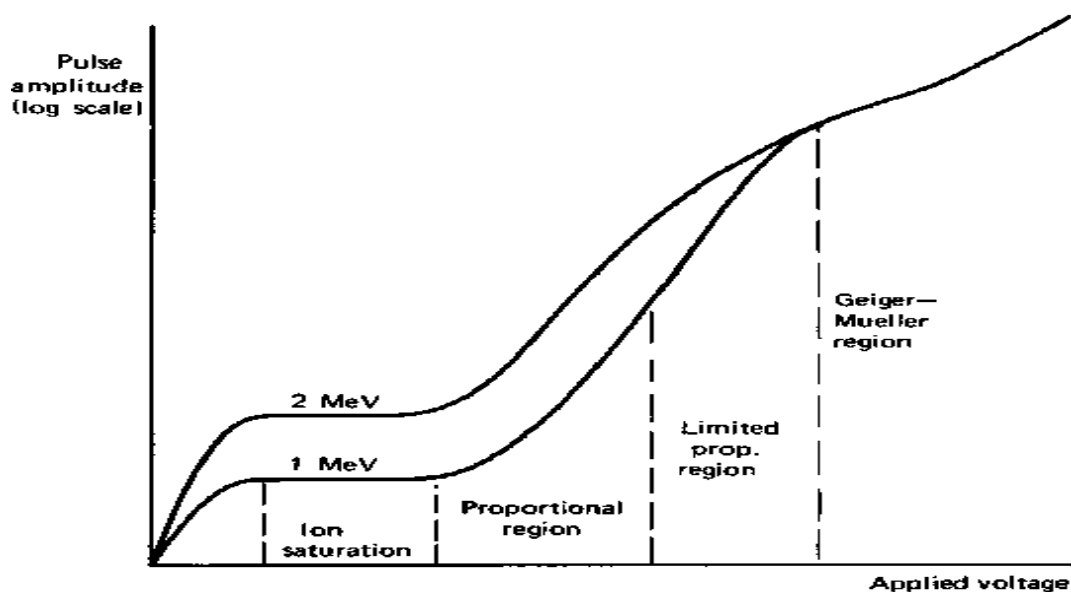


**Figure 2-5: The different regions of operation of gas-filled detectors [45].**

Gas-flow proportional counting is one of the most practical methods for performing gross alpha and/or beta measurements. Measuring the gross radioactivity in a sample provides a simple direct method of sample screening [48]. Figure (2-6) shows the diagram of the gas flow proportional counter with a loop anode wire and hemispherical volume. Tennelec LB system which has been used in this study is capable of providing accurate radioactivity measurements.

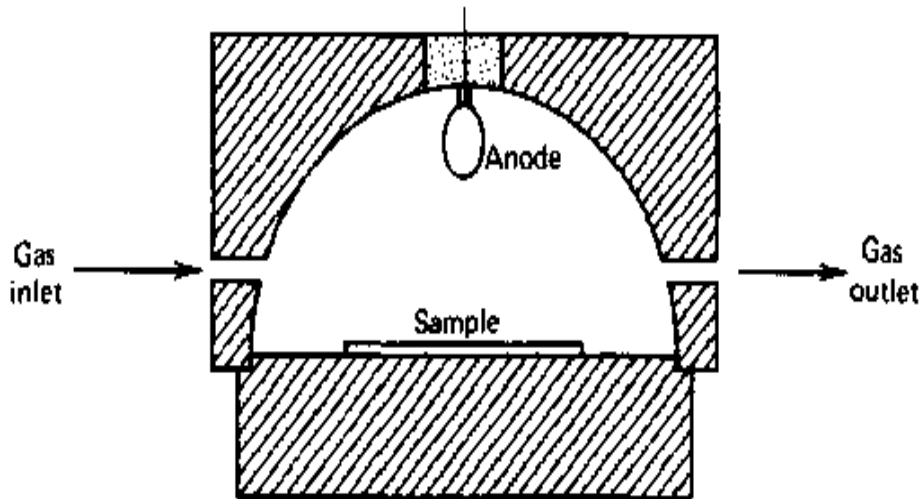


**Figure 2-6: Diagram of a gas flow proportional counter [45].**

## 2.7 Radioactive Waste

The radioactive waste contains irradiative material, it usually produces from nuclear power generation and other applications of nuclear fission or nuclear application, such as research and medicine. The radioactive waste is hazardous to all forms of life and the environment, therefore, it regulates by national and international control bodies or agencies in order to protect the human health and the environment. Due to the radioactivity naturally decays over time, the radioactive waste has to be isolated, confined and conserve in appropriate disposal facilities for a sufficient period, which depends on the type of waste and radioactive isotopes [49].

### 2.7.1 Sources of Radioactive Waste

There are several sources of radioactive waste like the nuclear power plants, nuclear weapon, or nuclear fuel treatment plants. The large portion and the majority of waste originates of producing radioactive waste is from the nuclear fuel cycle and nuclear weapons reprocessing, as shown in figure (2-7) [50]. Other radioactive waste sources include

medical and industrial wastes, as well as naturally occurring radioactive materials (NORM) which can be concentrated as a result of the processing and consumption of coal, oil and gas and some minerals [51,52].

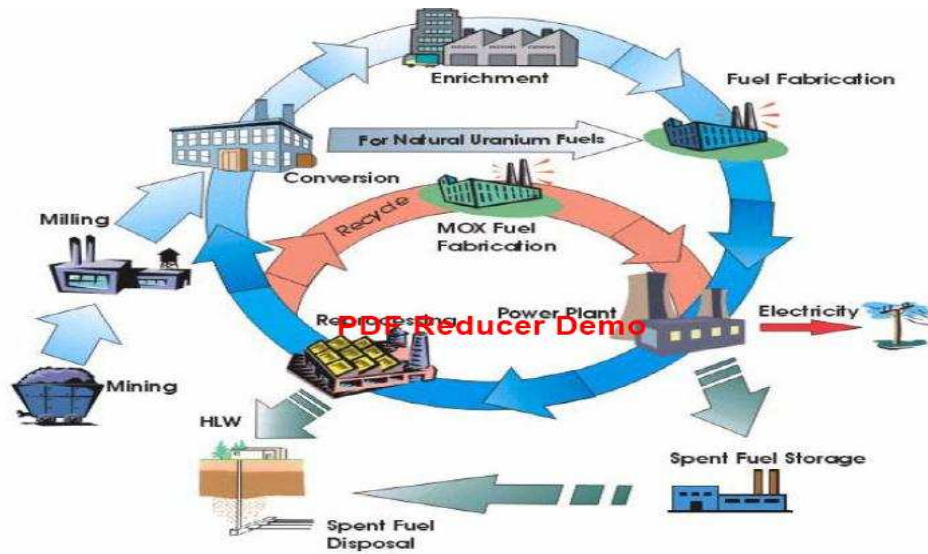


Figure 2-7: Nuclear fuel cycle [50].

### 2.7.2 Classification of Nuclear Waste

The classification of nuclear wastes depends on their types, source, and levels of emitting radiation [53]. In order to achieve the radioactive waste management with standards required, it classifies into a number of categories. The general considerations for classifying radioactive wastes are a long of the waste which remain radioactive, concentration of the radioactive material in the waste and whether the waste is heat-generating. These considerations also determine suitable disposal methods.

The generation of radioactive wastes varies from country to country depending on the scale of applications. The classification of these wastes is very helpful throughout their management phases from generation through collection, segregation, treatment, storage, transportation to final disposal. Classifications are usually derived from

different perspectives, *i.e.*, safety perspective, the physical/chemical characteristics of the waste, process engineering demands or regulatory issues. The international classification of waste in general of accepted categories are [54]:

- ❖ Exempt wastes (EW): Activity levels at or below clearance levels, which are based on an annual dose to members of the public of less than 0.01 mSv
- ❖ Very low-level waste (VLLW): It is the waste which contains negligible radioactivity.
- ❖ Low-level waste (LLW): It contains only small amounts of radioactivity with negligible amounts of long-lived radionuclides.
- ❖ Intermediate level waste (ILW): It is the waste which contains higher amounts of radioactivity.
- ❖ High-level waste (HLW): There are two sorts of high-level waste; spent fuel and the fission products released from spent fuel by reprocessing. HLW is highly radioactive and contains long-lived radioactivity [55], figure (2-8) illustrates the radioactive waste classification.

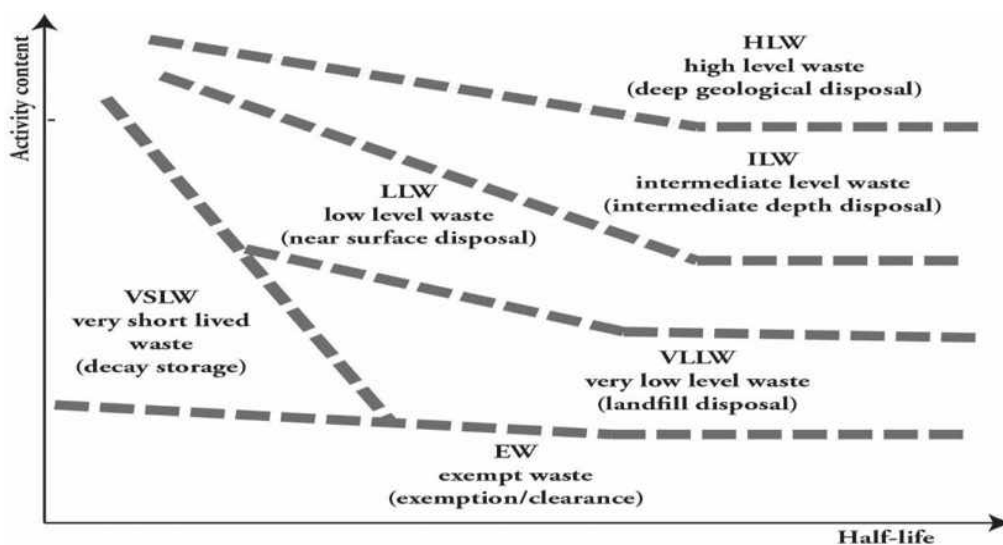
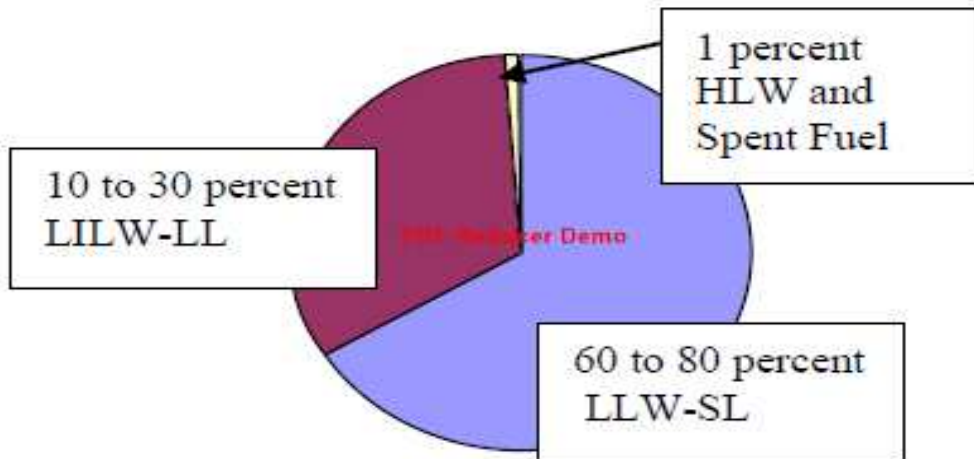


Figure 2-8: Conceptual illustration of waste classification scheme [55].

The low and intermediate-level wastes may combine and classify together as (LILW), which may be subdivided into short-lived and long-lived (LILW-SL), (LILW-LL) wastes [56,57]. Figure (2-9) shows the relative volume of radioactive waste type which produces in the commercial nuclear cycle.



**Figure 2-9: Relative volume of radioactive waste type nuclear cycle [56].**

### 2.7.3 Radioactive Liquid Waste

The radioactive liquid waste is generated during nuclear reactor operation and during industrial and institutional application of radioisotopes. The radioactive liquid wastes must be categorized into aqueous and organic liquid wastes to facilitate the management for them [58, 59].

### 2.7.4 Classification of Radioactive Liquid Waste

The radioactive liquid waste (RLW) can be classified by different ways, the RLW from waste nuclear fuel (WNF) storage pools, and the RLW from reactor coolant liquids. All these types of the RLW differ in chemical and radiochemical composition. The RLW divides into high-

active (higher than 10 Ci/L), middle-active (from 10 down to  $10^{-2}$  Ci/L), low-active (from  $10^{-2}$  down to  $10^{-5}$  Ci/L), and very low-active (from  $10^{-6}$  down to  $10^{-9}$  Ci/L) [60].

### 2.7.5 Cesium-137 and Strontium-90 as Nuclear Waste

The main two of the radioactive wastes produced by the nuclear plants are  $^{137}\text{Cs}$  and  $^{90}\text{Sr}$  with half-lives about 30 and 29 years, respectively. They usually generated by nuclear fission processes with a high yield fission product in fission products,  $^{137}\text{Cs}$  and  $^{90}\text{Sr}$  transfer to the environment and they pollute air, water and soil as a result of fallout from nuclear bomb tests and reactor accidents. Both bring some of the problems to environmental and health of the public. They can cause various diseases in living organisms, especially cancer in people. They do not lose their hazardous properties in a short time [61].

#### 2.7.5.1 Cesium

Cesium is an alkali metal which locates in group I A and period 6, S block in the periodic table. It is silvery gold, soft, electropositive (+), very toxic and ductile. It reacts easily with oxygen and explosively with water. Cesium is a high yield fission product and one of the highest specific activity radionuclide as well as present at high concentrations in fission products with a half-life of 30.2 years. Cesium is a volatile element, which exists as gases at high temperatures, its melting point  $28^\circ\text{C}$  and boiling point is  $671^\circ\text{C}$  [62]. Figure (2-10) shows cesium-137 ( $^{137}\text{Cs}$ ) decay diagram.  $^{137}\text{Cs}$  decays by beta emission to a metastable nuclear isomer of barium-137m ( $^{137\text{m}}\text{Ba}$ ) with half-life 153 seconds which is much shorter than  $^{137}\text{Cs}$ , the  $^{137\text{m}}\text{Ba}$  is responsible for all gamma rays emissions with large probability (85.1%) then it decays to ground state into stable  $^{137}\text{Ba}$  by emission of gamma-ray with energy

0.6617 MeV [63]. The specific activity of  $^{137}\text{Cs}$  (One gram of cesium-137) has an activity of 3.215 Tera-Becquerel (TBq/g).

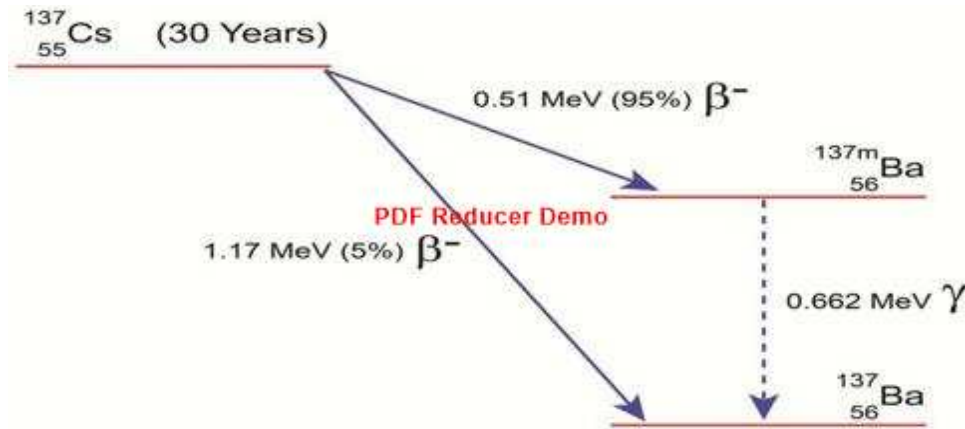


**Figure 2-10: The decay scheme of  $^{137}\text{Cs}$  [63].**

Cesium absorbs by humans and animals through the digestive system and chemically acting like potassium in the body, therefore, it can be replacing potassium in the body and combines very quickly to the organism, causing the growth of the cells everywhere of the body [64].

### 2.7.5.2 Strontium

Strontium is an alkaline earth element which locates in group II A and period 5, S block in the periodic table. Strontium does not be as a free element, it is softer than calcium and reacts and dissolves with water strongly and interacts with oxidants, and therefore, it ignites spontaneously in air. It has a white/silvery appearance and electropositive (++) . Strontium is a high yield nuclear fission product and the most abundant radionuclide with highest specific activity radionuclide as well as present at high concentrations in fission products whose half-life is about 28.79 years. Strontium is an insoluble oxides element, its melting point  $777^\circ\text{C}$  and boiling point is  $1382^\circ\text{C}$  [62]. Figure (2-11) shows strontium-90 ( $^{90}\text{Sr}$ ) decay diagram, the main features of this diagram, strontium-90 decays into unstable yttrium-90 ( $^{90}\text{Y}$ ) with a half-life (64



hours) which it is much shorter than that of  $^{90}\text{Sr}$ , the yttrium-90 decays into stable zirconium-90.  $^{90}\text{Sr}$  and  $^{90}\text{Y}$  are successively decaying almost by negative beta 100%, there are no accompanying gamma rays allowing to easily identifying the decays [65].

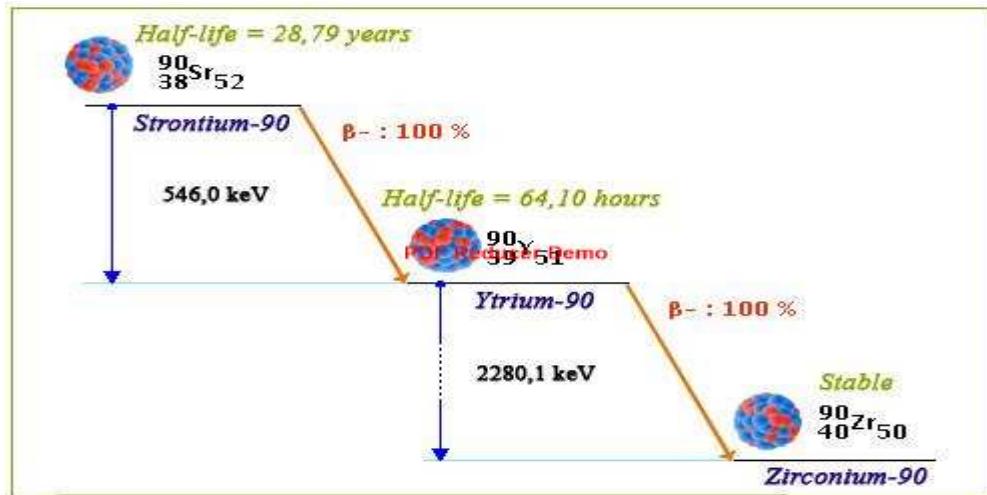


**Figure 2-11: The strontium-90 decay diagram [65].**

Chemically, strontium acting like calcium in the human body.  $^{90}\text{Sr}$  absorbed by the body and stored in the skeleton where calcium is found, therefore it can cause a result of multiple types of bone cancer [64].

## 2.8 Separation Techniques for Radioactive Wastes

The separation processes of cesium and strontium and remove them from the radioactive liquid waste are highly desired, therefore, there are many techniques for separating and removing them from aqueous solutions, which include [61]:

- Evaporation
- Filtration
- Precipitation
- Ion Exchange
- Sorption
- Membrane

## 2.9 The Zeolites

### 2.9.1 Definition of Zeolites

Zeolites are microporous, aluminosilicate minerals commonly used as commercial adsorbents and catalysts [66]. The zeolite is a Greek originated word, it means "boiling stone". In 1756, zeolites were discovered as a new group of minerals by the Swedish mineralogist Axel Fredrik Cronstedt, who observed that when it is heated, the material rapidly produces large amounts of steam from water which have been adsorbed by the material [67]. Natural zeolites contain other minerals such as quartz ( $\text{SiO}_2$ ),  $\text{SO}_4^-$  and amorphous glass, as well as other types of zeolite. Zeolites occur naturally but are also produced industrially on a large scale (figures (2-12 and 2-13)). There are about 232 unique zeolite frameworks have been identified, and over 40 naturally occurring zeolite frameworks are known possessing a variety of physical and chemical properties [68].



Figure 2-12: Natural zeolite [27]



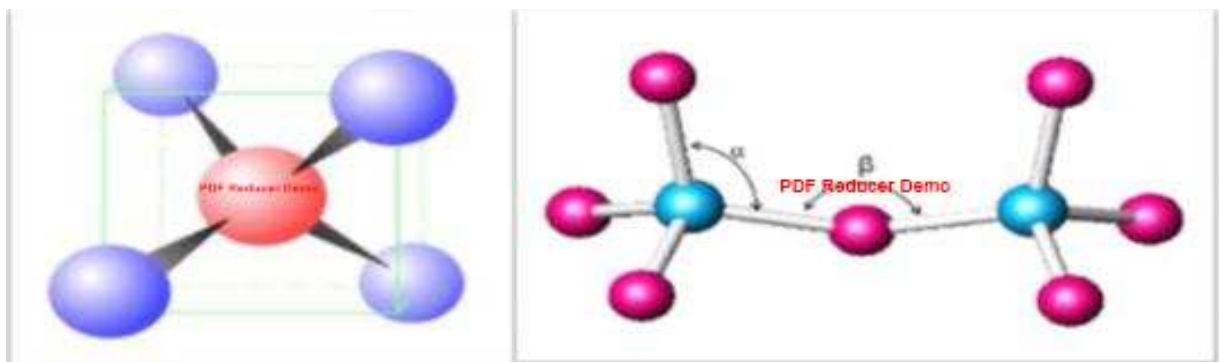
Figure 2-13: Synthetic zeolite [27]

### 2.9.2 General Properties of Zeolites and Structure

A zeolite is an aluminosilicate, whose framework a crystal structure of  $(\text{Si}, \text{Al})\text{O}_4$  tetrahedra contains pores filled with water molecules and exchangeable cations of both synthetic and natural forms exist. The skeletal structure of the zeolite contains holes occupied by

exchangeable ions and water molecules which have a considerable freedom of movement leads to ion exchange. The more common mineral zeolites are analcime, chabazite, clinoptilolite, heulandite, natrolite, phillipsite, and stilbite. An example of the mineral formula of a zeolite is  $\text{Na}_2\text{Al}_2\text{Si}_3\text{O}_{10}\cdot 2\text{H}_2\text{O}$  [9].

Zeolites have a framework structure arising from  $[\text{SiO}_4]^{-4}$  and  $[\text{AlO}_4]^{-5}$  tetrahedron. Tetrahedron structure consists of central core silicon or aluminum atom which is linked together by oxygen atoms. The primary building block of zeolite framework shows in figure (2-14). These linked structures are composed of infinite lattices made of crystalline materials [69]. The cavities and channels allow cations and water molecules to be held within the zeolite frameworks which are form about 50% of their total volume, while water represents 10 to 12% of their weight. The cations such as “ $\text{Na}^+$ ,  $\text{K}^+$ ,  $\text{Ca}^{+2}$ , and  $\text{Mg}^{+2}$ ” are also contained within the structure of the zeolite. These cations have a high degree of freedom of movement and ability to exchange with other cations [9]. These ions are rather loosely held and they can readily exchange for others in a contact solution.



(a)

(b)

**Figure 2-14:** (a-) Tetrahedral units ( $\text{SiO}_4$  or  $\text{AlO}_4$ ) are the basic structural component of zeolite networks , (b-)  $\text{TO}_4$  tetrahedral where  $\alpha$  is the O-T-O bond angle and  $\beta$  is the T-O-T bond angle (T= Si or Al) [69].

### 2.9.3 Applications of Zeolites

The properties of zeolite such as structural, availability and cost determine their industrial and agriculture use in many countries. The major industrial applications of zeolites can be summarized as follows:

- Treatment of nuclear effluents
- Wastewater treatment
- Use of zeolites in gas purification
- Zeolites as catalysts
- Adsorbent applications

### 2.9.4 Clinoptilolite

Clinoptilolite is a type of zeolite; it is the most widely distributed naturally in the world which has a Si /Al ratio above 4. This type of zeolite is commonly found in rocks enriched with potassium and sodium [70]. The formula for the chemical composition of clinoptilolite is  $(\text{Na}, \text{K})_6 (\text{Al}_6\text{Si}_{30}\text{O}_{72}) \cdot 20\text{H}_2\text{O}$ . The  $[\text{SiO}_4]^{-4}$  and  $[\text{AlO}_4]^{-5}$  are joined together via oxygen atoms in layers within the framework of the zeolite structure [71].

The figure (2-15-a) shows the two-dimensional channel system of clinoptilolite, while figure (2-15-b) shows the ten and eight-membered channels of clinoptilolite with their size.

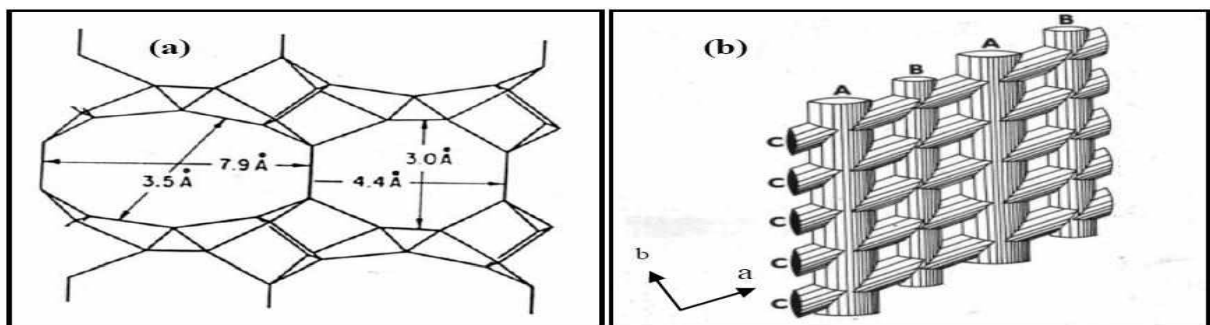


**Figure 2-15: a- two-dimensional channel system of clinoptilolite. b- ten and eight-membered channels of clinoptilolite with their size [72].**

### 2.9.5 Ion Exchange Properties of Clinoptilolite

Ion exchange process is a reversible chemical reaction where an ion from a solution is exchanged stoichiometrically for a similarly charged ion attached to a fixed solid particle. When a zeolite particles containing a mobile ion is placed in water containing a different ion of the same charge sign. In general, the cation exchange behavior of zeolites depends on [61]:

- ❖ The nature of cation species, the cation size, and cation charge
- ❖ The temperature
- ❖ The concentration of the cation species in the solution and the anion species associated with the cation in solution.
- ❖ The solvent.
- ❖ The structural characteristics of the zeolite which is under consideration.

The difference in the diameter of clinoptilolite pores, which range from 0.45 to 0.6 nm, cations are able to pass through and thus they do the ion exchange processes. Figure (2-16) shows pictures of natural clinoptilolite are presented according to cation type.

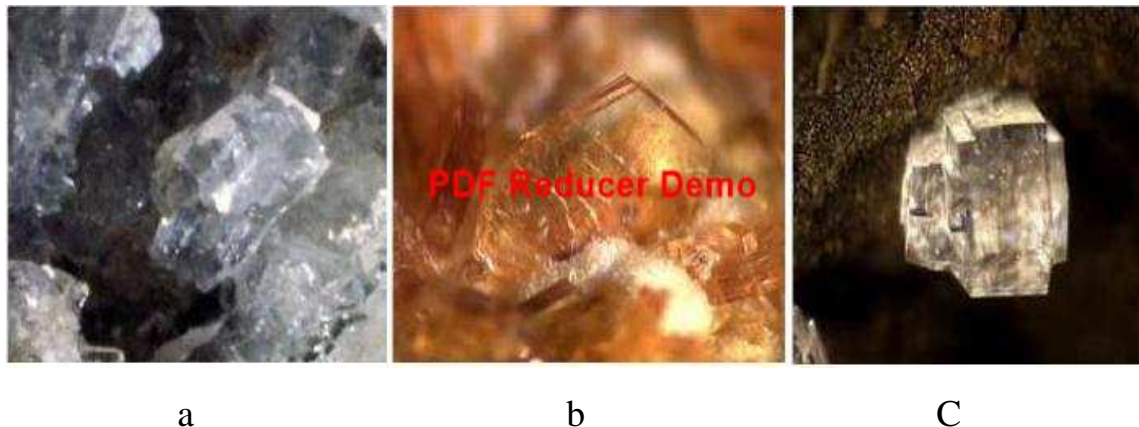


**Figure 2-16: Natural clinoptilolite [27]: (a) Clinoptilolite–K, (b) Clinoptilolite- Na, and (c) Clinoptilolite–Ca.**

The individual properties of natural clinoptilolite such as chemical stability in various caustic media, high rate of sorption equilibrium, and thermo-stability make it use in the environmental protection industry [73]. Due to these properties as well as the natural availability, clinoptilolite has been used in an extensive range of applications such as catalysis and ion-exchange, adsorption, solvent separation and removal, radioprotection, soil disinfection and biomedical applications. Extensive deposits of clinoptilolite are found in the Western United States, Russia, Bulgaria, Hungary, Yugoslavia and Japan [9]. Clinoptilolite (Turkish origin) was used in this study as a adsorbents material to remove  $^{137}\text{Cs}$  and  $^{90}\text{Sr}$  radionuclides.

# **CHAPTER THREE**

## **Experimental Technique**

---

## CHAPTER THREE

### Experimental Technique

#### 3.1 Introduction

In the present work, there are two parts of experiments, the first experiments is the measuring of radioactivity concentration of radionuclides for liquid samples which collected from the waste hall in the radiochemistry laboratories, by gamma spectroscopy technique for gamma-emitting radionuclides and by gross alpha beta gamma system for beta-emitting radionuclides.

The second part of experiment is the investigation of the ability of natural zeolite clinoptilolite to uptake the radionuclides in liquid samples.

The samples collection have been achieved with approval and aid of the Iraqi Decommissioning Directorate (IDD) and all the other experiments in this work have been done in Central Laboratories Directorate (CLD) at Ministry of Science and Technology (MoST) of Iraq.

#### 3.2 Description of Radioactive Liquid Waste System

The radioactive liquid waste system is the most important system in radiochemistry laboratories , which consists of six tanks, they located underground in the WH as shown in figure (3-1). The six liquid waste tanks are divided into three groups;

1. The first group includes three stainless steel tanks with a volume of  $5\text{m}^3$  for each one which were used to collect high-level liquid waste, another was used to collect the intermediate level waste and the third used as a spare storage tank. The three tanks were located inside a concrete closed pool with a concrete hatch, this pool called the high-



level liquid waste pool (HLLWP). The three tanks were filled with liquid waste, as well as, the pool was filled at (1.7) m height with liquid, the volume of this pool was (35.7) m<sup>3</sup> as shown in figure (3-2).

2. The second group included two stainless steel liquid waste tanks with a volume of 5m<sup>3</sup> for each one, the two tanks were located inside a concrete pool closed with a concrete hatch, the two tanks are empty, this pool called the organic liquid waste pool (OLWP), there are no liquid inside this pool just a sludge remain in it.
3. The third group included one stainless steel tanks with a volume of 10 m<sup>3</sup>, used for collecting low-level liquid waste, the tanks are located inside a concrete pool closed with a concrete hatch, this pool called the low-level liquid waste pool (LLLWP), the level of liquid in this pool was 1.65 m, therefore, the total volume of liquid in this pool is (19.8) m<sup>3</sup> [74].

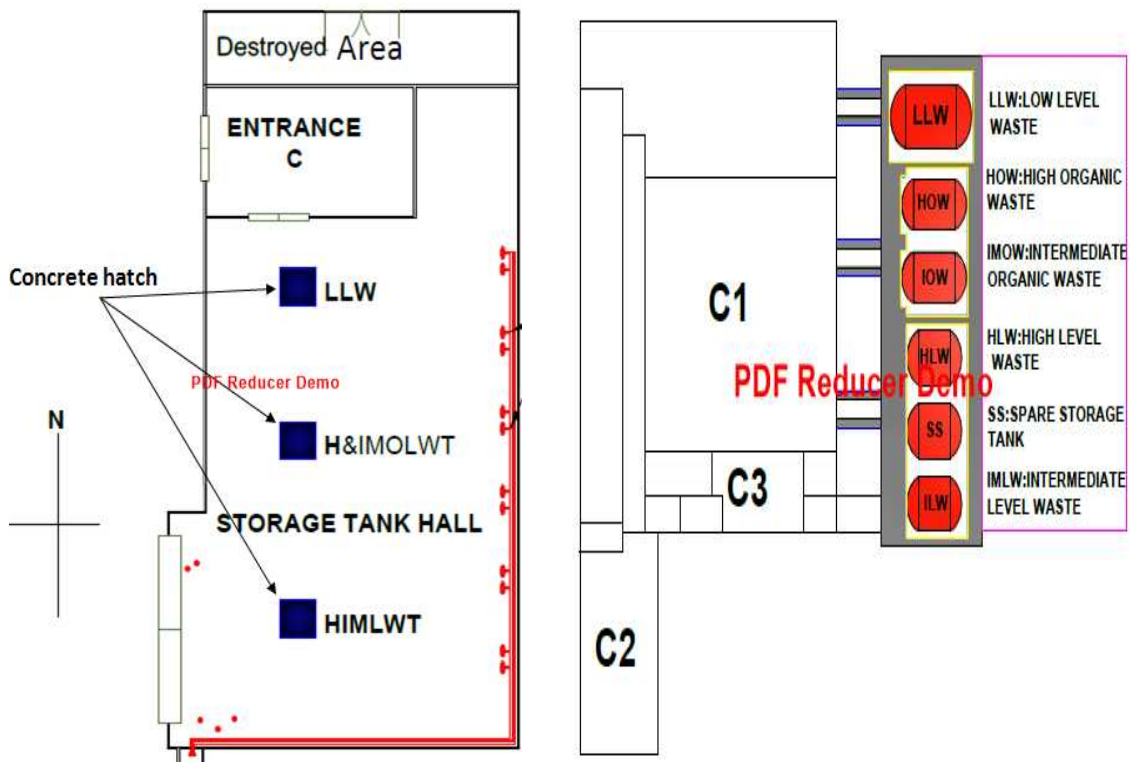


Figure 3-1: The scheme of waste hall (WH) in the RCL.



(a)



(b)



(c)



(d)

**Figure 3-2: a, b are the radioactive liquid waste hall, and c, d are the radioactive liquid waste pool and tanks.**

### 3.3 Radiological Characterization of Radioactive Liquid Waste Hall

Radiological characterization was done in and around the WH before the beginning of any activity in order to evaluate the radiological risk of this place.

#### 3.3.1 Dose Rate Measurement

LUDLUM 2241- 2RK is portable radiological survey device model 44-10 with sodium iodide (NaI) scintillation detector type. The crystal size is 2 inches diameter and 2 inches thick. It was used for measuring the

equivalent dose rate of gamma ( $\gamma$ ) rays in a unit ( $\mu\text{Sv/hr}$ ). Ludlum device is a digital instrument used for gamma rays investigation in the range of 60 keV- 2 MeV with a sensitivity of approximately 900 CPM per micro Roentgen per hour ( $\mu\text{R.hr}^{-1}$ ) for  $^{137}\text{Cs}$  isotope, as shown in figure (3-3).

The background of radiation was determined by measuring the dose rate level outside the Radiochemistry Laboratories (RCL) in open area and building to compare in-site buildings of similar construction, by walking at height (15 cm) and one meter above the ground level [75]. The radiation dose rate measurements carried out inside the WH, as presents in the table (3-1).

**Table 3-1: Dose rate Measurements inside and outside the WH.**

Point of measuring	Description of the measuring point	Dose rate $\mu\text{Sv.h}^{-1}$ at distance	
		0.15 m	1m
B.G-1	Background out Al-Tuwaitha site	0.065	0.062
B.G-2	Background inside liquid waste hall before opening the gates	0.082	0.098
B.G-3	Background out liquid waste hall	0.072	0.081
WH-I	The entrance of the liquid waste hall	0.156	0.145
WH-C	The center of the liquid waste hall	0.534	0.543
LLLWP	The entrance of low-level liquid waste pool after opening the gate	2.112	1.132
OLWP	The entrance organic waste pool after opening the gate	1.773	0.822
HLLWP	The entrance high-level waste pool after opening the gate	76	27



**Figure 3-3: The LUDLUM dose rate meter device.**

### **3.4 The Sampling**

Sampling is a process of collecting a part of an environmental medium as a representative of the wholly remaining medium. The samples should be collected and analyzed using the appropriate equipment and procedures analytical capabilities for the radionuclides of interest [76]. Analytical liquid samples need the laboratory procedures and significant requirements consist of several parts to counting preparation.

#### **3.4.1 Samples collection**

The sampling process from radioactive WH conducted after adjusting all radiation protection requirements such as radiation monitoring devices and personal dosimeter, preparing sampling tools such as (liquid pump 0.25hp, flex pipe, long meter and plastic containers with one liter capacity) and all necessary precaution equipment such as (working suits, mask, gloves, safety hat and safety shoes). Electric power was conducted for operating radiation monitoring devices, as well as light and air ventilation.

Three samples with volume one liter were collected from Low Level Liquid Waste Pool LLLWP from bottom, middle and surface of

liquid level of the pool. These samples were put in clean plastic container (one liter), and labeled with codes ( LLLW-P-S, LLLW-P-M and LLLW-P-B), the letters (S, M and B) refer to surface, middle and bottom respectively. One sample was taken from the tank by a liquid pump and coded as LLLW-T, where the letter T refers to tank.

Three samples with volume one liter were collected from High-Level Liquid Waste Pool HLLWP at the bottom, middle and surface of a liquid level of the pool. Samples labeled and coded as (HLLW-P-S, HLLW-P-M, and HLLW-P-B). One sample was taken from each tank by a liquid pump, samples coded as (HLLW-T- $\alpha$ , HLLW-T-SS, and HLLW-T-H) the letters (T- $\alpha$ , T-SS, and T-H) refer to alpha tank, spear storage tank and high tank respectively which are the real name of these tanks, as presented in table (3-2).

**Table 3-2: The location of samples in the waste hall.**

No.	Sample code	Location
1	LLLW-P-S	Low-level liquid waste from the surface of the pool
2	LLLW-P-M	Low-level liquid waste from the middle of the pool
3	LLLW-P-B	Low-level liquid waste from the bottom of the pool
4	LLLW-T	Low-level liquid waste from the tank
5	HLLW-P-S	High-level liquid waste from the surface of the pool
6	HLLW-P-M	High-level liquid waste from the middle of the pool
7	HLLW-P-B	High-level liquid waste from the bottom of the pool
8	HLLW-T- $\alpha$	High-level liquid waste from the $\alpha$ tank
9	HLLW-T-SS	High-level liquid waste from the SS tank
10	HLLW-T-H	High-level liquid waste from the H tank

Some important data were fixed on each sample such as the location of the sample, collecting date, volume, contact dose rate equivalent and above one meter of the sample as presented in table (3-3) and figure (3-4).

Table 3-3: Dose rate measurements of samples of the waste hall.

Sample code	Dose rate $\mu\text{Sv.h}^{-1}$ at distance	
	touch	1 m
LLLW-P-S	0.120	0.094
LLLW-P-M	0.108	0.085
LLLW-P-B	0.112	0.087
LLLW-T	0.435	0.144
HLLW-P-S	46	1.21
HLLW-P-M	45	1.112
HLLW-P-B	46	1.181
HLLW-T- $\alpha$	41	0.734
HLLW-T-SS	38	0.825
HLLW-T-H	28	1.08



(a)



(b)



(c)



(d)

Figure 3-4: a, b samples collecting from WH and c, d samples preservation.

**3.4.2 Preparing Samples**

The preparation of samples was divided into three parts; the first was for gamma spectroscopy system measurements, the second was for gross alpha beta gamma system measurements and the third part was preparation liquid samples for treatment, as illustrated below in details. Figure (3-5) shows some of devices and tools which were used in this study.

**3.4.3 Samples Preparing Tools, materials and Equipment**

1. Distilled water
2. Filter papers type Whatman with diameter ( $\phi$ ) 125mm
3. pH meter
4. Sensitive digital scale
5. Plastic wrap
6. Holders of sample
7. Stainless steel counting planchets
8. Burn oven with a wide range of temperature degree (MUFFLE FURNACE)
9. Hot plate
10. Drying Oven
11. Glass Beakers
12. Micro and disposable pipettes
13. Graduated cylinders (10,20) mL

**3.4.4 Preparing Samples for Gamma Analyzing**

The liquid samples of the low-level liquid waste pool (LLLW) were filtered by filter papers type (Whatman, 125mm  $\phi$ ) and putting in a suitable container that belongs to gamma spectroscopy system called Marinelli beaker with 500 mL volume. The four LLLW samples (LLLW-P-S, LLLW-P-M, LLLW-P-B and LLLW-P-T) were prepared without

dilution and put in Marinelli beaker then closed by a secured tape (Poly Tetrafluoroethene) and labeled to be ready for measurements.

The Liquid samples of the high-level liquid waste pool (HLLWP) were filtered. The sample HLLW-P-B was diluted to four samples as a test for gamma spectroscopy system to achieve the best dead time, therefore (1,2,5,10)mL from HLLW-P-B- sample were diluted with distilled water to fill Marinelli beakers with 500 mL volume, with different dilution percent, (0.2, 0.4, 1, 2)% respectively for the four diluted samples. All others HLLW samples diluted at 0.2% percent by adding 1 mL from initial samples to 499 mL distilled water to fill the Marinelli beaker by using a graduated beaker and digital scale. The six HLLW samples (HLLW-P-S, HLLW-P-M, HLLW-P-B, HLLW-T- $\alpha$ , HLLW-T-SS, and HLLW-T-H) were prepared at dilution percent 0.2% and put in Marinelli beaker then closed by the secured tape and labeled to be ready for measurements [77]. The HLLW-P-M sample coded as C-sample because it was depended on next experiments.

### **3.4.5 Preparing Samples for Gross Alpha Beta Gamma Counting**

One samples from each pool (HLLWP and LLLWP) which were measured by the gamma spectroscopy system were measured by gross alpha beta gamma system (HLLW-P-M and LLLW-P-M) by deposit a specific volume from these prepared liquid samples on stainless steel counting planchets 5.1 cm (2in.) sample tray diameter [78, 79].

The HLLW-P-M sample of the high-level liquid waste pool was chosen to represent this pool and named C-sample with dilution percent 0.2%. Ten samples were prepared from sample-C by depositing (1-10)mL on stainless steel counting planchets at temperature 100°C for one hour by a hot plate which already put in a fume hood. These samples were



coded as (C-1,C-2,C-3,C-4,C-5,C-6,C-7,C-8,C-9 and C-10) by depending on their deposit liquid volume. These samples were heated to 300 °C for one hour by burn oven with a wide range of temperature degree (MUFFLE FURNACE), and measured by gross alpha beta gamma system by putting these samples in carriers belong to the system. The samples (C-2, C-4, C-7 and C-10) were heated at temperature 500 °C and 700 °C and were measured in each step.

The sample (LLLW-M) of the low-level liquid waste pool was chosen to represent this pool and called sample-L without dilution. Three samples were prepared from LLLW-M sample by depositing (2, 4 and 7)mL on stainless steel counting planchets at temperature 100 °C for one hour by the hot plate, these samples coded as (L-2, L-4, L-7). The samples were heated at temperature (300,500 and 700) °C for one hour by the FURNACE oven and were measured in each step by gross alpha beta gamma system.

### **3.4.6 Preparing Samples for Treatment**

The samples were prepared for treatment and for calculating the removal efficiency of gamma emitters radionuclides for the high-level liquid waste pool (HLLWP). The liquid sample HLLW-P-M (sample-C), which belongs to HLLWP was depended in this work without dilution. Initially, the potential of Hydrogen pH and laboratory temperature of sample were determined.

Five samples with (15 mL) of each sample were taken from sample-C, they filtered by filter papers and put in in 20-ml vials a suitable container with secured cap. Five amount of natural clinoptilolite zeolite were prepared by a sensitive four digit scale at (0.025, 0.05, 0.075, 0.1 and 0.15)g, and added to the prepared liquid samples (15mL). The

samples were coded as (C-A1, C-A2, C-A3, C-A4 and C-A5), (the letter A refers to words; after treatment). A 10 mL was taken from C-sample (C-ST) to be the sixth sample as a standard (initial sample without treatment) to compare it with the five treated samples. The five samples were subjected to shaking at two hours (time contact between the contaminated liquid and zeolite material) by a roller shaker at about 2 Hz (round per second) and temperature 22 °C (laboratory temperature). This time is considered sufficient for the establishment of sorption equilibrium [9]. The solids (the zeolite which dissolved into solution) were then separated from the liquid by filtration through filter paper. A 10 mL was taken from each sample as a treated sample and measured by gamma spectroscopy system along 1000 s by putting each sample directly on the detector.

The preparing samples for treatment or decontamination of beta emitters radionuclides was carried out by using the previous six liquid samples after measuring them by gamma spectroscopy system. They were diluted at percent 0.2% with distilled water. A 7 mL of each sample was deposited on the counting planchets (2in.) by the hot plate at 100 °C for one hour. The six deposit samples heated at (300,500 and 700) °C by burn oven for one hour and measured in each step by gross alpha beta gamma system. The equipment which was used for preparation of samples for radiological measurements and for treatment are shown in figure (3-5).

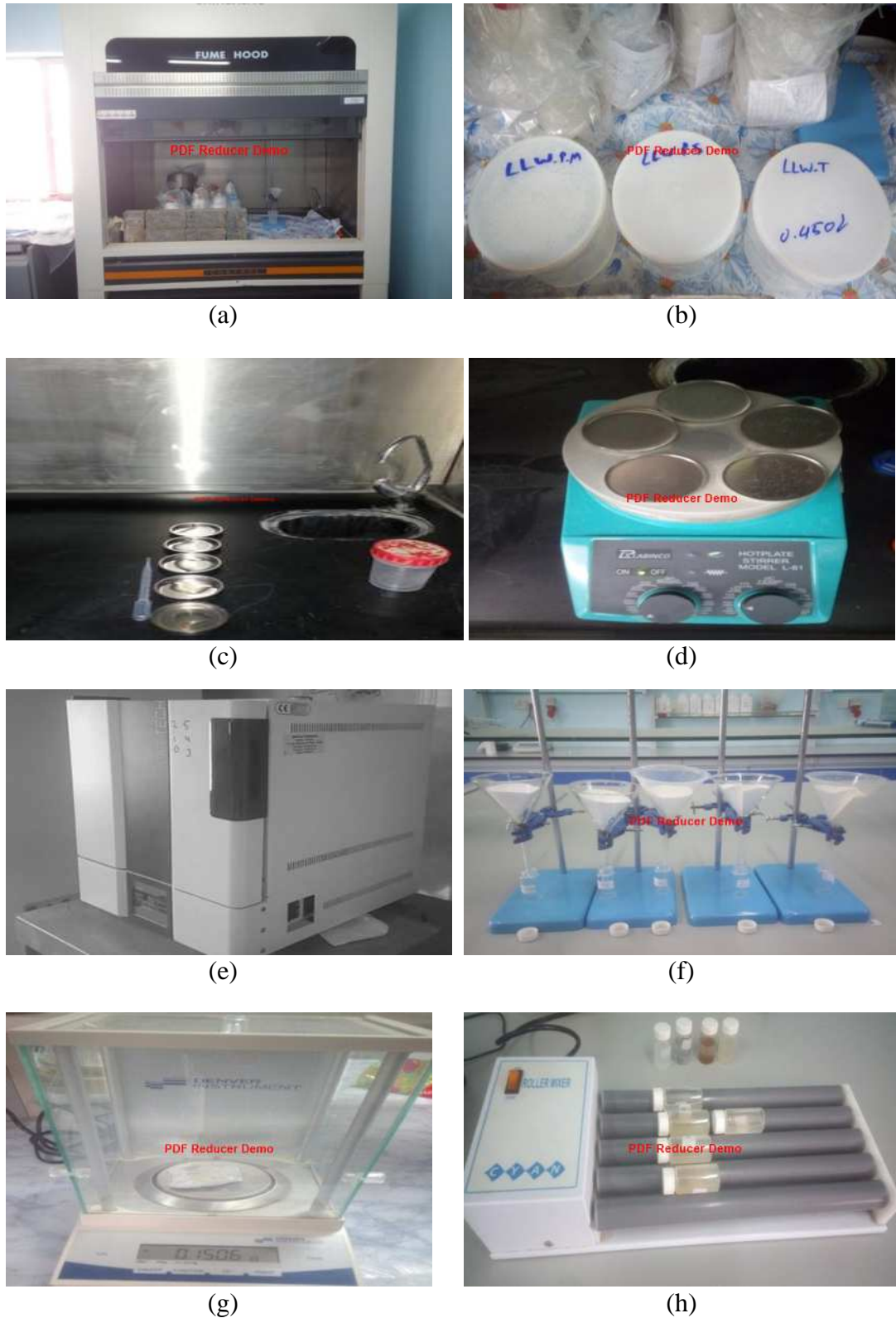


**Figure 3-5: a- The fume hood, b- The prepared samples, c- 2 in. planchets, d- The hot plate, e- The burn oven MUFFLE FURNACE, f- samples preparation for treatment, g- The sensitive scale with zeolite and h-The shaker.**

**3.4.7 Preparing Samples for Acidity Solution Run-1 Test**

The samples were prepared for treatment and calculation the removal efficiency for the gamma-ray emitters radionuclides to HLLWP with different pH of the solution. Four samples (20 mL) for each sample were taken from sample-C, they were filtered and the pH of sample-C was determined by pH meter. The four samples were modified at a pH (3, 6, 9, 12) by adding a strong acid type nitric acid ( $\text{HNO}_3$ ) to the first and second samples and adding a strong base type sodium hydroxide ( $\text{NaOH}$ ) to the last two samples. Four equal amount of natural clinoptilolite zeolite (0.2g) added to these samples (20 mL), The samples were coded as (CA-pH(3), CA-pH(6), CA-pH(9) and CA-pH(12)). The four samples were shaken at two hours by roller shaker. The four samples were filtered and 10 mL was taken from each sample as a treated sample and measured by gamma spectroscopy system for 1000 s by putting each sample on the detector directly.

The preparing samples for treatment of beta emitters radionuclides for HLLWP was carried out by using the previous four liquid samples (CA-pH(3), CA-pH(6), CA-pH(9) and CA-pH(12)) which were used in gamma spectroscopy system measurements. The samples were diluted at percent 0.2% with distilled water. A 7 mL of each sample was deposited on counting planchet by hot plate at 100 °C for one hour. Samples were coded as (CA-pH(3), CA-pH(6), CA-pH(9) and CA-pH(12)) and measured by gross alpha beta gamma system. This represents run-1 for liquid decontamination.

**3.4.8 Preparing Samples Run-2 Test to Improving Removal Efficiency**

The samples were prepared for treatment to calculate the removal efficiency for gamma emitters radionuclides to HLLWP with different pH

of the solution. A 0.15g of natural clinoptilolite zeolite were added to the treated previous four samples from run-1 test with volume 15 mL for each sample. The samples were coded as (CA2-pH(3), CA2-pH(6), CA2-pH(9) and CA2-pH(12)). The four samples were subjected for shaking at two hours, then the four samples were filtered and 10 mL were taken from each sample as a treated sample (run-2 test) and measured by gamma spectroscopy system for 1000 s by putting each sample directly on the detector.

The preparing samples of beta emitters radionuclides for HLLWP were carried out by taking two samples (CA2-pH(6) and CA2-pH(9)) which were used in the previous gamma spectroscopy measurements experiment and diluted at percent 0.2% with distilled water. A 7 mL from each sample was deposited on counting planchets (2in.) by the hot plate at 100 °C for one hour and measured by gross alpha beta gamma system, this represents run-2 for the liquid decontamination.

### **3.5 Gamma-ray Spectroscopy System**

Gamma-ray spectrometry system was used in this study to determine the activity concentration of radionuclides by depending on the analysis of the energies and the peaks areas of the full-energy peaks of gamma lines. These techniques non-destructive and allow the identification and the quantification of the radionuclides concentration in the sample [80]. Figure (3-6) shows the gamma-ray spectroscopy system which was used in the current study. The system manufactured by ORTEC company, it consists of the following component [82]:

#### **a- High Purity Germanium (HPGe) Detector**

The high purity germanium detector HPGe model GEM65P4-95, coaxial p-type which was manufactured by ORTEC company with the

relative efficiency 65% and the resolution  $\leq 1.9$  keV was used in this study. The full width at half maximum (FWHM) is 1.95keV at energy line of 1.33 MeV of  $^{60}\text{Co}$  and 1keV at energy line of 122 keV of  $^{57}\text{Co}$ , the operation positive voltage is 1500 volts. The crystal of HPGe detector dimension is (71.9, 73.1) mm diameter and length respectively. It is surrounded by lead shielded with a 10cm thickness to reduce the radiation background. A graded shield consists of layers of cadmium (Cd) and copper (Cu), the copper layer is directly viewed of the detector in order to absorb the characteristic X-rays from lead (Pb) shield and to reduce their peaks in the background spectrum. The HPGe detector is cooled at 77 K (-196 °C) by using liquid nitrogen to reduce the leakage current, as shown in figure (3-7).

**b- High voltage supply**

The high voltage power supply provided the detector with the voltage required to operate. The required high voltage for the detector that was used is a positive 1500 volts.

**c- Preamplifier**

The preamplifier model (A257P) was used to collect and integrate the charge from the detector and produce an output voltage pulse and to reduce the noise. It is located nearest point to the detector [81].

**d- Main amplifier**

The main amplifier role is amplifying and shaping the pulses which produces from preamplifier 1000 times or more and converting the output signals of the preamplifier into a suitable form to the desired measurements. The amplifier is a linear increasing where the pulse height is a proportion to the absorbed energy [81].

**e- Multi-channels analyzer**

The multichannel analyzer (MCA) function is recording and storing electric pulses according to their height. Each storage unit is called a channel, the height of the pulse has some known relationship usually proportional to the energy of the photon that enters into the detector. Each pulse stores in a particular channel corresponding to the certain energy. The pulses distribution in the channels is spectral of the distributed energies of the particles [81]. At the end of a counting period, the spectrum which was recorded displayed on a screen. The multi-channel analyzer used in this study has 8000 channels.



**Figure 3-6: Gamma-ray spectroscopy system which used in the current study.**

All main amplifier, the multichannel analyzer (MCA) and high voltage power supply are compacted in one device called digital signal processing (DSP) as shown in figure (3-8).



Figure 3-7: The HPGe detector



Figure 3-8: The multichannel analyzer

### 3.5.1 The software

The personal computer used to display the measurement spectra and to treat the information which is provided by the multi-channel analyzer. The analysis of gamma-ray spectra was performed using Gamma Vision-32 software version-6 from ORTEC Company. GammaVision-32 integrates acquisition control, "Smart" MCA and quantitative analysis functions for use in conjunction with PC-based gamma spectroscopy workstations [82].

### 3.5.2 Dead Time Mode

The collection time (real time) of the achievement to correct for input pulse train losses incurred during achievement due to system dead time. This corrected time value known as the live time is then used to determine the net peak count rates necessary to determine nuclide activities. The total real time will be [83]:

$$Real\ Time = \left\{ \frac{Live\ time\ x\ 100\%}{100\ \% - Dead\ Time\ \%} \right\} \quad (3 - 1)$$

### 3.5.3 Calibration

Gamma spectroscopy system must calibrate both in terms of energy and efficiency, in order to obtain reliable results such as radionuclide identification, qualitative and quantitative analysis.



### 3.5.3.1 Energy calibration

The energy calibration is the determination of the energy position of the incident photon for each channel [84]. The energy calibration was conducted to appear the relationship between the channel numbers and photon energy, the multi-peak of the standard source (multi-nuclide radioactive emitting gamma) was used. The multi-nuclides radioactive with different energy type (CBS 2S) has certification No. 9031-OL-506/13 was used for energy calibration with volume 500 mL (Marinelli beaker). It was with the same geometry as that used to measure the liquid samples. Table (3-4) shows the multi-nuclides radioactive standard source which used for the energy calibration. The standard source put in the system for 3600 seconds. The channel number and associated peaks were recorded and the graph between them was plotted. Figure (3-9) shows the spectrum of the gamma ray of standard mixed radionuclides calibration source, while, figure (3-10) shows the relationship between gamma energy and channel numbers.

**Table 3-4: The mixture of radioactive source data and the detection efficiency for each radionuclide.**

Nuclide	Channel number	Energy (keV)	Net area (CPS/h)	Activity (Bq)	FWHM (keV)	Efficiency %
<sup>241</sup> Am	162.2	59.54	123445	3953.3	1.99	2.0903
<sup>109</sup> Cd	240.19	88.03	38082	4663.2	1.35	7.561
<sup>57</sup> Co	372.48	136.06	3620	129.08	2.02	7.895
<sup>165</sup> Ce	453.75	165.85	4918	21.98	1.27	8.131
<sup>113</sup> Sn	1070.51	391.69	4817	41.04	1.94	5.02
<sup>137</sup> Cs	1808.89	661.66	204519	2162.9	1.62	2.962
<sup>60</sup> Co	3206.73	1173.24	126997	1794.5	2.04	1.906
	3642.14	1332.5	116137	1771.2	2.39	1.814
<sup>88</sup> Y	5017.82	1836.01	2031	36.44	2.55	1.582

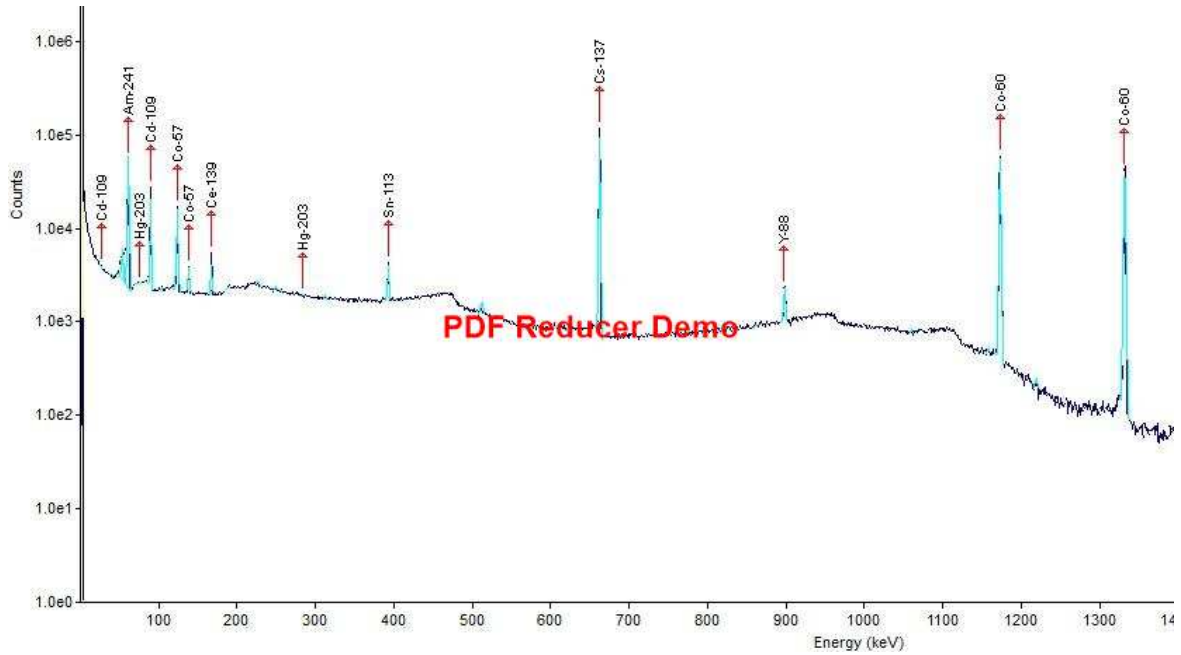


**Figure 3-9: Gamma-ray spectrum of mixed radionuclides which used as a calibration source.**

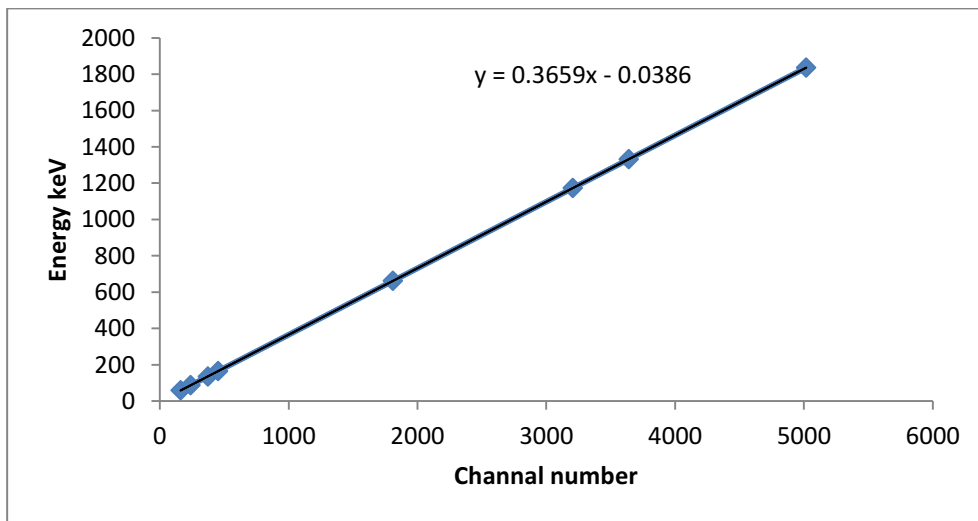


**Figure 3-10: The relationship between gamma energy and channel numbers.**

From figure (3-10), it is noticed the linear relationship between the channel number and gamma-ray energies which mathematically represented by the following equation:

$$Energy (keV) = 0.3659 \times Channel\ number - 0.0386 \quad (3 - 2)$$

Where: 0.3659 and -0.0386 are fitting coefficients respectively.

### 3.5.3.2 Efficiency calibration

The same standard source of multi-gamma energy which used in energy calibration used also in efficiency calibration HPGe detector. In order to achieve efficiency calibration, the type of samples must be taken into account. The density of standard source ( $0.985 \pm 0.01$ )  $\text{g.cm}^{-3}$  is approximately equal to the liquid density which used in this study. The efficiency calibration allows establishing the detection efficiency of the detector as a function of the gamma photons energy, as well as finding the efficiency for energies of gamma rays which are not found in the standard source which has been used [85]. Figure (3-11) shows the detection efficiency curve of HPGe detector. The efficiency of the detector is the relation between the numbers of gamma rays emitted from the source to the number of gamma rays collected in the full-energy peak. The efficiency for all energies of isotopes can be calculated from the following equation [86]:

$$\varepsilon_{E_\gamma} = \frac{N_{net}}{t_c \times A_t \times I_\gamma} \times 100\% \quad 3 - 3$$

$$N_{net} = N_S - N_B \quad (3 - 4)$$

where:

$\varepsilon_{E_\gamma}$ : The detection efficiency of gamma emitters radionuclides.

$N_{net}$ : The net peak area under the specific peak at gamma energy (counts).

$N_S$ : The peak area in the sample spectrum.

$N_B$ : The corresponding peak area in the background spectrum.

$t_c$ : The counting time of measurement (sec)

$A_t$ : The corrected activity in (Bq) of the standard source at the measuring time.

$I_\gamma$ : The abundance (dimensionless) of specific gamma energy  $E_\gamma$ .

Table (3-4) presents the mixture radioactive source data and the detection efficiency of HPGe detector for each radionuclide in this source which used in this study.

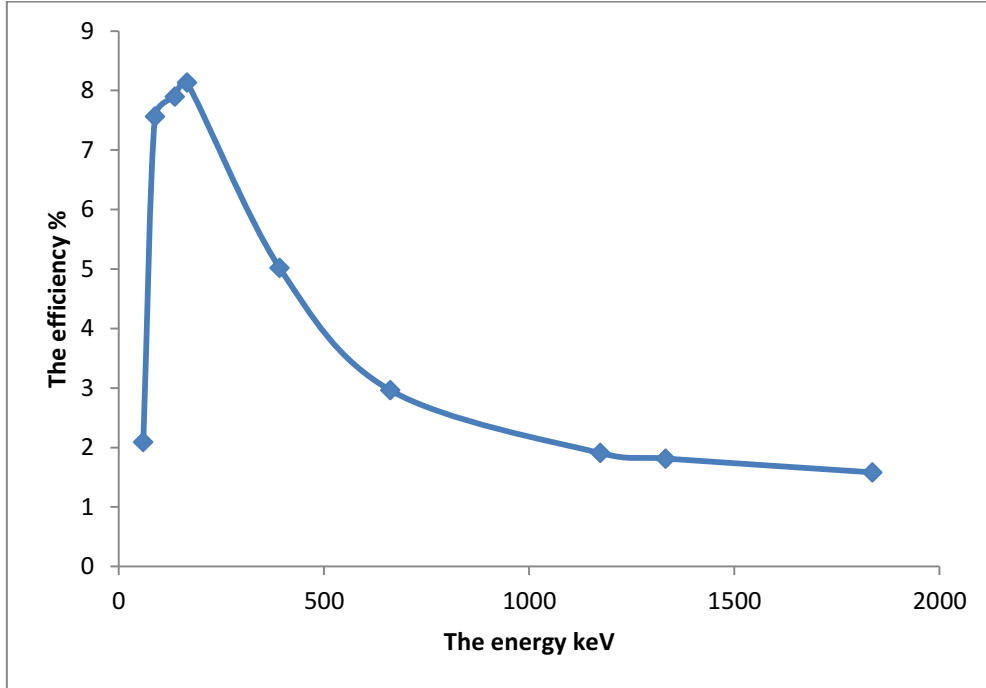


**Figure 3-11: The efficiency calibration curve.**

### 3.5.4 Interpolative Fit

A straight line between the data points between two points uses to obtain the efficiency at any energy in interpolative fit. The efficiency/energy formula is [86]:

$$\varepsilon(E) = \frac{\varepsilon_1 + (\varepsilon_2 - \varepsilon_1) * (E - E_1)}{(E_2 - E_1)} \quad (3 - 5)$$

Where :  $\varepsilon(E)$  : Efficiency at energy  $E$ ,  $E$ : The target energy to determine the efficiency,  $\varepsilon_1$ : The efficiency at energy  $E_1$ ,  $E_1$  : The energy point below the target energy,  $\varepsilon_2$ : The efficiency at energy  $E_2$  , and  $E_2$  : The energy point above the target energy.

### 3.5.5 Energy Resolution

The germanium detector has an excellent energy resolution for gamma-ray spectroscopy. The energy resolution of a gamma-ray detector is the measurement of the possible variation in the size of the electrical pulses resulting from the complete absorption of a gamma ray of the same energy. A small value of a calculated resolution (R), as in equation below means the high energy resolution which means that the detector can distinguish between gamma-rays with closely energies [87]. The resolution of a detector calculates as [88]:

$$R = \text{FWHM} \times \left( \frac{\Delta E}{\Delta \text{ch}} \right) \quad (3 - 6)$$

Where: R: Energy resolution (keV), FWHM: Full width at half maximum (ch),  $\Delta E$ : Difference between two-separated gamma lines (keV) and  $\Delta \text{ch}$ : Difference between the photo-peaks of the two gamma lines (ch).

### 3.5.6 Determination of Detection Limits and Minimum Detection activity

Detection limit expresses on the detection capability of a measuring system under certain conditions. It varies according to the instrumentation and analytical techniques that used, and it is estimated for the lowest amount of activity of a specific gamma-emitting radionuclide that can be detected at the time of measurement. The detection limit concept was established by Currie in 1968 [89]. The detection limit by Currie method can be given by the following equation:

$$L_D = 2.706 + 4.653 \cdot \sigma_{Nb} \quad (3 - 7)$$

Where:

$L_D$ : The detection limit.

$\sigma_{Nb}$ : The standard deviation of the counts number where the blank sample is measured to determine the background level.

The Minimum Detectable Activity (MDA) is a measure of smaller an activity could be presented and not be detected by the analysis. There are many factors affecting the MDA such as; the calibration geometry, the background, the detector resolution and the particular nuclide. The MDA can be calculated using detection limit ( $L_D$ ) and some factors [90] as:

$$MDA = \frac{L_D}{\varepsilon_{E_\gamma} \times I_\gamma \times t_c} \quad (3 - 8)$$

Where;  $\varepsilon_{E_\gamma}$  is the detection efficiency,  $t_c$  is the counting time of measurement (sec), and  $I_\gamma$  is the abundance of specific gamma energy  $E_\gamma$ . Table (3-5) shows the values of MDA for some isotopes in the liquid samples, which were measured in gamma-ray spectrometry.

**Table 3-5:** The values of MDA of isotopes in the liquid samples have been obtained from the measurements system.

Sample code	Nuclide	Energy (keV)	MDA (Bq.L <sup>-1</sup> )
HLLW-P-B	Cs-137	661.66	1.603
	K-40	1460.83	0.6
HLLW-P-S	Cs-137	661.66	1.317
	K-40	1460.83	0.601
HLW-P-M (c)	Cs-137	661.66	1.45
	K-40	1460.83	0.6015
LLLW-P-S	Cs-137	661.66	0.597
	K-40	1460.83	0.6015
	Bi-214	609.32	0.586
LLLW-P-M	Cs-137	661.66	1.037
	K-40	1460.83	0.763
	Bi-214	609.32	0.582

### 3.5.7 Calculation of Radioactivity Concentration

The radioactivity concentration of each liquid sample were measured by placing the Marinelli beaker which contained the prepared liquid sample in the gamma-ray spectroscopy system for 3600 seconds. The gamma-ray spectrum of the sample were obtained via Gamma Vision software. Gamma Vision performed result report includes many information such as real-time, live time, dead time, radionuclides activity concentration of each energy, MDA, and etc. The radioactivity concentration of radionuclide in the sample can be calculated using the following equation [91]:

$$A(Bq/L) = \frac{N_{net}}{t_c \times I_\gamma \times \varepsilon_{E_\gamma} \times V} \quad (3 - 9)$$

Where:

$A(Bq/L)$ : The radioactivity concentration of radionuclide at energy E.

$N_{net}$ : The net peak area under the specific peak at gamma energy (counts).

$\varepsilon_{E_\gamma}$ : The counting efficiency of the specific radionuclide's energy.

$I_\gamma$ : The transition probability by gamma decay of the energy ( $E_\gamma$ ) or the abundance of specific gamma energy  $E_\gamma$ .

$t_c$ : The counting live-time of the sample spectrum collection in seconds.

$V$ : volume of measured sample (Liter).

### 3.6 Gross Alpha Beta Gamma System

The gross alpha, beta, gamma system enhanced low background capability was used in this study. The system was manufactured by Canberra Company. This system consists of two detectors; the first is the proportional gas-flow type for detection of alpha and beta rays, while the second detector is sodium iodide scintillation type for detecting gamma

rays, as shown in figure (3-12). The gross alpha beta gamma system was connected with computer provided with Eclipse LB software program to manage and display the output results with custom reports. This program presents all the information which needed to operate the system and analyze the data.

This system displays total or gross alpha beta and gamma count per minute (CPM), gross activity (Bq, Ci and  $\mu\text{Ci}$ ), activity concentration ( $\text{Bq.g}^{-1}$ ,  $\text{Bq.L}^{-1}$ ) or disintegration per minute (DPM) without determining the type of radionuclide. This system displays count rate of a sample about 500000 CPM with ( $\leq 1.5\%$ ) dead time loss with counting time adjustable as between 0.2 and 9999 minutes and the sample changer capacity standard – 50 samples and optional – 100 samples with identification external coded positive sample carrier or sample changer based bar code reader. This system consists of the following component:

a- Detectors

The alpha and beta detector is a 2.25 inches diameter pancake style gas-flow proportional detector with P-10 gas. The detector features twin anodes for uniformity counting and an ultra-thin entrance window  $80 \mu\text{g/cm}^2$ . The gamma ray detector in this system is sodium iodide (NaI) scintillation detector type, the crystal size is (2x2) inches. The individual lead shield components have a maximum weight of 60 pounds, and it surrounds the counting detectors.

b- Preamplifier

The system includes individual charge-sensitive preamplifiers. The preamplifiers distribute the high voltage bias to the detectors.



## c- Amplifier

The system amplifier board contains separate amplification /shaping/ discrimination sections for the guard and sample channel information.

## d- Power Supply

The system requires connection to the AC mains power for operation.



a

b

**Figure 3-12:** The gross alpha beta gamma system.

### 3.6.1 Gas Regulation and Control

The proportional gas-flow detector P-10 (10% Methane in Argon), the compressed gas system is supplied from a high pressure (about 3000 psi) gas cylinder. A regulator is fixed to the cylinder and regulates the gas pressure delivered to the system at 10 psi.

### 3.6.2 Determining Operating Voltages

The alpha and beta simultaneous mode of operation voltage was selected from Eclipse LB program. In order to determine these voltages, alpha and beta plateaus were generated. The alpha plateau determines the operating voltage at which the detector is sensitive only to alpha. The

beta plateau determines the operating voltage at which alphas and beta are detected and separated based on pulse height.  $^{241}\text{Am}$  and  $^{90}\text{Sr}$  standard sources were used for alpha and beta emitting in this study. Both of these two operating voltages are required for this mode of operation [92]. Therefore, the operation voltage was selected based on the beta plateau voltage, it was 1410 volt, as shown in figures (3-13 and 3-14).

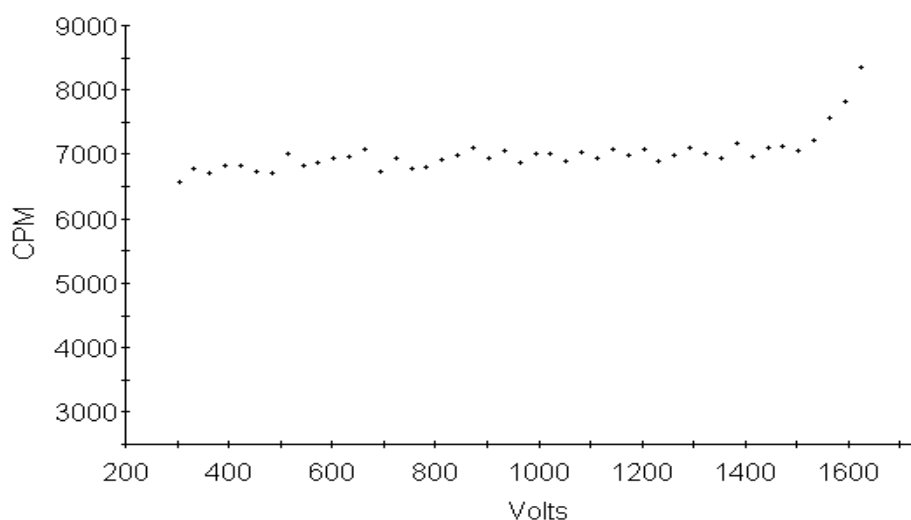


**Figure 3-13: Alpha plateau graph**

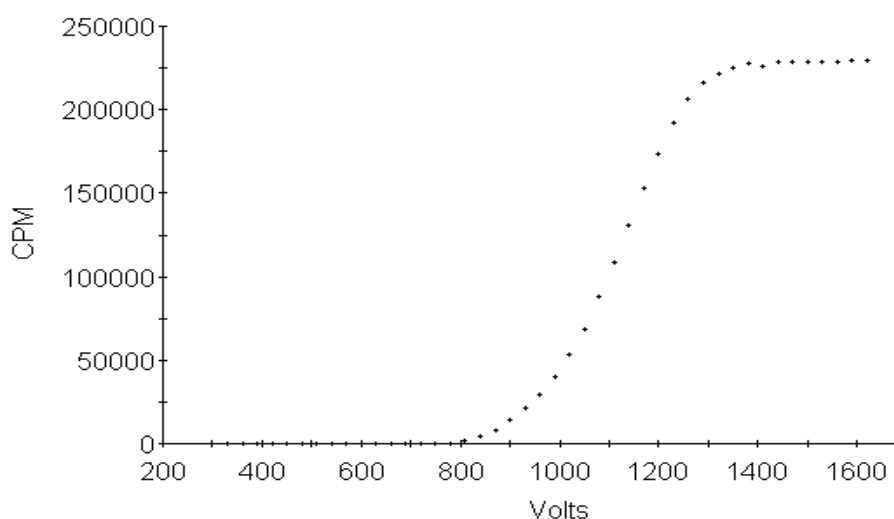


**Figure 3-14: Beta plateau graph.**

### 3.6.3 Beta Counting

For beta and alpha particles of typical energies, a differential pulse height spectrum as illustrates in the left portion of figure (3-15) [93]. The counting curve shows two plateaus; the first presents only alpha particles were counted, and the second shows both alpha and beta particles were counted. Because the beta particle pulse height distribution is wider and less well separated from the low-amplitude noise, the beta plateau is generally shorter and shows a greater slope than the alpha plateau [45].

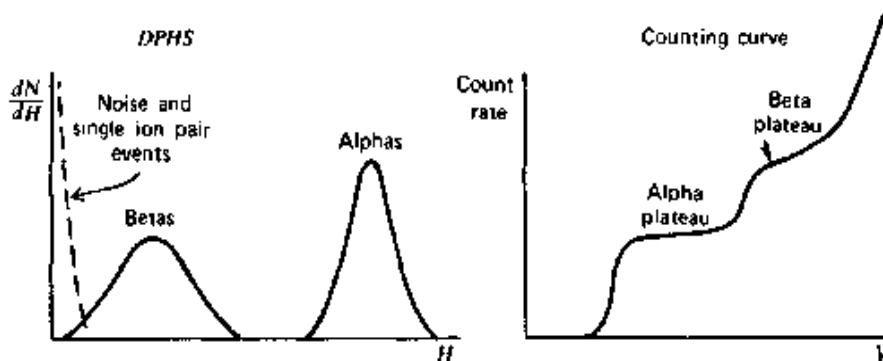


**Figure 3-15: Changing the Operating Voltage**

### 3.6.4 Efficiency Calibration

The same sources were used to generate the alpha and beta plateaus used for the efficiency calibration. In order to report the results of samples that have been counted in units of activity, alpha and beta efficiencies must be determined. These efficiencies must be determined under the same conditions as the samples that will be measure.

For gross alpha and gross beta measurement, the detector was calibrated to obtain the ratio of count rate to disintegration rate.  $^{90}\text{Sr}$  and  $^{137}\text{Cs}$  have both been used as standard sources for gross beta emitting activity. The efficiency counting for the beta can be calculated from the following equation [93]:

$$\epsilon_{E\beta} = \frac{C_{net} \text{ (cpm)}}{A(dpm) \cdot I_{\beta}} \times 100\% \quad (3 - 10)$$

$\epsilon_{E\beta}$ : The counting efficiency of beta particles radionuclides.

$C_{net}$ : The measured net count rate (CPM of sample minus CPM of background).

A: The activity of the standard source.

$I_{\beta}$ : The transition probability by beta decay, it is equal to 1 for  $^{90}\text{Sr}$  ( $E_{\beta\text{max}} = 2.28 \text{ MeV}$ ) and 0.95 for  $^{137}\text{Cs}$  ( $E_{\beta\text{max}} = 0.514 \text{ MeV}$ ).

The calibration for beta particle measurements can be accomplished for the beta plus alpha plateau counting. Table (3-6) display the counting efficiency of beta for  $^{90}\text{Sr}$  and  $^{137}\text{Cs}$ . The total activity of  $^{90}\text{Sr}$  standard sources which was used at the experiment time (3145 Bq) and (387.47kBq) for  $^{137}\text{Cs}$ .

**Table 3-6: The counting efficiency of beta for  $^{90}\text{Sr}$  and  $^{137}\text{Cs}$ .**

Radionuclide source	Beta CPM	Source decay corrected (DPM)	Beta efficiency %
$^{90}\text{Sr}$	44520	116020.55	38.372
	44139	116020.54	38.044
	44668	116020.59	38.500
	44458	116020.58	38.319
The average efficiency of $^{90}\text{Sr}$			38.40
$^{137}\text{Cs}$	3054182	23239456.69	13.142
	3050087	23239454.38	13.124
	3049980	23239452.07	13.124
	3050842	23239449.74	13.127
The average efficiency of $^{137}\text{Cs}$			13.11

### 3.6.5 Gross Beta Radioactivity

The gross beta radioactivity calculations were done in order to convert the counts per minute (CPM) into disintegration per minute (DPM) by depending on beta detector efficiency and finally into units of activity per sample weight or volume ( Bq Kg<sup>-1</sup> or Bq L<sup>-1</sup>). A blank planchet was used as a background count, the dry residue of liquid samples count refers to gross beta radioactivity, as the equation below [81]:

$$A_{\beta}(Bq. L^{-1}) = \frac{C_{net}(cpm) \times 1000}{\varepsilon_{E_{\beta}} \times V \times 60} \quad (3 - 11)$$

Where:  $A$  is the beta radioactivity concentration.

$C_{net}$ : The net beta count rate.

$\varepsilon_{E_{\beta}}$ : The beta efficiency.

$V$ : volume of sample (mL).

### 3.7 The X-Ray Fluorescent (XRF)

X-rays fluorescence technology was used to measure the concentrations of elements, XRF is one of the most important techniques for the analysis of metals and trace elements which is independent to the chemical form of the elements, it is undistracted technique [94].

In this work, the used X-ray tube which manufactured by Spectro Xepos Company, with a detector silicone-lithium, as shown in figure (3-16). It is connecting with the computer via XLab-pro program. The X-ray tube energy has resolution 45eV in 5.9Kev of iron (Fe-55) isotope. The analysis works out using the comparative method with standard sources. Several targets were used to generate different X-ray energy. The targets

are highly oriented pyrolytic graphite (HOPG), alumina ( $\text{Al}_2\text{O}_3$ ) and Molybdenum.

### 3.7.1 Zeolite Sample Preparing for Analyzing

An amount of clinoptilolite natural zeolite was crushed into a fine powder, then drying in an oven at (100-120)°C for 6 h. sample mixed carefully with a binder (PVC) and pressed by the hydraulic press into 5 Ton/cm<sup>2</sup> in diameter 32 mm (pellet) [94], sample coded as Z- sample. The pellet was loaded into the sample chamber for measurement.

### 3.7.2 Liquid Sample Preparing for Analyzing

Two liquid samples were prepared; the first one (15 mL) from the liquid sample (HLLW-B) without dilution, was deposited on filter paper [95], this sample coded as F-sample. The second sample was prepared by depositing 15 mL from distilled water on filter paper as a background sample, it coded F-BG-sample, the two samples were dried by the drying oven at (100-120)°C for 6 h, as shown in figure (3-16).



(a)



(b)



(c)

**Figure 3-16:** a- XRF system, b- zeolite sample and c- filter paper sample.

# **CHAPTER FOUR**

## **RESULTS, DISCUSSION, AND CONCLUSIONS**

## CHAPTER FOUR

### RESULTS, DISCUSSION, AND CONCLUSIONS

#### 4.1 Introduction

The present work consists of two parts, the first part is determining of the radioactivity concentration of the main radionuclides such as cesium ( $^{137}\text{Cs}$ ) and strontium ( $^{90}\text{Sr}$ ) of liquid samples which were collected from the radiochemistry waste hall in Al-Tuwaitha site. The samples were measured by using two techniques:-

1. Gamma-ray spectroscopy system with high purity germanium (HPGe) detector for measuring the radioactivity concentration for gamma-ray emitters radionuclides.
2. Gross alpha beta gamma system with gas flow detector was used for measuring the radioactivity concentration of beta emitter radionuclides.

The second part is evaluating the removal efficiency of natural zeolite (clinoptilolite) to remove the  $^{137}\text{Cs}$  and  $^{90}\text{Sr}$  radionuclides from the high level liquid waste pool (HLLW) in the radiochemistry waste hall by using ion exchange technique.

#### 4.2 Gamma Spectroscopy Measurements

The main purposes of the gamma spectrometry technique is to determine the quantity of the radioactivity concentration and type of gamma-emitters radionuclides in the samples. The activities of gamma rays emitters radionuclides belonging to natural and man-made were measured by using gamma spectrometry system based on the analysis of the area under the peak of the gamma lines energies.

The radioactivity concentration ( $\text{Bq.L}^{-1}$ ) of the cesium ( $^{137}\text{Cs}$ ) and the potassium ( $^{40}\text{K}$ ) radionuclides have been calculated using their single



gamma-ray transitions energies at 661.65 keV with intensity 85.1% and 1460.81 keV with intensity 10.66% respectively. The radioactivity concentration of the bismuth isotope ( $^{214}\text{Bi}$ ) was calculated at the energy 609.31 keV with intensity 45.59%. While the radioactivity concentration of the radium isotope ( $^{226}\text{Ra}$ ) was calculated at the energy 186.21 keV with intensity 3.64 %.

#### 4.2.1 The Radioactivity Concentration of HLLW Pool Samples

The first experiment was done to determine the acceptable dead time for gamma spectrometry system. The HLLW-P-B sample was used in this experiment at four dilution percent, as shown in the table (4-1). The results show that radioactivity concentration of  $^{137}\text{Cs}$  varies from  $(6931.9 \pm 42.7$  to  $64037 \pm 75.2)$   $\text{Bq.L}^{-1}$  at dilution percent (0.2 to 2) % with dead time (2.28% to 13.16%) to HLLW-P-B-4 and HLLW-P-B-1 respectively. The dilution percent 0.2% has been depended on this research because it represents accepted dead time, therefore all radioactivity concentration for each radionuclide in any samples should integrate to initial concentration (100%) by multiply by percent factor (PF). The percent factor was derived from direct proportional between the dilution percentage and the radioactivity concentration of the radionuclide as in equation (4-2), therefore, the actual radioactivity concentrations of HLLWP samples which are shown in table (4-2) must be integrated to their actual radioactivity as presented in table (4-3). The samples which were taken from the low level liquid waste pool (LLLWP) without dilution because of their dead time were not high.

The results of HLLWP samples show that radioactivity concentration of cesium ( $^{137}\text{Cs}$ ) varies from  $(2118.3 \pm 13.6$  to  $6403.12 \pm 23.68)$   $\text{Bq.L}^{-1}$  for HLLW-T-H sample and sample-HLLW-P-B respectively. The radioactivity concentration of potassium ( $^{40}\text{K}$ ) varies

from  $(8.87 \pm 3.7$  to  $15.34 \pm 4.31)$   $\text{Bq.L}^{-1}$  for HLLW-T- $\alpha$  sample and HLLW-P-M sample respectively. The radioactivity concentration values of radium ( $^{226}\text{Ra}$ ) are  $<\text{MDA}$  for all samples except HLLW-T-H sample which is  $(42.07)$   $\text{Bq.L}^{-1}$ . The radioactivity concentration values of Bismuth ( $^{214}\text{Bi}$ ) are  $<\text{MDA}$  for all samples except HLLW-T-SS which is  $(17.439 \pm 0.1)$   $\text{Bq.L}^{-1}$ .

The radioactivity concentration results of gamma spectroscopy system for HLLW pool samples were approximately equal to each other of the selected samples HLLW-P-S, HLLW-P-M, and HLLW-P-B except the radioactivity concentration of the three tanks, therefore, the HLLW-P-M sample was depended in measurements and calculation in the next experiments which belong to characterization of HLLW pool because it represents the sample in the middle of pool as well as it represents about the mean of radioactivity concentration value between surface and bottom level, the HLLW-M was coded sample-C.

**Table 4-1: The radioactivity concentration results in liquid samples at different dilution percent for HLLW-P-B liquid samples.**

Sample code	Dilution percent %	Radioactivity concentration $\text{Bq.L}^{-1}$		dead time %
		$^{137}\text{Cs}$	$^{40}\text{K}$	
HLLW-P-B-1	2	$64037 \pm 75.2$	$9.77 \pm 3.86$	13.16
HLLW-P-B-2	1	$32490 \pm 90.75$	$<\text{MDA}$	7.22
HLLW-P-B-3	0.4	$13434 \pm 59.46$	$<\text{MDA}$	3.62
HLLW-P-B-4	0.2	$6931.9 \pm 42.7$	$<\text{MDA}$	2.28

**Table 4-2: The radioactivity concentration results in liquid samples at dilution percent 0.2% for HLLW pool.**

Sample code	Radioactivity concentration (Bq.L <sup>-1</sup> )			
	<sup>137</sup> Cs	<sup>226</sup> Ra	<sup>214</sup> Bi	<sup>40</sup> K
HLLW-P-S	4532.63±19.9	<MDA	<MDA	10.226±3.5
HLLW-P-B	6403.12±23.6	<MDA	<MDA	10.82±3.62
HLLW-P-M	5193.01±21.3	<MDA	<MDA	15.34±4.31
HLLW-T-α	2951.8±16.08	<MDA	<MDA	8.87±3.7
HLLW-T-SS	2706.9±15.4	<MDA	17.439±0.1	12.632±3.9
HLLW-T-H	2118.3±13.6	42.07±40.2	<MDA	10.527±3.5

$$\frac{DP_1}{DP_2} = \frac{AC_1}{AC_2} \dots\dots\dots (4 - 1)$$

$$AC_2 = \frac{DP_2 \cdot AC_1}{DP_1}$$

$$PF = \frac{DP_2}{DP_1} \dots\dots\dots (4 - 2)$$

$$PF = \frac{100\%}{0.2\%}$$

$$PF = 500$$

Therefore;

$$AC_2 = PF \times AC_1$$

Where:

*DP*<sub>1</sub>: Dilution percent of used solution concentration at the experiment.

*DP*<sub>2</sub>: Initial solution concentration percent (100%).

*AC*<sub>1</sub>: Radioactivity concentration of solution at the experiment.

$AC_2$ : Actual radioactivity concentration of the solution.

$PF$  : Percent factor.

Table (4-3) lists the initial radioactivity concentration results of liquid samples at dilution percent 100% for HLLW pool and its tanks, therefore, the average value of  $^{137}\text{Cs}$  radioactivity concentration for only HLLWP is  $2688126.6 \text{ Bq.L}^{-1}$ . Figures (4-1 and 4-2) show gamma-ray spectrum of maximum radioactivity concentration for  $^{137}\text{Cs}$  of liquid sample HLLW-P-S and HLLW-M.

**Table 4-3: The radioactivity concentration results of liquid samples at dilution percent 100% for HLLW pool.**

No.	Sample code	Radioactivity concentration for $^{137}\text{Cs}$ ( $\text{Bq.L}^{-1}$ )
1	HLLW-P-S	2266315
2	HLLW-P-B	3201560
3	HLLW-P-M	2596505
4	HLLW-T- $\alpha$	1475900
5	HLLW-T-SS	1353450
6	HLLW-T-H	1059150

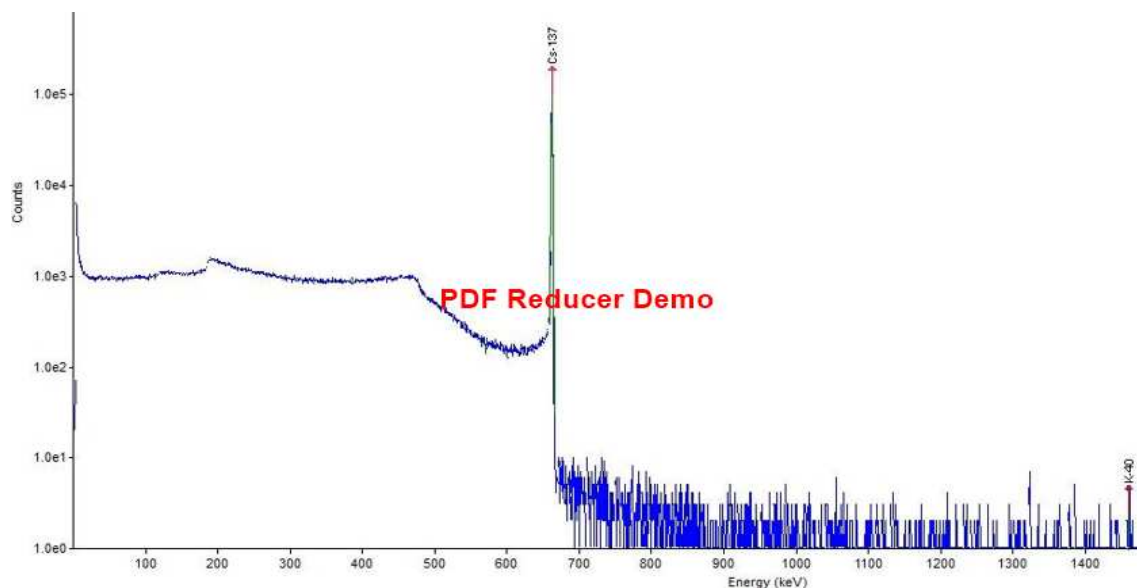


**Figure 4-1: Gamma-ray spectrum of HLLW-P-S liquid sample.**

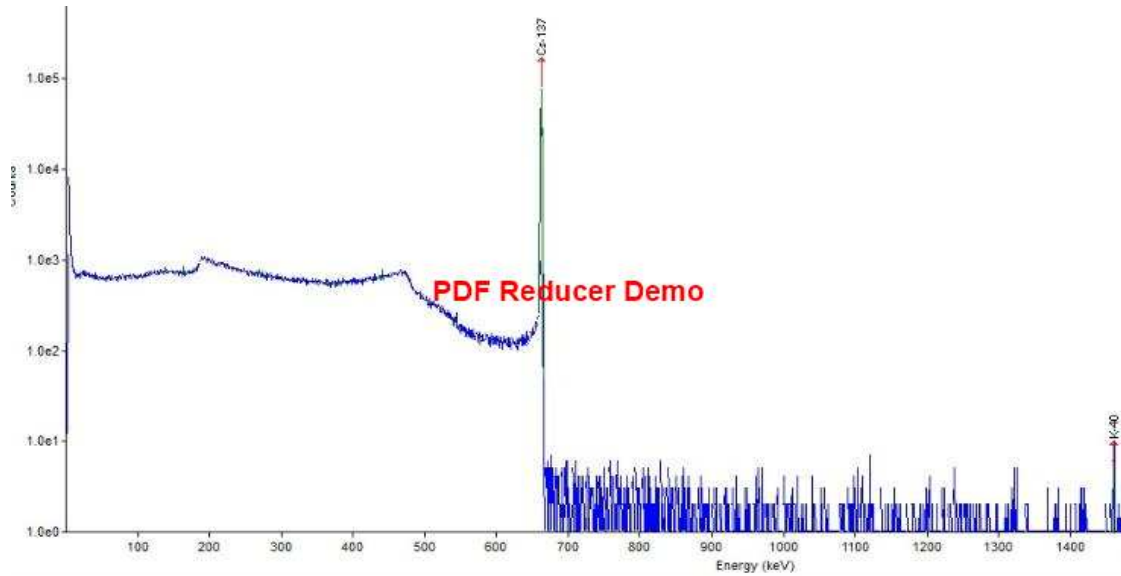


**Figure 4-2: Gamma-ray spectrum of HLLW-M (C) liquid sample.**

#### 4.2.2 The Radioactivity Concentration of LLLW Pool Samples

The radioactivity concentration results of radionuclides for four liquid samples which have been taken from the low-level liquid waste pools show that radioactivity concentration of cesium ( $^{137}\text{Cs}$ ) for LLLW pool varies from  $(833.13 \pm 8.5 \text{ to } 22255.4 \pm 46.6) \text{ Bq.L}^{-1}$  for the sample-LLLW-P-S and sample-LLLW-T respectively, as presented in the table (4-4). The radioactivity concentration of potassium ( $^{40}\text{K}$ ) varies from  $(13.38 \pm 4.3 \text{ to } 17.29 \pm 4.9) \text{ Bq.L}^{-1}$  for the sample-LLLW-P-M and sample-LLLW-P-B respectively. The radioactivity concentration of Bismuth ( $^{214}\text{Bi}$ ) varies from below MDA to LLLW-P-B and LLLW-T to  $10.89 \pm 3.03$  to LLLW-P-S. The results of radioactivity concentration of gamma spectroscopy system for LLLW pool samples were approximately equal to each other of the selected samples LLLW-P-S, LLLW-P-M, and LLLW-P-B except for the radioactivity concentration of the tank, therefore, the LLLW-M sample was depended in measurements and calculation in the next experiments which belong to characterization of LLLW pool because it represents the sample in the middle of pool as well

as it represents about the mean radioactivity concentration value between surface and bottom level, the LLLW-P-M was coded sample-L. The average value of  $^{137}\text{Cs}$  radioactivity concentration for LLLWP is  $850.63 \text{ Bq.L}^{-1}$ .

Figures (4-3 and 4-4) shows the gamma-ray spectrum of maximum radioactivity concentration for  $^{137}\text{Cs}$  in liquid sample LLLW-P- B and LLLW-P- S.

**Table 4-4: The radioactivity concentration of LLLW pool liquid samples.**

Sample code	Radioactivity concentration ( $\text{Bq.L}^{-1}$ )		
	$^{137}\text{Cs}$	$^{40}\text{K}$	$^{214}\text{Bi}$
LLLW-P-S	$833.13 \pm 8.54$	$15.94 \pm 4.37$	$10.89 \pm 3.03$
LLLW-P-M	$853.2 \pm 8.63$	$13.38 \pm 4.3$	$10.711 \pm 3.1$
LLLW-P-B	$865.56 \pm 8.7$	$17.29 \pm 4.9$	<MDA
LLLW-T	$22255.4 \pm 46.56$	$17.15 \pm 5.52$	<MDA

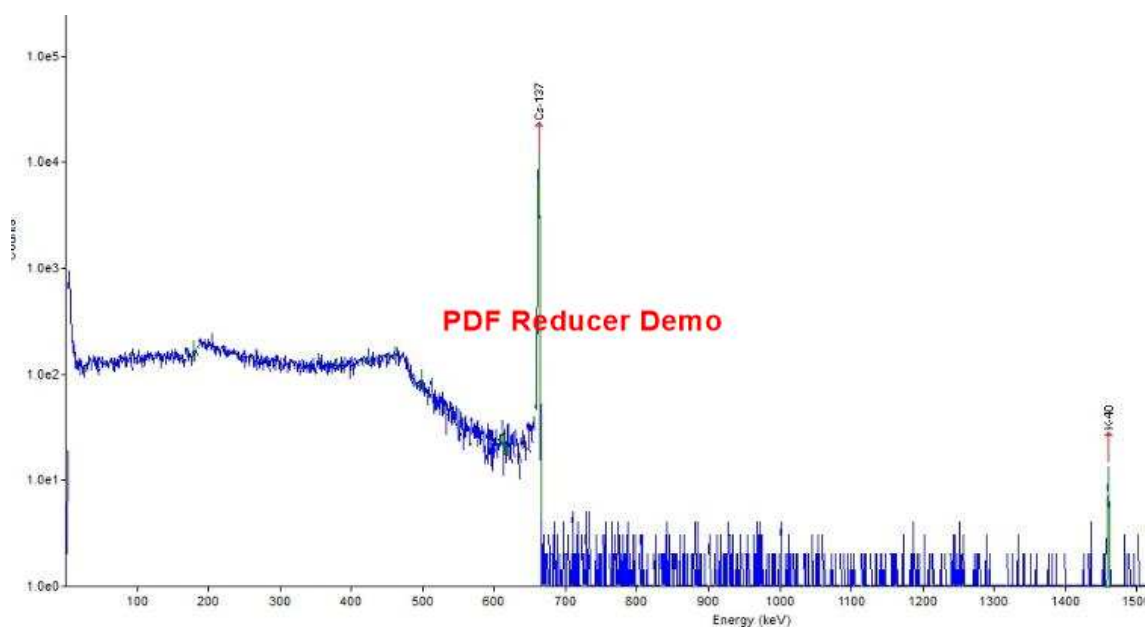


**Figure 4-3: Gamma-ray spectrum of liquid sample LLLW-P-B.**

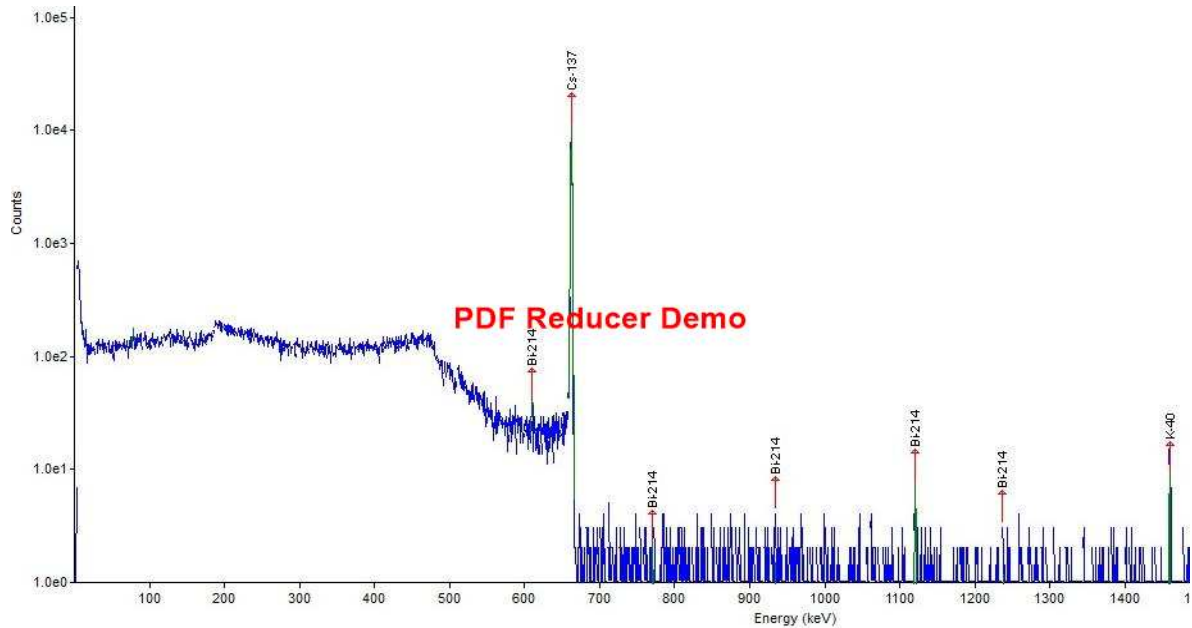


**Figure 4-4: Gamma-ray spectrum of liquid sample LLLW-P-S.**

### 4.3 Gross Alpha Beta Gamma System Measurements

The gross alpha beta gamma system with proportional gas flow detector has been used to determine the radioactivity concentration of strontium-90 ( $^{90}\text{Sr}$ ) by three steps. The first step was a depositing the liquid samples at 100 °C on a 2 inch stainless steel planchet. The second step was heating the deposit samples at a different temperature 300, 500 and to 700°C, while the third step included measuring these samples at each temperature by the gross alpha beta gamma system and gamma spectroscopy system.

#### 4.3.1 The Count Rate of HLLW Pool Samples

The radioactivity concentration of  $^{90}\text{Sr}$  estimated in count per minute (CPM) units for high-level liquid waste pool HLLW by deposit ten samples with volume (1 to 10) mL from HLLW-M (C) sample with dilution 0.2% on planchets. Table (4-5) presents the radioactivity of alpha, beta, and gamma for ten deposit samples at 300°C and background radiation level of gross alpha beta gamma system. The results of alpha

radioactivity varied from  $(0.1 \pm 0.1$  to  $0.6 \pm 0.24)$  CPM, while beta radioactivity varied from  $(138.7 \pm 3.72$  to  $1605.4 \pm 12.67)$  CPM and gamma radioactivity vary from  $(46.1 \pm 2.15$  to  $109.7 \pm 3.31)$  CPM for (C-1 to C-10) samples respectively. Figure (4-5) presents the relation between gross beta radioactivity and sample volume, obviously the count rate of beta radioactivity increase with increase of liquid sample volume from 1 mL to 10 mL without attenuation or self-absorption in sample because of the thin layer of the residual deposit liquid, there is no ideal sample from the ten samples because of the curve is approximately linear, therefore, four samples were selected (C-2, C-4, C-7, C-10) to continue this experiment. Table (4-6) presents the radioactivity of alpha, beta and gamma for four selected samples from the previous ten samples at  $500^{\circ}\text{C}$ , the results of alpha radioactivity varies from  $(0.4 \pm 0.20$  to  $1 \pm 0.32)$  CPM and beta radioactivity vary from  $(287.7 \pm 5.36$  to  $1522.9 \pm 12.34)$  CPM for (C-2, C-10) samples respectively, while gamma radioactivity vary from  $(48.7 \pm 2.21$  to  $94.1 \pm 3.07)$  CPM for (C-2, C-7) samples respectively. Table (4-7) presents the radioactivity of alpha, beta and gamma for four samples at  $700^{\circ}\text{C}$ , the results of alpha radioactivity vary from  $(0.2 \pm 0.14$  to  $0.6 \pm 0.24)$  CPM and beta radioactivity vary from  $(272 \pm 5.22$  to  $1385.3 \pm 11.77)$  CPM for C-2, C-10 samples respectively, while gamma radioactivity vary from  $(49.4 \pm 2.22$  to  $58.5 \pm 2.42)$  CPM for C-2, C-7 samples respectively. Figure (4-6) shows the gross beta radioactivity CPM for different HLLW samples (2, 4, 7 and 10) mL as a function of temperature.



**Table 4-5: The radioactivity of alpha, beta and gamma at 300°C for HLLWP.**

Sample code	The radioactivity (CPM) of		
	Alpha	Beta	Gamma
B.G	0.2±0.14	18.9± 1.37	41.7±2.04
C-1	0.1±0.1	138.7±3.72	46.1±2.15
C-2	0.3±0.17	284±5.33	44.1±2.10
C-3	0.2±0.14	398.9±6.32	48.6±2.20
C-4	0±0.00	581.4±8.26	60.4±2.46
C-5	0.3±0.3	683±8.26	58.1±2.41
C-6	0.6±0.24	962.1±9.81	68.3±2.61
C-7	0.1±0.1	1286.5±11.77	109.7±3.31
C-8	0.4±0.2	1374.5±10.38	74±2.72
C-9	0.3±0.17	1415.5±11.90	74.6±2.73
C-10	0.4±0.2	1605.4±12.67	85.8±2.93

**Table 4-6: The radioactivity of alpha, beta samples at 500°C for HLLWP.**

Sample code	The radioactivity (CPM) of		
	Alpha	Beta	Gamma
B.G/	0.2±0.14	22.2±1.49	41.5±2.04
C-2	0.4±0.20	287.7±5.36	48.70±2.21
C-4	0.4±0.20	580.2±7.62	57.5±2.40
C- 7	1±0.32	1196.8±11.39	94.1±3.07
C-10	0.4±0.20	1522.9±12.34	79.1±2.81

**Table 4-7: The alpha and beta radioactivity of samples at 700°C to HLLWP.**

Sample code	The radioactivity (CPM) of		
	Alpha	Beta	Gamma
B.G/	0.2±0.14	19.7±1.40	45.2±2.13
C-2	0.2±0.14	272±5.22	49.4±2.22
C-4	0.3±0.17	518.8±7.20	49.2±2.22
C-7	0.4±0.20	1001.6±10.25	58.5±2.42
C-10	0.6±0.24	1385.3±11.77	54.2±2.33

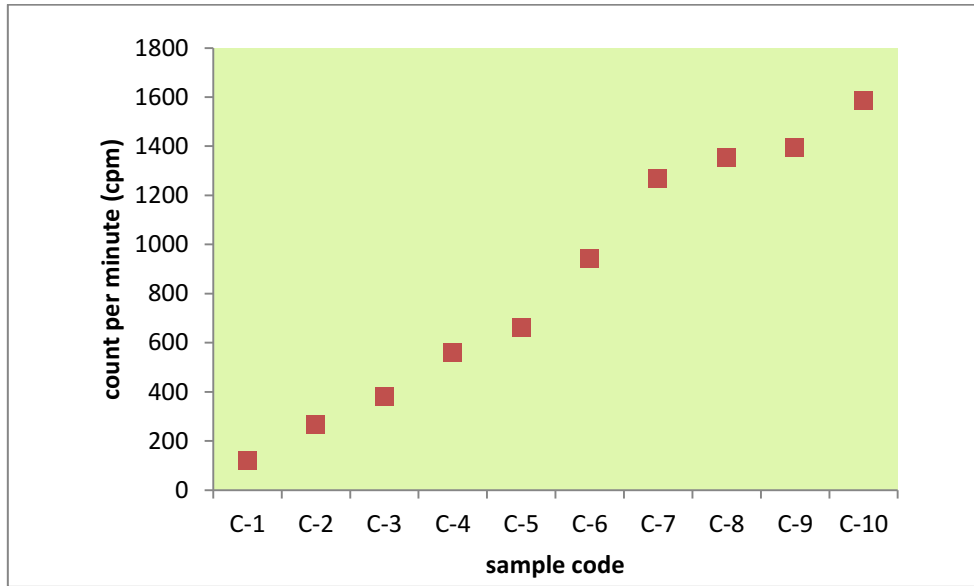


Figure 4-5: Gross beta radioactivity CPM of HLLW-P samples as a function of samples volume at 300 C°.

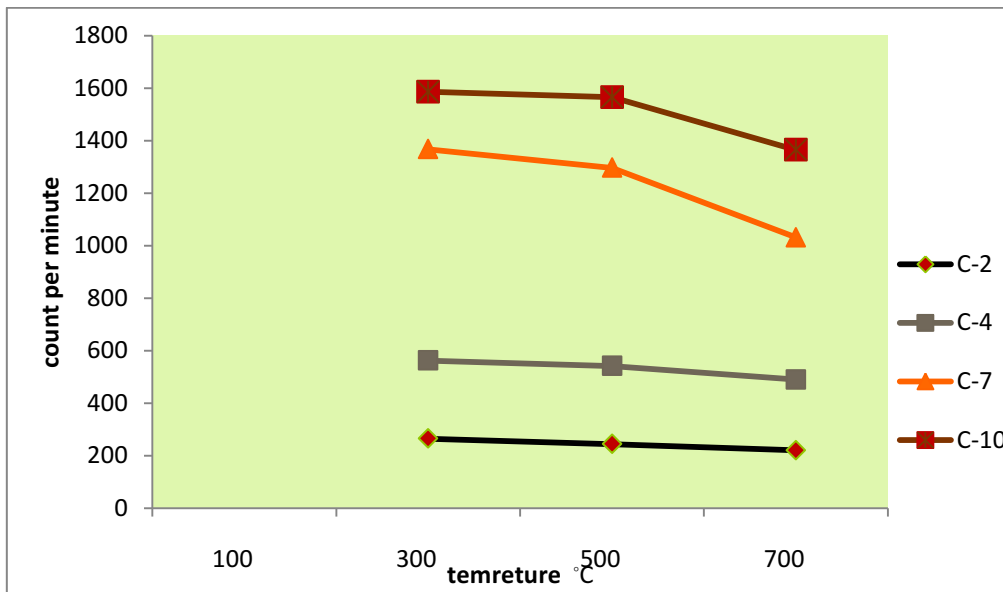


Figure 4-6: Gross beta radioactivity CPM for different HLLW samples as a function temperature.

#### 4.3.1.1 Calculation of Strontium Radioactivity Concentration for HLLWP

The alpha radioactivity (counts rate) was neglected because it in the background range of gross alpha beta gamma system, the gross gamma radioactivity in this system not depended in calculation just

indicator for the decreasing of gamma count rate with increasing of temperature as well as the radionuclide with gamma emission ( $^{137}\text{Cs}$ ) were measured by gamma spectroscopy system to the samples in each step of the experiments in this study. This part of the study focuses to determine the gross beta radioactivity of strontium and cesium ( $^{90}\text{Sr}$  and  $^{137}\text{Cs}$ ) which are the main beta emitters radionuclides with a long half-life in this radioactive liquid waste. The radioactivity concentration of cesium for HLLWP was measured by gamma spectroscopy system with mean value (2596505)  $\text{Bq.L}^{-1}$ , it belongs to HLLW-P-M sample (sample-C) as in the table (4-3) with dilution percent 0.2% (the percent factor  $PF=500$ ). Strontium-90( $^{90}\text{Sr}$ ) isotope cannot detect by the same technique because of it is a pure beta emission. The cesium is volatile at elevated temperatures above  $450^{\circ}\text{C}$ . In this research, the evaporation process was used to separate cesium element from deposit samples to determine the radioactivity of  $^{90}\text{Sr}$  due to their differences in boiling points, as a mentioned in chapter two.

The deposit liquid samples (C-2, C-4, C-7, C-10) on the planchets were depended in this experiment to determine the radioactivity concentration of strontium radionuclide ( $^{90}\text{Sr}$ ). The count rate of beta for these samples at  $700^{\circ}\text{C}$  represents the count of  $^{90}\text{Sr}$  with small amount of  $^{137}\text{Cs}$  counts in the same sample because it is not evaporate completely, therefore a correction reading for the remain beta count of  $^{137}\text{Cs}$  in these samples at  $700^{\circ}\text{C}$  was derived to subtract from total beta count of sample (C-2, C-4, C-7, C-10). According to work history of the radiochemistry laboratories, this waste is nuclear fission products of uranium-235 ( $^{235}\text{U}$ ) isotope, therefore the remaining radioactivity refers to strontium-90( $^{90}\text{Sr}$ ) radionuclide due to its long half-life.

**4.3.1.2 Developing a New Method to Separating <sup>90</sup>Sr from <sup>137</sup>Cs**

The liquid samples of high and low-level liquid waste pools have contained a radioactivity for <sup>137</sup>Cs as shown in the tables (4-2 and 4-4), the deposit liquid samples (C-2, C-4, C-7, C-10) are depended in this process. These samples were heated to different temperatures (300, 500 and 700) °C. Gamma spectroscopy system was used to measure these samples in each step of heating to determine the count rate for <sup>137</sup>Cs which remaining in them, as presented in table (4-8) and figures (4-7, 4-8 and 4-9). These figures show that the radioactivity (total count per 1000 second) of <sup>137</sup>Cs decreases with increasing the temperature. The results show that the radioactivity of <sup>137</sup>Cs in the samples which heated to 700 °C was less than of their activity at 300 °C, with presents a small amount of <sup>137</sup>Cs activity, that means the <sup>137</sup>Cs does not completely evaporated, therefore, the remain radioactivity factor of <sup>137</sup>Cs ( $RAF_{137Cs}$ ) derived as in equation (4-3). The correction factor of beta efficiency ( $CF_{eff}$ ) for gross alpha beta gamma system was derived by equation (4-4) because of the deference of <sup>90</sup>Sr and <sup>137</sup>Cs efficiencies for this system of beta detection. The correction factor for <sup>137</sup>Cs ( $CF_{137Cs}$ ) was derived by equation (4-5), therefore the correction reading for <sup>137</sup>Cs ( $CR_{137Cs}$ ) derived by equation (4-6) to estimate the total count rate (CPM) of <sup>137</sup>Cs in the sample. The correction reading for <sup>90</sup>Sr ( $CR_{90Sr}$ ) calculates by equation (4-7) by subtracting <sup>137</sup>Cs count rate from the total count rate of the sample, therefore, the radioactivity concentration of <sup>90</sup>Sr calculates by equation (4-8). Table (4-9) presents the calculation of <sup>90</sup>Sr radioactivity concentration, therefore, the average radioactivity concentration of <sup>90</sup>Sr in HLLWP is 2606217.144 Bq.L<sup>-1</sup>.

$$(RAF_{137Cs})_i = \left[ \frac{CPS(700)}{CPS(300)} \right]_i \dots \dots \dots (4 - 3)$$

$$CF_{eff} = \frac{eff_{137Cs}}{eff_{90Sr}} \dots \dots \dots (4 - 4)$$

$$CF_{eff} = \frac{13.1\%}{38.4\%} = 0.341$$

$$(CF_{137Cs})_i = CF_{eff} \cdot (RAF_{137Cs})_i \dots \dots \dots (4 - 5)$$

$$(CR_{137Cs})_i = CPM_i \cdot (CF_{137Cs})_i \dots \dots \dots (4 - 6)$$

$$(CR_{90Sr})_i = CPM_i(at\ 700C) - (CR_{137Cs})_i \dots \dots \dots (4 - 7)$$

$$[A_{90Sr} (Bq. L^{-1})]_i = \frac{[(CR_{90Sr})_i - B]x1000}{eff_{90Sr} \cdot V_i \cdot 60} \cdot xPF \dots \dots (4 - 8)$$

Where: *i*: sample number

*PF*: The percent factor (500 for HLLW samples and 1 for LLLW samples)

*RAF<sub>137Cs</sub>*: The remain radioactivity factor of <sup>137</sup>Cs in the sample

*CPS (700)*: Count per second for <sup>137</sup>Cs in the sample at 700 °C by gamma spectroscopy system

*CPS (300)*: Count per second for <sup>137</sup>Cs in the sample at 300 °C by gamma spectroscopy system

*CF<sub>eff</sub>* : Correction efficiency factor

*eff<sub>137Cs</sub>*: Gross alpha beta gamma system efficiency of <sup>137</sup>Cs

*eff<sub>90Sr</sub>*: Gross alpha beta gamma system efficiency of <sup>90</sup>Sr

*CF<sub>137Cs</sub>* : Correction factor of the remain radioactivity for <sup>137</sup>Cs in sample

*CR<sub>137Cs</sub>* : Correction reading of radioactivity for <sup>137</sup>Cs in sample

*CPM<sub>i</sub>* : Count per minute for the initial sample (code *i*) at 700 °C

*CR<sub>90Sr</sub>*: Net count per minute for <sup>90</sup>Sr at 700 °C

*B* : The background of beta radioactivity

*A<sub>90Sr</sub>* : The total radioactivity concentration of <sup>90</sup>Sr in the sample.

**Table 4-8: The radioactivity of  $^{137}\text{Cs}$  for HLLW pool by gamma spectrometry system and the derived RAF for  $^{137}\text{Cs}$ .**

Sample code	Radioactivity for $^{137}\text{Cs}$ (count/1000seconds) at a temperature			The derived <b>RAF</b> $_{137\text{Cs}}$
	300 °C	500 °C	700 °C	
C-2	16	15	6	0.375
C-4	44	27	20	0.45
C-7	222	130	23	0.103
C-10	142	91	36	0.253

**Table 4-9: The calculated radioactivity concentration of  $^{90}\text{Sr}$  to HLLW-M sample in HLLW pool.**

Sample code	Beta radioactivity (CPM) at 700 °C	RAF $_{137\text{Cs}}$	CF $_{137\text{Cs}}$	CR $_{137\text{Cs}}$ (CPM)	CR $_{90\text{Sr}}$ (CPM)	A $_{90\text{Sr}}$ (Bq. L $^{-1}$ )
C-2	272	0.375	0.13	34.78	237.22	2360221.35
C-4	518.8	0.45	0.15	79.61	439.19	2275879.66
C-7	1051.6	0.103	0.04	36.94	1014.66	3084587.84
C-10	1385.3	0.253	0.09	119.51	1265.78	2704179.72
C- ave						2606217.144

The total activity of high level liquid waste pool for the main radionuclides ( $^{137}\text{Cs}$  and  $^{90}\text{Sr}$ ) can calculate as in table (4-10).

**Table 4-10: The total activity of high level liquid waste pool.**

Volume of HLLWP (liter)	radioactivity concentration of $^{137}\text{Cs}$ (MBq.L $^{-1}$ )	Total radioactivity of $^{137}\text{Cs}$ (MBq)	radioactivity concentration of $^{90}\text{Sr}$ (MBq.L $^{-1}$ )	Total radioactivity of $^{90}\text{Sr}$ (MBq)	Total radioactivity $^{137}\text{Cs}+^{90}\text{Sr}$ (MBq)
35700	2.688	95961.6	2.606	93034.2	188995.8

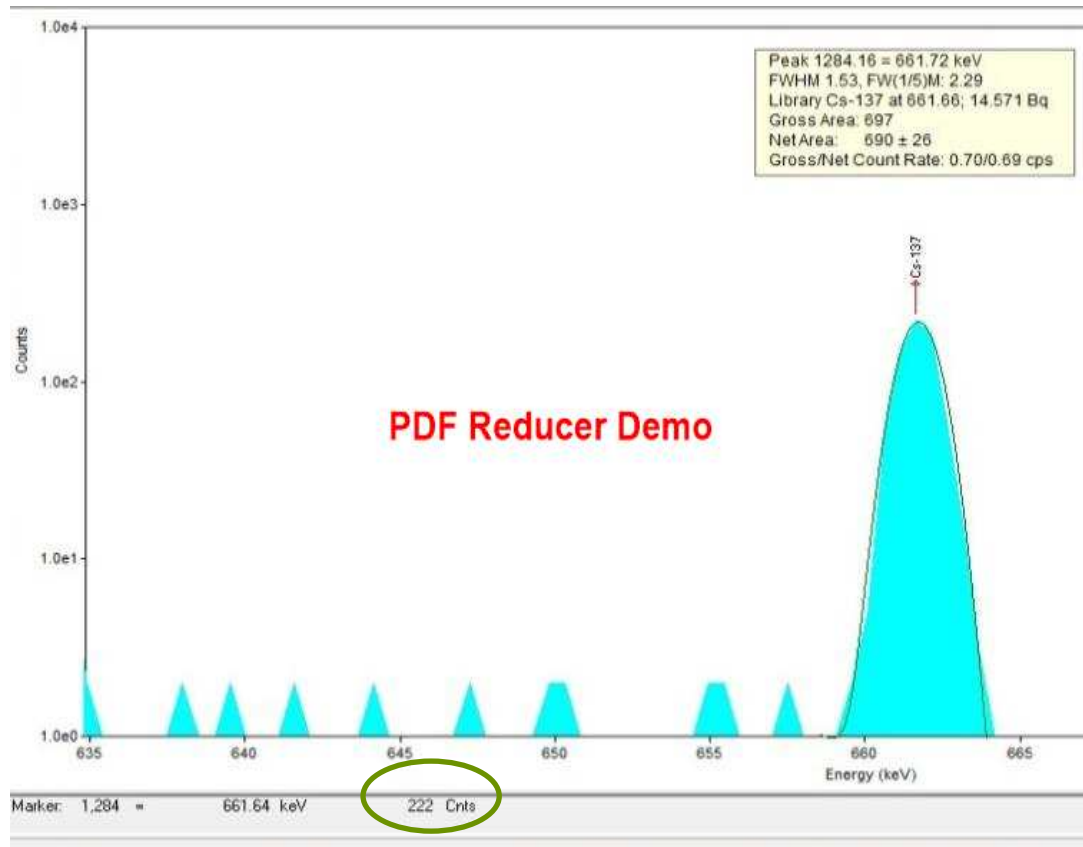


Figure 4-7:  $^{137}\text{Cs}$  spectrum of C-7 sample (planchet) at 300 °C.

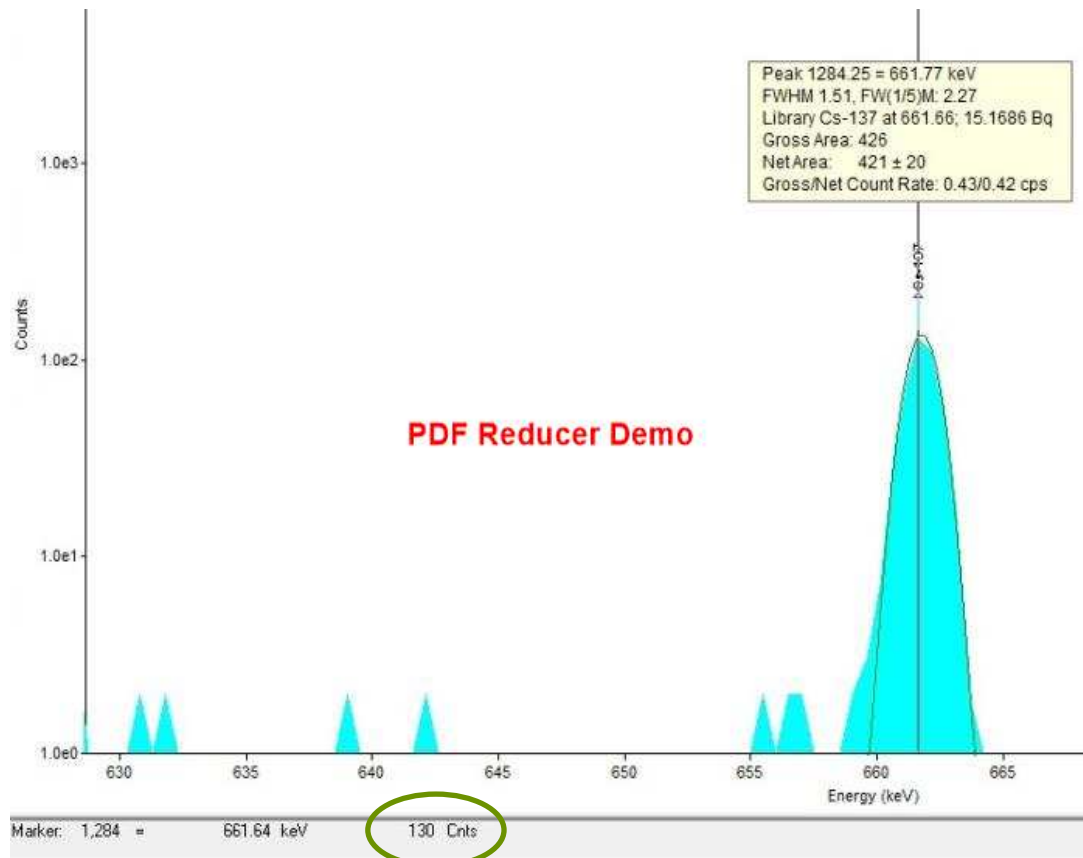
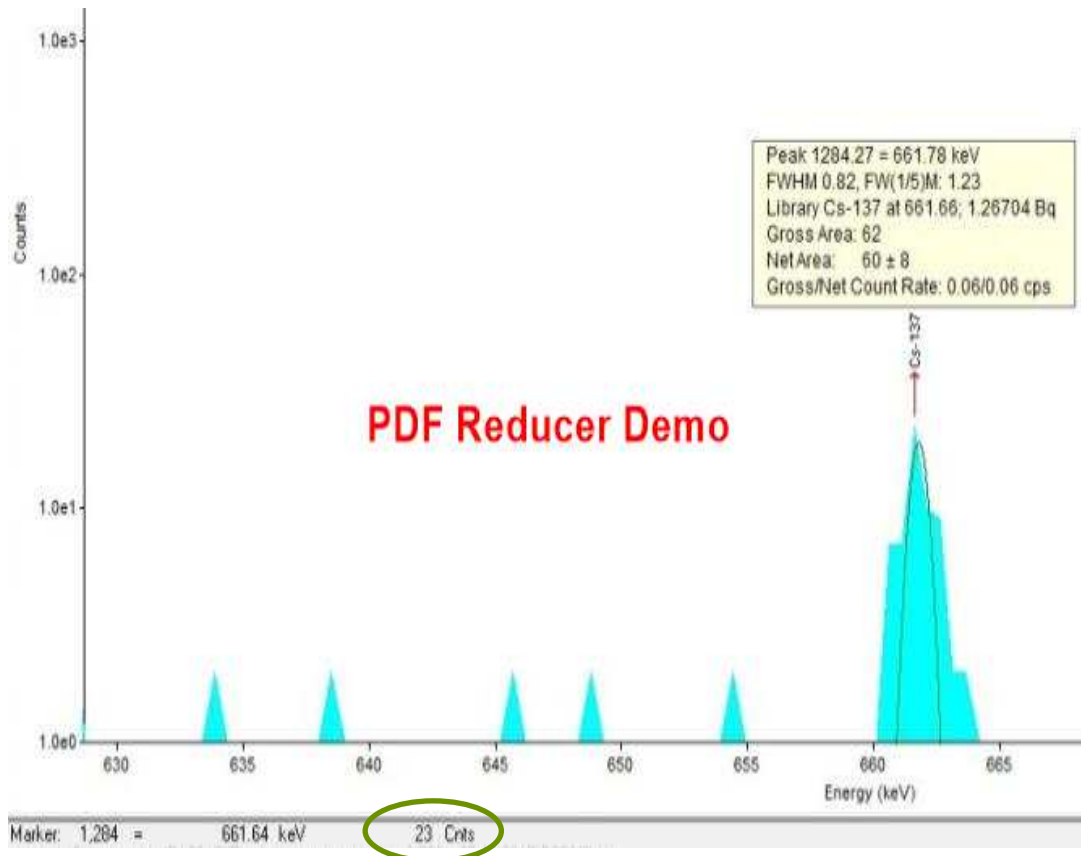


Figure 4-8:  $^{137}\text{Cs}$  spectrum of C-7 sample (planchet) at 500 °C.



**Figure 4-9:**  $^{137}\text{Cs}$  spectrum of C-7 sample (planchet) at 700 °C.

#### 4.3.1.3 The Radioactivity Concentration of Strontium for LLLWP

The radioactivity concentration of strontium ( $^{90}\text{Sr}$ ) for low-level liquid waste pool LLLWP was determined by gross alpha beta gamma system by depositing three samples with volume (2,4 and 7) mL from LLLW-M sample without dilution (the percent factor  $PF = 1$ ) on the planchets. The samples L-2, L-4, and L-7 refer to the volume of the deposited liquid on planchets (mL). Table (4-11) shows the gross radioactivity for alpha, beta and gamma for the three deposit samples at 100°C and background limit, the results of gross alpha radioactivity vary from  $(0.4 \pm 0.2$  to  $1.7 \pm 0.41)$  CPM and gross beta radioactivity vary from  $(596.6 \pm 7.072$  to  $1165 \pm 10.79)$  CPM for (L-2, L-7) samples respectively while gross gamma radioactivity vary from  $(109.2 \pm 3.3$  to  $194.9 \pm 4.41)$  CPM for (L-4, L-7) samples respectively. Table (4-12) presents the gross radioactivity of alpha, beta and gamma for the three deposit samples at



300°C and background limit, the results of gross alpha radioactivity vary from  $(0.7 \pm 0.26$  to  $1.2 \pm 0.35)$  CPM for L-2, L-4 respectively, while gross beta radioactivity vary from  $(589.3 \pm 7.68$  to  $1218.2 \pm 11.04)$  CPM for L-2, L-7 respectively and gross gamma radioactivity vary from  $(115.3 \pm 3.4$  to  $192.3 \pm 4.39)$  CPM for (L-4, L-7) samples respectively. Table (4-13) presents the gross radioactivity for alpha, beta and gamma for the three deposit samples at 500°C and background limit, the results of gross alpha radioactivity vary from  $(0.3 \pm 0.17$  to  $1.2 \pm 0.35)$  CPM for L-2, L-7 respectively and gross beta radioactivity vary from  $(501.3 \pm 7.08$  to  $1056.6 \pm 10.28)$  CPM for L-4, L-7 respectively, while gross gamma radioactivity vary from  $(97.5 \pm 3.12$  to  $171 \pm 4.14)$  CPM for (L-4, L-7) samples respectively. Table (4-14) presents the gross radioactivity for alpha, beta and gamma for the three deposit samples at 700°C, the results of gross alpha radioactivity vary from  $(0.1 \pm 0.1$  to  $0.7 \pm 0.26)$  CPM for L-2, L-7 respectively, while gross beta radioactivity vary from  $(98.1 \pm 3.13$  to  $348.6 \pm 5.9)$  CPM for L-2, L-7 respectively and gross gamma radioactivity vary from  $(43.2 \pm 2.08$  to  $63.6 \pm 2.52)$  CPM for (L-4, L-7) samples respectively.

The radioactivity concentration of strontium for LLLW pool determined by the same way of HLLW pool by depending on the three deposit samples (L-4, L-2, L-7) at 700°C and deriving the same correction factors, as presented in tables (4-14 and 4-15). Figure (4-10) shows the reduction of beta radioactivity of samples at 700 °C. Gamma spectroscopy system was used to measure these samples in each step of heating to determine the count rate for  $^{137}\text{Cs}$  which remain in them, as shown in figures (4-11 and 4-12), these figures show the reduction of  $^{137}\text{Cs}$  radioactivity (count per 1000 seconds) with increasing temperature. Table (4-15) which represent  $^{137}\text{Cs}$  radioactivity at different temperature.

The radioactivity concentration of  $^{90}\text{Sr}$  calculated by equation (4-8) with percent factor equal one (PF=1) because of the LLLW-M sample which was depended to determining  $^{90}\text{Sr}$  radioactivity concentration was not diluted. Table (4-16) presents the calculation of the mean  $^{90}\text{Sr}$  radioactivity concentration of low level liquid waste pool which is  $1703.89 \text{ Bq.L}^{-1}$ , therefore, the total activity of  $^{137}\text{Cs}$  and  $^{90}\text{Sr}$  in LLLWP is  $50579496 \text{ Bq}$  as present in table (4-17).

**Table 4-11: The radioactivity of alpha, beta, and gamma for the deposit samples at  $100^\circ\text{C}$  to LLLW pool.**

Sample code	The radioactivity (CPM)		
	Alpha	Beta	Gamma
B.G/	$0.1\pm 0.10$	$20\pm 1.41$	$46.2\pm 2.15$
L-2	$0.4\pm 0.20$	$596.6\pm 7.72$	$128.2\pm 3.58$
L-4	$0.6\pm 0.24$	$561.6\pm 7.49$	$109.2\pm 3.30$
L-7	$1.7\pm 0.41$	$1165\pm 10.79$	$194.9\pm 4.41$

**Table 4-12: The radioactivity of alpha, beta, and gamma for the deposit samples at  $300^\circ\text{C}$  to LLLW pool.**

Sample code	The radioactivity (CPM)		
	Alpha	Beta	Gamma
B.G/	$0.1\pm 0.10$	$20\pm 1.41$	$46.2\pm 2.15$
L-2	$0.7\pm 0.26$	$589.3\pm 7.68$	$125.8\pm 3.55$
L-4	$1.2\pm 0.35$	$589.9\pm 7.68$	$115.3\pm 3.40$
L-7	$1.1\pm 0.33$	$1218.2\pm 11.04$	$192.3\pm 4.39$

**Table 4-13: The radioactivity of alpha, beta, and gamma for the deposit samples at  $500^\circ\text{C}$  to LLLW pool.**

Sample code	The radioactivity (CPM)		
	Alpha	Beta	Gamma
B.G/	$0\pm 0.00$	$21.8\pm 1.48$	$41.7\pm 2.04$
L-2	$0.3\pm 0.17$	$509.3\pm 7.14$	$113.8\pm 3.37$
L-4	$0.3\pm 0.17$	$501.3\pm 7.08$	$97.5\pm 3.12$
L-7	$1.2\pm 0.35$	$1056.6\pm 10.28$	$171\pm 4.14$

**Table 4-14: The radioactivity of alpha, beta, and gamma for the deposit samples at 700°C to LLLW pool.**

Sample code	The radioactivity (CPM)		
	Alpha	Beta	Gamma
B.G/	0±0.00	21.8±1.48	41.7±2.04
L-2	0.1±0.10	98.1±3.13	44.6±2.11
L-4	0.7±0.26	163.4±4.04	43.2±2.08
L-7	0.7±0.26	348.6±5.90	63.6±2.52

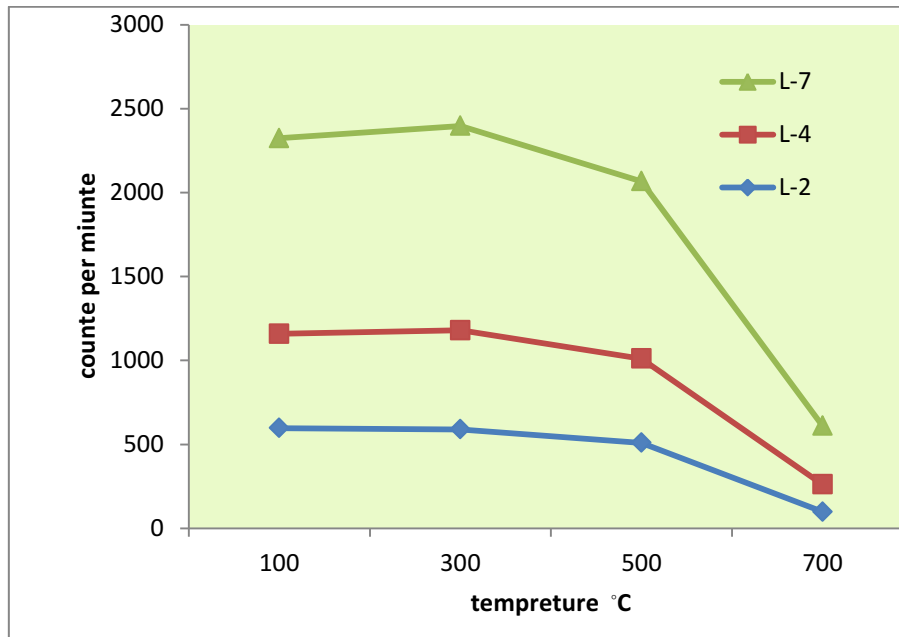


**Figure 4-10: Gross beta radioactivity (CPM) of LLLW pool samples (L-2,4 and 7) with temperature degree C°.**

**Table 4-15: The  $^{137}\text{Cs}$  radioactivity of the deposit samples at a different temperature to LLLW pool by gamma spectrometry system and the derived RAF for  $^{137}\text{Cs}$ .**

Sample code	Radioactivity of $^{137}\text{Cs}$ (count/1000seconds) at a temperature				RAF $_{137\text{Cs}}$
	100 C°	300 C°	500 C°	700 C°	
L-2	303	238	143	8	0.026
L-4	244	195	133	5	0.02
L-7	530	424	354	55	0.103

**Table 4-16: The radioactivity concentration of <sup>90</sup>Sr for LLLW pool.**

Sample code	Radioactivity of beta (CPM)	RAF <sup>137</sup> Cs	CF <sup>137</sup> Cs	CR <sup>137</sup> Cs (CPM)	CR <sup>90</sup> Sr (CPM)	A <sub>90Sr</sub> (Bq.L <sup>-1</sup> )
L-2	98.1	0.026	0.009	0.869	97.23	1636.941
L-4	163.4	0.02	0.007	1.114	162.285	1524.366
L-7	348.6	0.103	0.035	12.244	336.356	1950.373
L-ave						1703.89

**Table 4-17: The total activity of low level liquid waste pool.**

Volume of LLLWP (liter)	The radioactivity concentration of <sup>137</sup> Cs (Bq.L <sup>-1</sup> )	Total radioactivity for <sup>137</sup> Cs (Bq)	The radioactivity concentration of <sup>90</sup> Sr (Bq.L <sup>-1</sup> )	Total radioactivity of <sup>90</sup> Sr (Bq)	Total radioactivity <sup>137</sup> Cs+ <sup>90</sup> Sr (Bq)
19800	850.63	16842474	1703.89	33737022	50579496

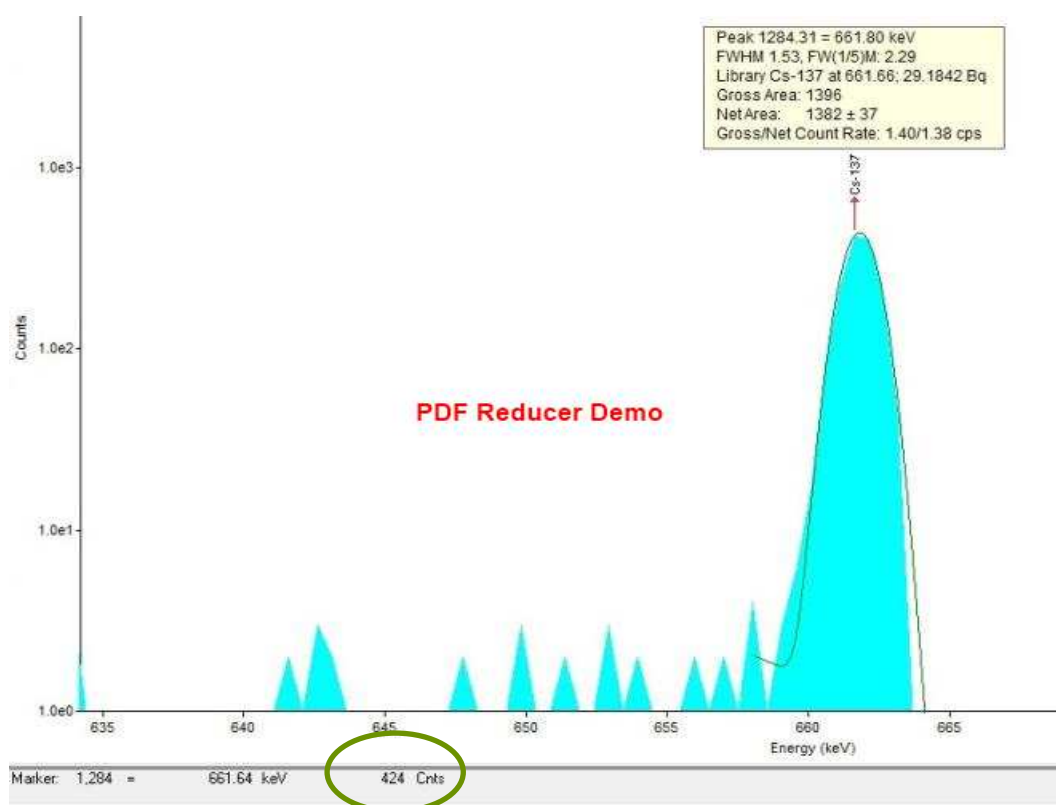


**Figure 4-11: <sup>137</sup>Cs spectrum for L-7 planchet sample at 300 °C.**

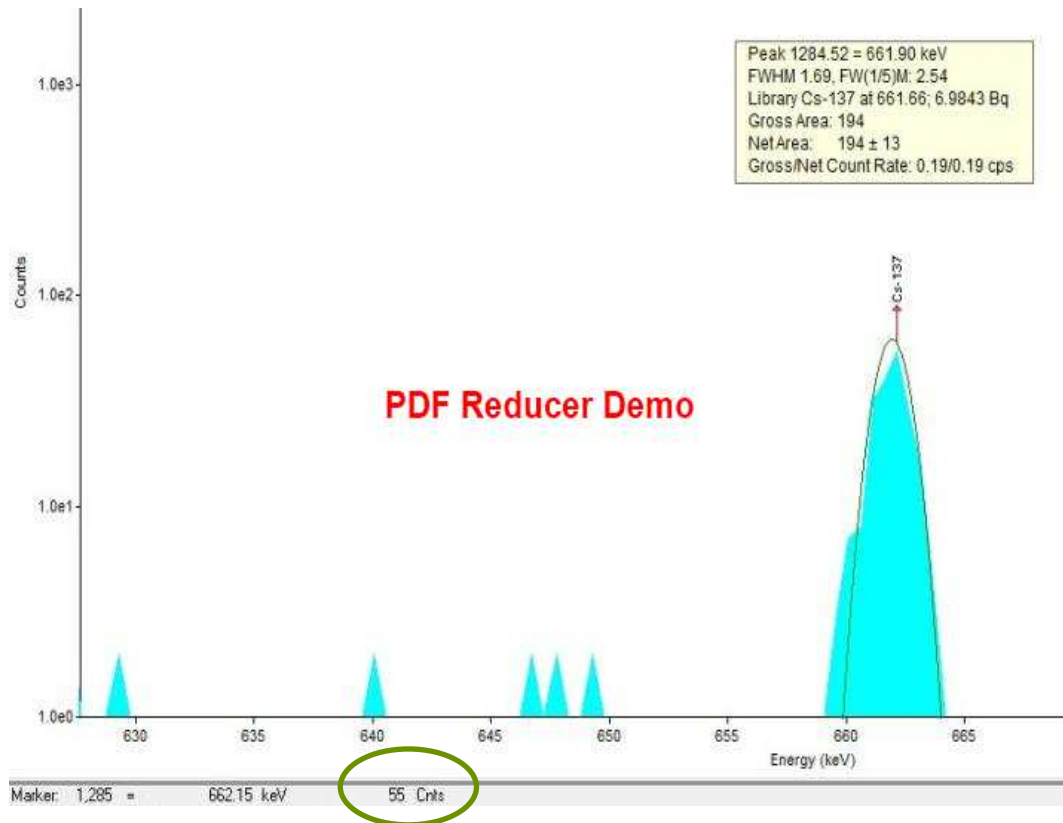


**Figure 4-12:**  $^{137}\text{Cs}$  spectrum for L-7 planchet sample at 700 °C.

#### 4.4 The Reduction of Total Radioactivity for HLLW Pool

This part of study concern on the ability of natural clinoptilolite zeolite in removing  $^{137}\text{Cs}$  and  $^{90}\text{Sr}$  from liquid waste by batch operation. There are some factors affecting on removal efficiency such as the weight of clinoptilolite, solution acidity, contact time and temperature. The weight of the clinoptilolite and the solution acidity were studied in two separated experiments. The removal efficiency (%) of radionuclides calculated as [95]:

$$\text{Removal efficiency (\%)} = \frac{C_0 - C_e}{C_0} \times 100\% \quad (4 - 9)$$

Where:

$C_0$ : the initial concentrations of the radionuclide.

$C_e$ : the concentrations of radionuclides after treatment.

#### 4.4.1 Effecting of Clinoptilolite Weight on Removal Efficiency for $^{137}\text{Cs}$

This section displays the ability of the natural clinoptilolite zeolite to remove cesium from liquid waste for HLLW pool to HLLWP-M sample (sample-C). The C-ST sample (10 mL) was measured by gamma spectroscopy system without dilution with pH (6.5) and laboratory temperature (22 °C). This sample represents a reference sample because it is without treatment. The average radioactivity of  $^{137}\text{Cs}$  for C-ST sample (area under the peak) is 468946 count per 1000 second (CPS) as presents in table (4-18). Figure (4-13) and table (4-18) show that natural clinoptilolite zeolite is efficient in removing cesium ions at all ranges of used weight. The removal efficiency of  $^{137}\text{Cs}$  was ranged from 69% at 0.025g of zeolite (C-A1 sample) to 89% at 0.15 g of zeolite (C-A5 sample), it can be seen that higher removal efficiency was achieved at 0.15g of clinoptilolite, “that because of possibly of the higher number of ion-exchange sites of zeolite”, which agree with more of previous studies [27]. It can see from the figure (4-13) that the removal efficiency does not significantly change at a high value of clinoptilolite weight at (0.1 and 0.15) g, because of the saturation of solution was happened. Figures (4-14, 4-15 and 4-16) show the  $^{137}\text{Cs}$  spectrum of 10ml from liquid samples for C-ST, C-A1, and C-A5 sample.

**Table 4-18: Removal efficiency of  $^{137}\text{Cs}$  by gamma spectroscopy system.**

No.	Sample code	Clinoptilolite weight (g)	Area under peak for $^{137}\text{Cs}$ (count/1000 s)		Removal Efficiency for $^{137}\text{Cs}$ (%)
1	C-ST	0	C-ST-1	408910	---
			C-ST-2	484215	
			C-ST-3	513715	
			C-ST-ave	468946.7	
2	C-A1	0.025	143479		69
3	C-A2	0.05	121445		74
4	C-A3	0.075	86685		82
5	C-A4	0.1	58492		88
6	C-A5	0.15	53100		89

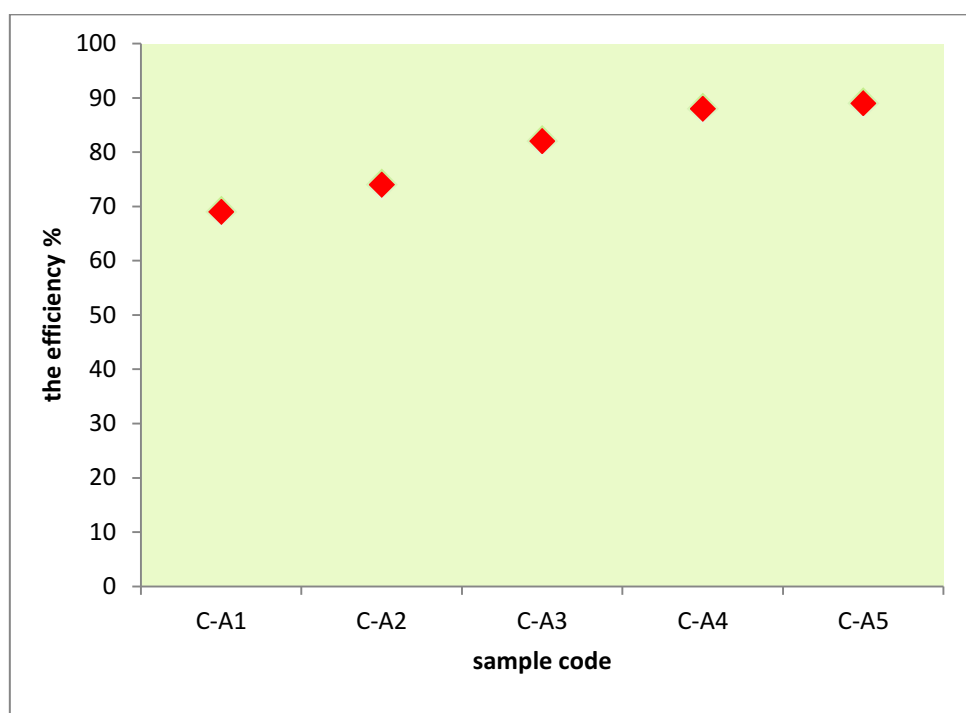


**Figure 4-13: Removal Efficiency of  $^{137}\text{Cs}$  for five samples.**

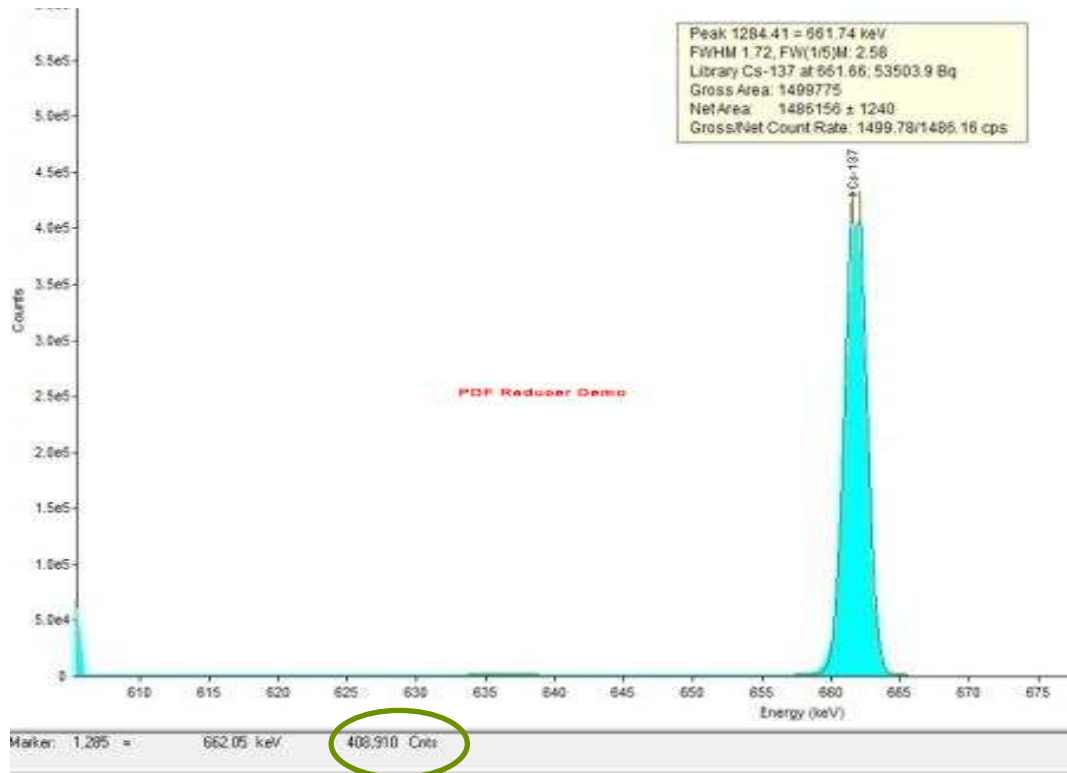


Figure 4-14:  $^{137}\text{Cs}$  spectrum of C-ST (10ml) sample.

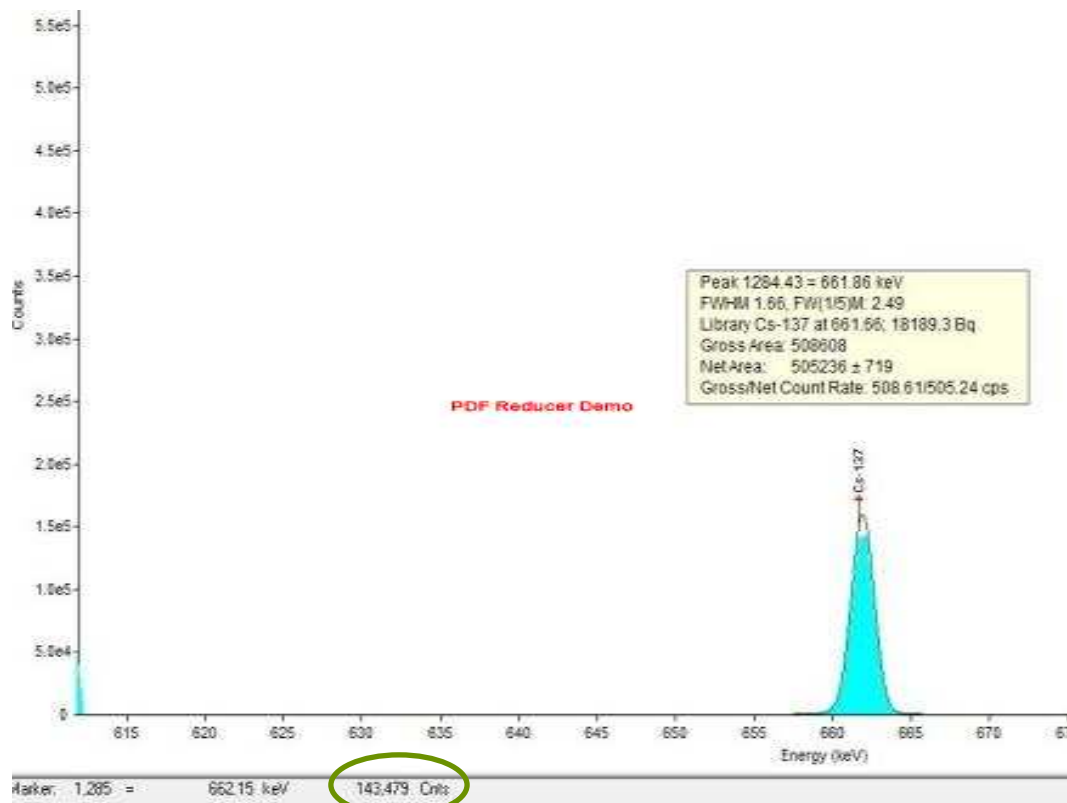
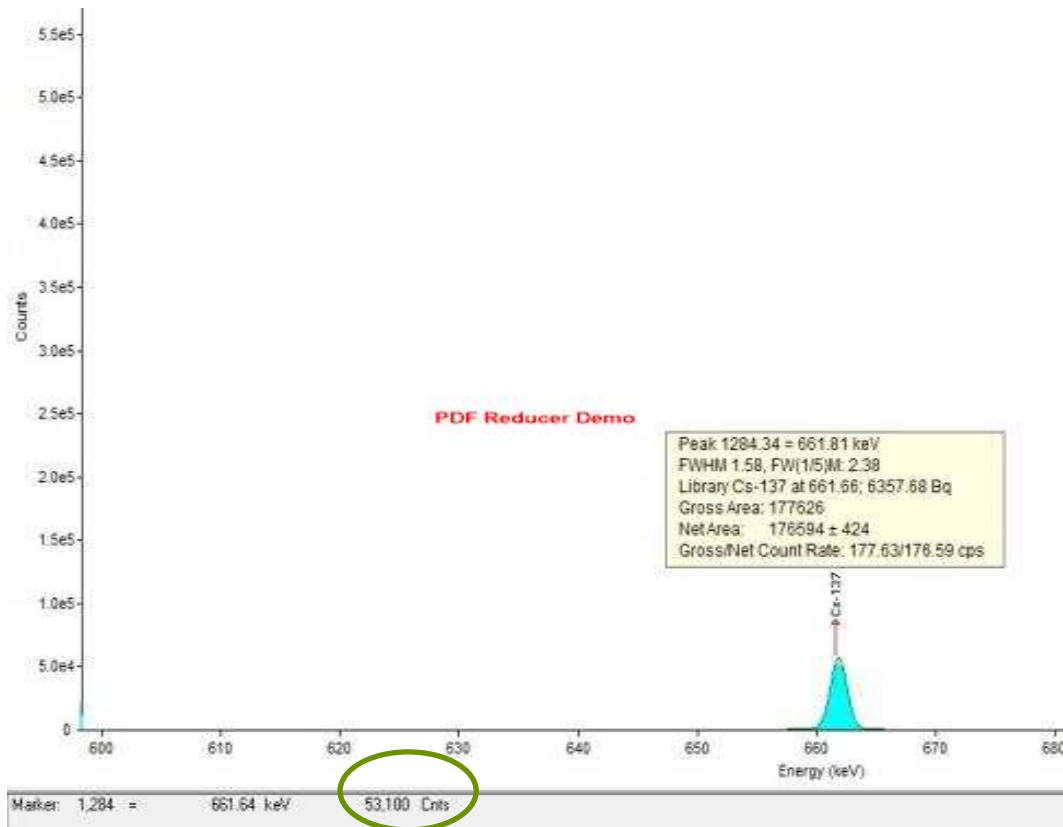


Figure 4-15:  $^{137}\text{Cs}$  spectrum of C-A1 (10ml) sample with 0.025g of clinoptilolite.





**Figure 4-16:**  $^{137}\text{Cs}$  spectrum of C-A5 (10ml) sample with 0.15g of clinoptilolite.

#### 4.4.2 Effecting of Clinoptilolite Weight on Removal Efficiency for $^{90}\text{Sr}$

This section displays the ability of natural zeolite (clinoptilolite) in removing strontium from liquid waste for HLLW pool for the same samples HLLWP-M (sample-C) with different zeolite weight in the previous experiment. A 7mL from each sample deposited on a 2-inch stainless steel planchet with dilution percent 0.2%. The six samples (C-A1, C-A2, C-A3, C-A4, C-A5, and C-ST) were used in this experiment with initial radioactivity (gross beta count rate) 2313.1CPM, pH (6.5) and laboratory temperature (22  $^{\circ}\text{C}$ ). Table (4-19) and figures (4-17, 4-18) show that natural clinoptilolite zeolite efficiency in removing strontium ions at all ranges of zeolite weight that used. The removal efficiency was ranged from 13% at 0.025g of zeolite (C-A1 sample) to 44% at 0.15 g of zeolite (C-A5 sample), it can be seen that higher removal efficiency was

achieved at 0.15g of clinoptilolite. The results of this study agree with the most previous studies which present that the zeolite clinoptilolite has high selectivity for  $\text{Cs}^+$  and  $\text{Sr}^{2+}$  with the selectivity sequence  $\text{Cs}^+ > \text{Sr}^{2+}$  [24].

**Table 4-19: Removal efficiency of  $^{90}\text{Sr}$  with clinoptilolite zeolite weight by gross alpha beta gamma system.**

Sample code	Weight of zeolite (g)	Beta count rate (CPM) at temperature				Removal efficiency (%)
		100 °C	300 °C	500 °C	700 °C	
C-ST	0	2313.1±15.3	2324±15.65	2100±14.23	1959.7±13.3	---
C-A1	0.025	1808.6±13.5	1785.6±13.4	1772.9±13.3	1706.0±13.1	13
C-A2	0.05	1674.7±13.2	1610±12.2	1589±12.14	1530±12.16	22
C-A3	0.075	1489.6±12.2	1463±12.1	1472.2±12.1	1382.1±11.7	29
C-A4	0.1	1206.3±10.9	1239.6±11.1	1237.1±11.1	1168.1±10.8	40
C-A5	0.15	1156.3±10.7	1145.1±10.7	1158±10.76	1099.2±10.5	44

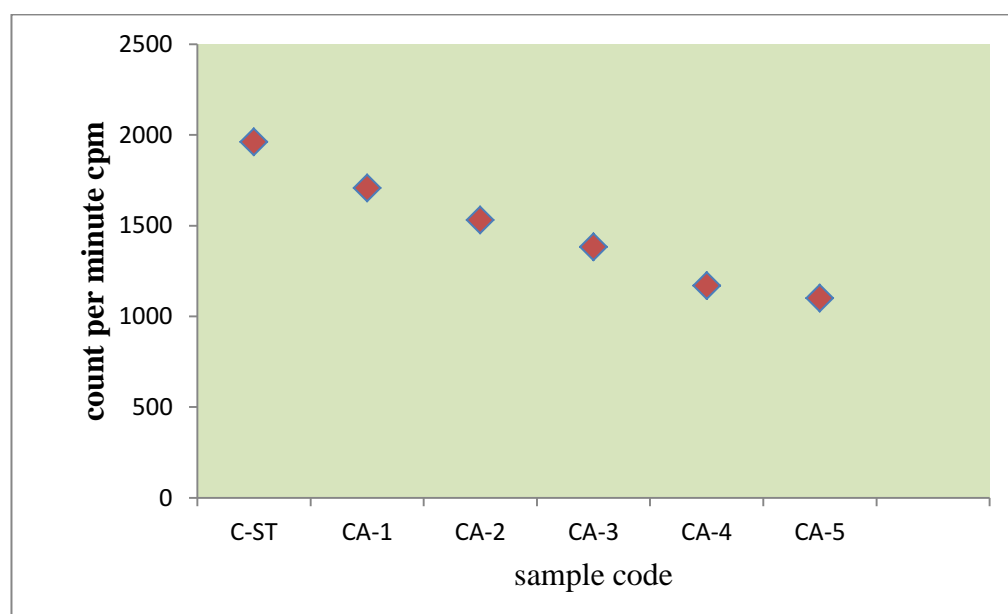


**Figure 4-17: The count rate of  $^{90}\text{Sr}$  for samples.**

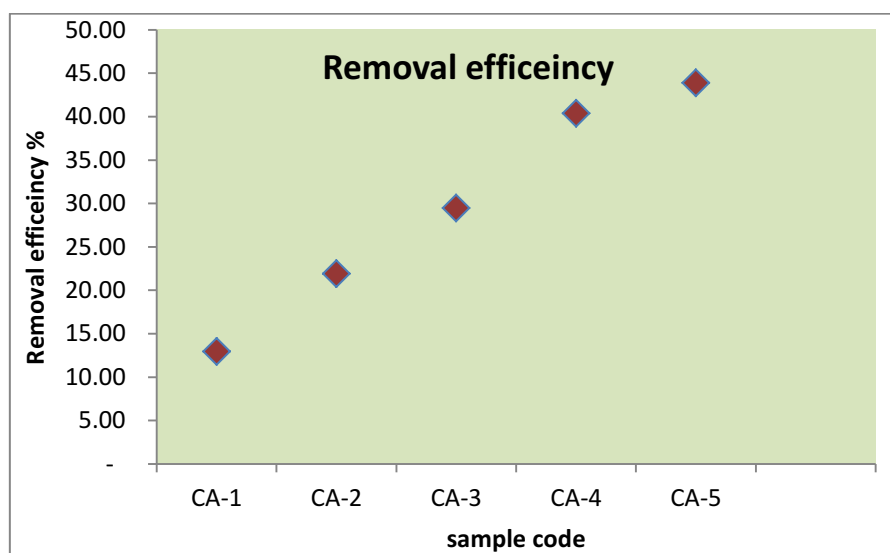


**Figure 4-18: Removal Efficiency of  $^{90}\text{Sr}$  for five samples.**

#### 4.4.3 Effect of Acidic Solution on Removal Efficiency for $^{137}\text{Cs}$

This section displays the ability of clinoptilolite zeolite in removing cesium from liquid waste for HLLW pool (sample-C) with different solution acidity by adding 0.2 g clinoptilolite to 20 mL liquid waste (sample-C) to four sample at pH(3,6,9,12). The average initial radioactivity (area under the peak) of  $^{137}\text{Cs}$  is 468946.7 counts at 1000 second from table (4-18) for 10 mL, the pH (6.5) without dilution and laboratory temperature (22  $^{\circ}\text{C}$ ). Table (4-20) and figure (4-19) show that natural clinoptilolite zeolite is efficient in removing cesium ions at all range of solution acidity that used (3,6,9 and 12). The removal efficiency was ranged from 92.7% at pH(12) , 94.1% at pH(3) and 93.8% at pH(6). The observation of removal efficiency of cesium does not significantly change with increasing or decreasing the solution acidity, which is going in same tuning with the previous study “at pH range of 3–12 the adsorption of  $\text{Cs}^+$  remains almost constant” [24].

**Table 4-20: Removal efficiency for  $^{137}\text{Cs}$  by gamma spectroscopy system at different pH.**

No.	Sample code	Area under peak for $^{137}\text{Cs}$ (cps)	Removal Efficiency for $^{137}\text{Cs}$ %
1	C-ST	468947.7	----
2	CA-pH(3)	27471	94.1
3	CA-pH(6)	29212	93.8
4	CA-pH(9)	27918	94.0
5	CA-pH(12)	34009	92.7

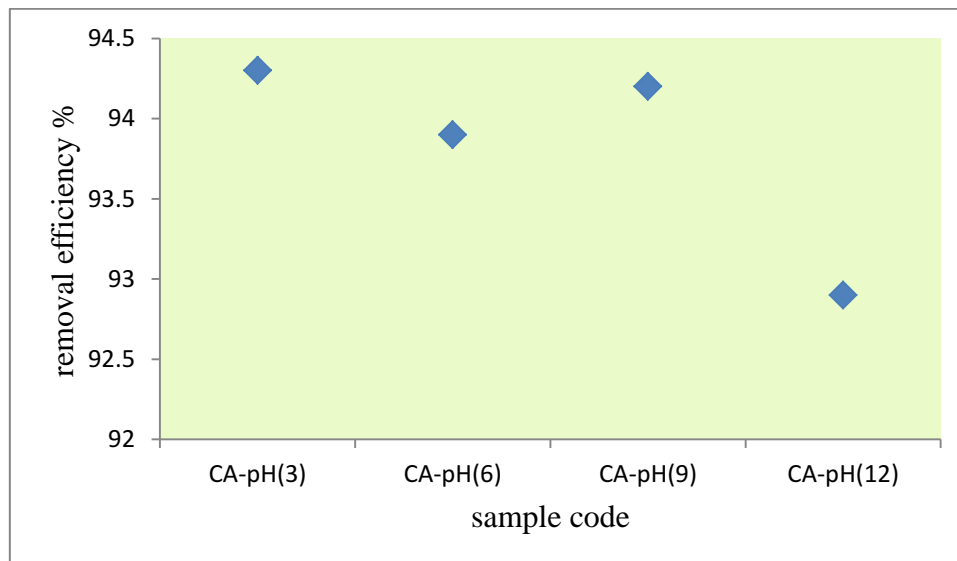


**Figure 4-19: Removal Efficiency of  $^{137}\text{Cs}$  for four samples at different pH.**

#### 4.4.4 The Acidic Effect on Removal Efficiency for $^{90}\text{Sr}$

This section displays the ability of clinoptilolite in removing strontium from liquid waste for HLLW pool (sample-C) by using the same four samples of the previous experiment of  $^{137}\text{Cs}$ , the liquid sample at pH(3,6,9,12) were diluted at percent 0.2%, the initial radioactivity (gross beta count rate) for 7mL with dilution was 1706.4 count per

minute (CPM). A 7mL from each liquid sample deposit on the planchet at pH(3,6,9,12) and measured in this experiment. Table (4-21) shows the clinoptilolite efficiency in removing strontium ions at all range of acidity that used.

The removal efficiency was ranged from 23.22% at pH(3) to 68.91% at pH(6), it can be seen that higher removal efficiency was achieved at pH(6) to the solution. The observation of the removal efficiency significantly changes with the solution acidity. It was found that the pH range 6-9 is suitable which agree with many other previous studies [9].

**Table 4-21: Removal efficiency of  $^{90}\text{Sr}$  at different pH.**

Sample code	Radioactivity concentration (CPM)			Removal Efficiency for $^{90}\text{Sr}$ %
	Alpha	Beta	Gamma	
B.G/	0±0.0	21.8±1.44	41.7±2.12	---
C-ST	0.40±0.20	1706.4±13.06	249.2±4.99	---
CA-pH-3	0.8±0.28	1310.2±11.50	91.3±3.02	23.22
CA-pH-6	0.7±0.26	530.6±7.28	68.2±2.61	68.91
CA-pH-9	0.70.26	672.9±8.20	67.7±2.6	60.57
CA-pH-12	0.2±0.14	938.3±9.69	76.2±2.76	45.01

#### 4.4.5 Improving Removal Efficiency for $^{137}\text{Cs}$ and $^{90}\text{Sr}$

The HLLW pool contains two major radionuclides ( $^{137}\text{Cs}$  and  $^{90}\text{Sr}$ ), therefore, the treatment of this liquid waste must take into account the behavior of two radionuclides. From the last experiment of solution acidity effect of removal efficiency, the pH(6) of the solution is suitable media to achieve good results for the two ions ( $\text{Sr}^{++}$  and  $\text{Cs}^{+}$ ).

The four treated samples of last experiment as shown in table (4-20) which were used as a run-1 treatment at different pH were used as repeating of treatment of these samples (run-2). The run-2 experiment

ried out by adding 0.15 g to 15 mL to these samples as a separated experiment. The table (4-22) presents the removal efficiency for  $^{137}\text{Cs}$  of four samples by measuring them by gamma spectroscopy system (run-2), while the figure (4-20, 4-21, 4-22, and 4-23) show the area under peak of  $^{137}\text{Cs}$  for the samples. The removal efficiency of  $^{137}\text{Cs}$  was ranged from (97.6% to 98.9%) for CA-pH(3) and CA-pH(12) respectively, while 98.8% at pH(6).

To improve the removal efficiency of  $^{90}\text{Sr}$ , the pH(6-9) were found a good media for uptake strontium. Two samples (CA2-pH-6, CA2-pH-9) were taken from the run-2 in order to determine the removal efficiency for  $^{137}\text{Cs}$  and diluted at percent 0.2%. A 7mL from (CA2-pH-6, CA2-pH-9) liquid samples was deposited on two planchets and measured in this experiment by gross alpha beta gamma system as a repeat treatment for  $^{90}\text{Sr}$  (run-2). Table (4-23) presents the initial radioactivity (1706.4(CPM)) of gross beta count rate for 7mL of original diluted sample (without treatment C-ST). The first treatment (run-1) as in table (4-21) was found to be (530.6 and 672.9) CPM for (CA-pH-6, CA-pH-9) respectively. Table (4-23) shows the final beta radioactivity to (CA2-pH-6, CA2-pH-9) samples after the run-2 process, it was (335.1 and 399.2) CPM respectively and shows the removal efficiency of natural clinoptilolite zeolite of strontium at two points of acidity solution that used (run-2). The removal efficiency of strontium was 80.36% at pH(6) and 76.61% at pH(9). It can be seen that higher removal efficiency of  $^{90}\text{Sr}$  was achieved at pH(6) to the solution.

Table (4-24) presents the remain radioactivity of  $^{137}\text{Cs}$  and  $^{90}\text{Sr}$  in HLLWP-M sample and their removal efficiencies at pH(6) after double treatment.

**Table 4-22: Removal efficiency of  $^{137}\text{Cs}$  by gamma spectroscopy system by run-2 for the solution.**

No.	Sample code	Area under peak for $^{137}\text{Cs}$ (cps)	Removal Efficiency for $^{137}\text{Cs}$ %
1	C-ST	468947.7	----
2	CA2-ph(3)	11192	97.6
3	CA2-ph(6)	5484	98.8
4	CA2-ph(9)	6212	98.7
5	CA2-ph(12)	5298	98.9

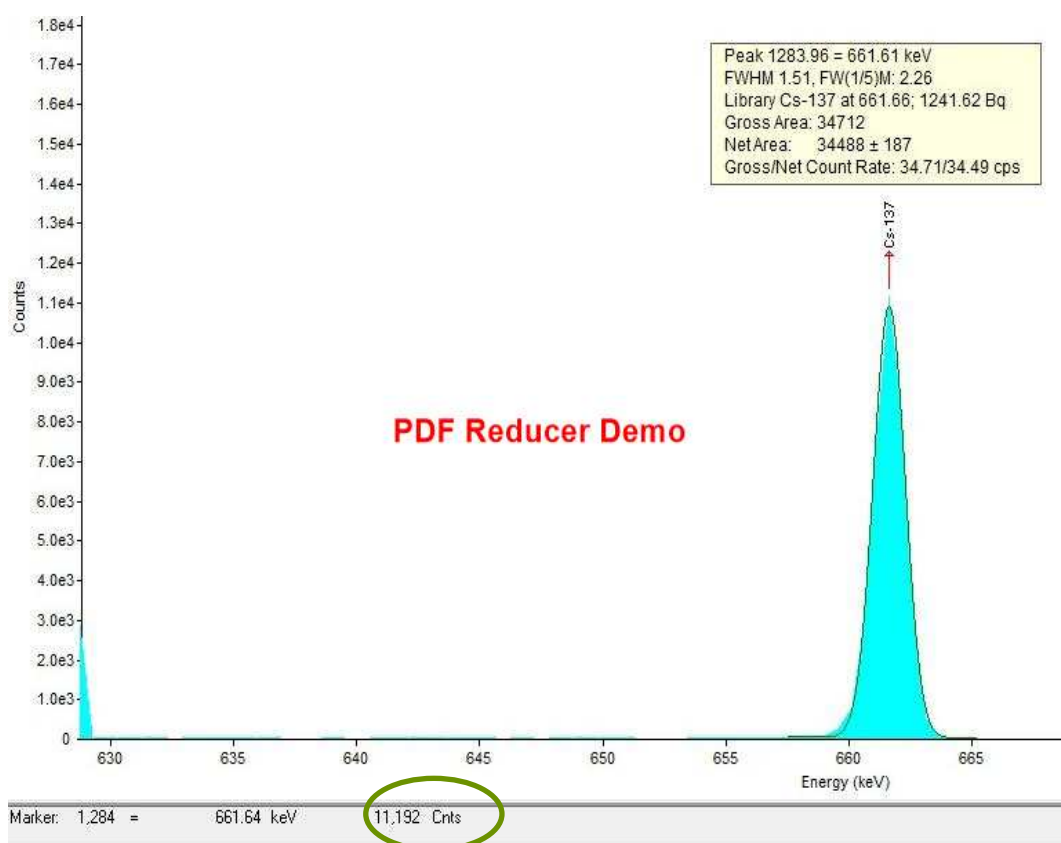


**Figure 4-20:  $^{137}\text{Cs}$  spectrum of CA2-ph(3) (10ml) sample.**

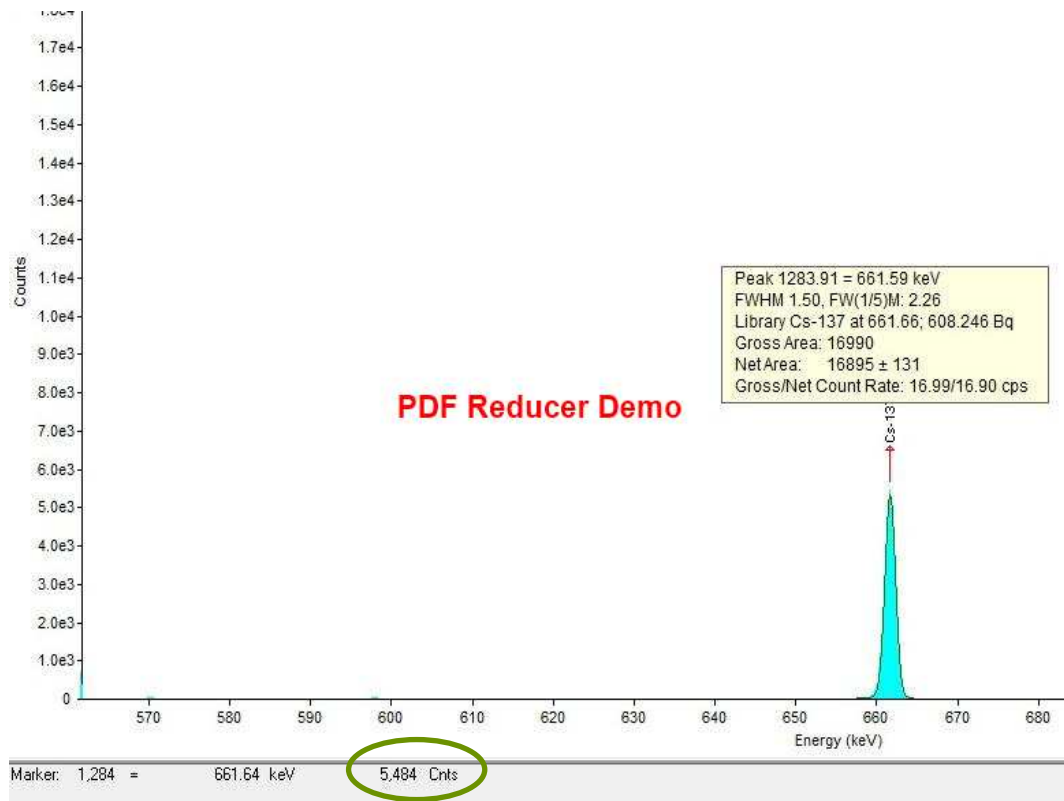


Figure 4-21:  $^{137}\text{Cs}$  spectrum of CA2-ph(6) (10ml) sample.

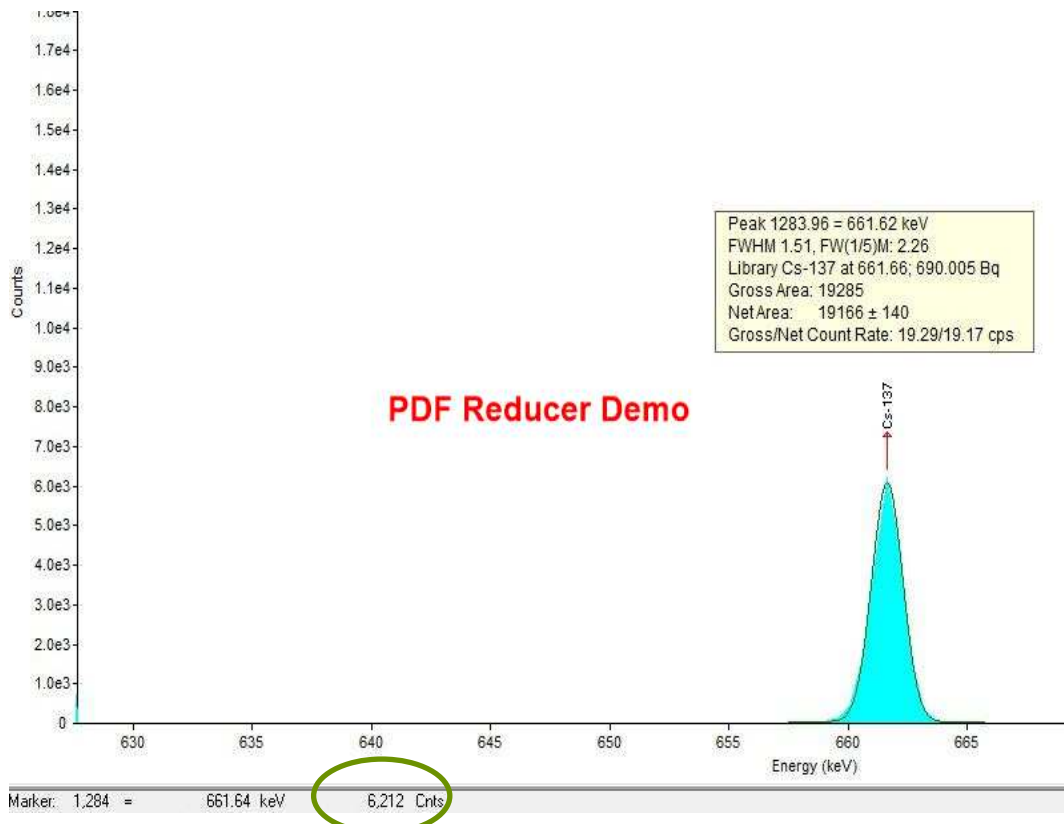


Figure 4-22:  $^{137}\text{Cs}$  spectrum of CA2-ph(9) (10ml) sample.



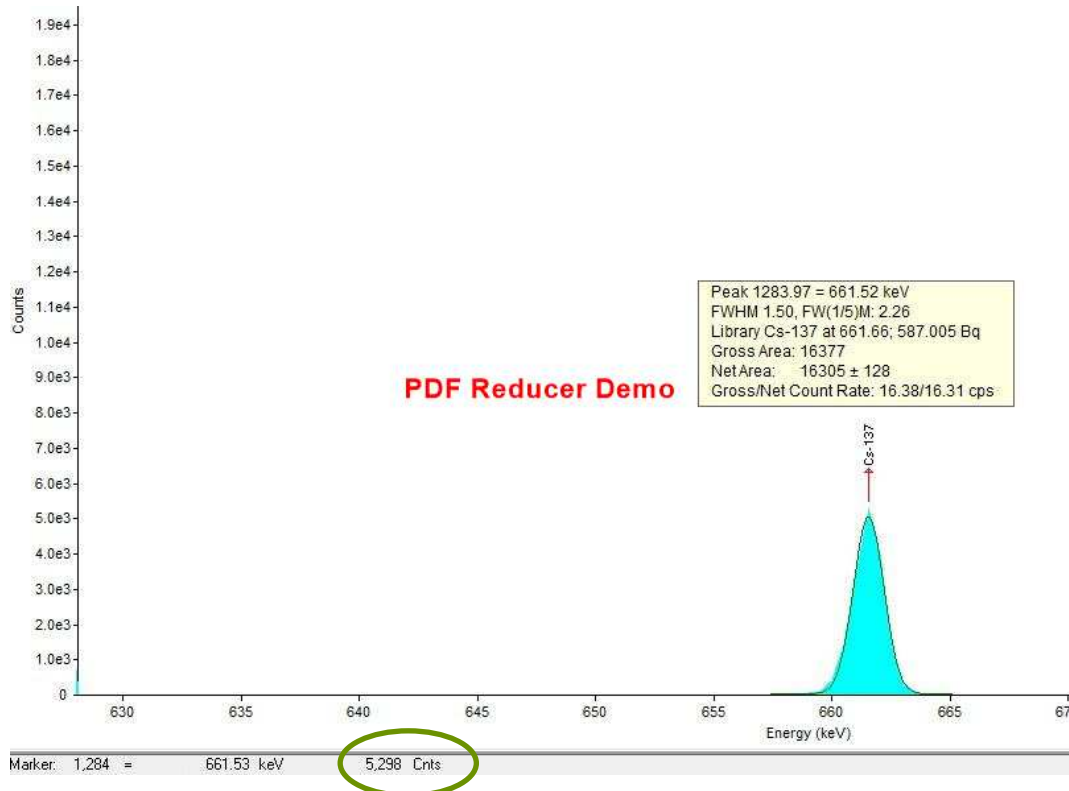


Figure 4-23: <sup>137</sup>Cs spectrum of CA2-ph(12) (10ml) sample.

Table 4-23: Removal efficiency for <sup>90</sup>Sr by gross alpha beta gamma system by run-2 for the solution.

Sample code	Radioactivity concentration (CPM)			Removal Efficiency for <sup>90</sup> Sr %
	Alpha	Beta	Gamma	
B.G/	0±0.0	21.8±1.44	41.7±2.12	---
C-B	0.40±0.20	1706.4±13.06	249.2±4.99	---
CA2-pH(6)	0.50±0.22	335.1±5.79	77.10±2.78	80.36
CA2-pH(9)	0.30±0.17	399.2±6.32	96.4±3.10	76.61

Table 4-24: The remain radioactivity of <sup>137</sup>Cs and <sup>90</sup>Sr in HLLWP-M sample and their removal efficiencies at pH(6).

Sample code	Isotope	Initial radioactivity concentration (Bq.L <sup>-1</sup> )	Removal efficiency %	Remain radioactivity (Bq.L <sup>-1</sup> )
C-BT	<sup>137</sup> Cs	2688126.6	98.8	32257.519
C-B	<sup>90</sup> Sr	2606217.14	80.36	511861.04
C-tot		5684587.84	---	544118.56

#### 4.5 XRF Results

The X-rays fluorescence technology used to measure the percent of elements concentrations from sample weight for the natural clinoptilolite and for the liquid sample which has been used in this study.

The results of the contaminated liquid samples (filter paper sample) was used to confirm the abundance of  $^{90}\text{Sr}$  and its daughter  $^{90}\text{Y}$  into this sample as presented in table (4-25) in comparison with the table (4-26) which represent the background (clean sample). The result as present in the table (4-27) of the natural zeolite clinoptilolite revealed the Si/Al ratio larger than 4 [35].

**Table 4-25: The major concentration elements of HLLWP sample (F-sample).**

Element symbol	Measured Concentration %	Error %	Element symbol	Measured Concentration %	Error%
Si	0.0113	0.0019	Zn	0.0025	0.0002
S	0.2381	0.0016	Br	0.00158	0.00008
Cl	0.3469	0.0014	Rb	0.00077	0.00011
K	0.521	0.011	Sr	0.02293	0.00024
Ca	2.712	0.016	Y	0.00116	0.0001
V	0.00317	0.0002	Hg	0.00051	0.00017
Mn	0.0020	0.0010	Pb	0.00096	0.00018
Fe	0.0351	0.0016	Bi	0.00032	0.00014
Co	0.00156	0.0004	Th	0.00033	0.00013
Ni	0.0022	0.0003	U	0.00026	0.00004
Cu	0.00095	0.0002			

**Table 4-26: The concentration elements of clean liquid sample (F-BG sample).**

Element symbol	Measured Concentration %	Error %	Element symbol	Measured Concentration %	Error %
Si	0.0173	0.0013	Zn	0.00176	0.00011
P	0.00628	0.00097	Ga	0.00014	0.00007
S	2.163	0.004	Se	0.00013	0.00004
Cl	0.5780	0.0014	Br	0.00204	0.00005
K	0.0164	0.0032	Rb	0.00013	0.00007
Ca	0.2192	0.0035	Sr	0.00059	0.00007
V	0.00129	0.0001	Y	0.00113	0.00006
Cr	0.00174	0.00068	Mo	0.0022	0.0017
Mn	0.00199	0.00062	Hg	0.00013	0.00008
Fe	0.0136	0.00078	Pb	0.00039	0.00011
Co	0.00043	0.00021	Bi	0.00030	0.0009
Ni	0.00162	0.00017	Th	0.0002	0.00009
Cu	0.00085	0.00013	U	0.00019	0.00003

**Table 4-27: The concentration elements of clinoptilolite (Z-sample)**

Element symbol	Measured Concentration %	Error%	Element symbol	Measured Concentration%	Error%
Na	0.185	0.063	Ge	0.00016	0.00006
Mg	0.083	0.012	As	0.0018	0.00011
Al	0.5668	0.0061	Se	0.00013	0.00004
Si	6.851	0.014	Br	0.00004	0.00004
P	0.00521	0.00003	Rb	0.0133	0.00012
K	1.14	0.007	Sr	0.05806	0.00022
Ca	1.541	0.007	Y	<0.00298	0.00006
Ti	0.0169	0.00045	Sb	0.00132	0.00023
Cr	0.0049	0.0077	Te	0.00264	0.0003
Mn	0.0373	0.0011	I	0.00313	0.00055
Fe	1.164	1.164	Ba	0.0771	0.0019
Co	0.00236	0.0023	Hg	0.002	0.0001
Ni	0.00092	0.00092	Pb	0.005	0.00015
Cu	0.000053	0.00053	Bi	0.00031	0.00008
Zn	0.0033	0.00011	Th	0.0028	0.00011
Ga	0.00119	0.00008	U	0.00067	0.00013

**4.6 Conclusions**

The main objectives of this work are the radiological characterization and the radiation treatment of the radioactive liquid wastes in the radiochemistry laboratories at AL-Tuwaitha site in Iraq.

This study contained two parts as follows; the first part focused on radiation measurements which carried out by two techniques; the first is by gamma-ray spectroscopy which is the high resolution to detect gamma emitters radionuclides and the second technique is by gross alpha beta gamma system to determine the total radioactivity and the radioactivity concentration of beta emitters radionuclides.

While the second part deals with the treatment of radioactive liquid waste content cesium and strontium using natural zeolite clinoptilolite. Based on the results of this study, the following conclusions can be inferred:

**4.6.1 The Results Related to the Radiation Measurements**

The radiation measurements of liquid samples revealed the following:

- 1- Cesium ( $^{137}\text{Cs}$ ) is the main radionuclide was detected in the liquid samples which collected from LLLWP, HLLWP and their tanks by gamma-ray spectroscopy.
- 2- The count rate of alpha radioactivity around background limit, therefore there are no significant alpha emitters radionuclides in high and low-level liquid waste pools.
- 3- The counts rate of beta radioactivity of the deposit samples by gross alpha beta gamma system refers to a high beta radioactivity concentration in samples ( $5096726 \text{ Bq.L}^{-1}$  average to C-2,4,7 and 10 samples at  $300^\circ\text{C}$ ) which exceed the mean concentration of  $^{137}\text{Cs}$  ( $2688126.6 \text{ Bq.L}^{-1}$ ) when

we convert the count rate to radioactivity concentration ( $\text{Bq.L}^{-1}$ ) of  $^{137}\text{Cs}$  by equation (3-11), therefore, the remain activity belongs to  $^{90}\text{Sr}$  because of the  $^{137}\text{Cs}$  and  $^{90}\text{Sr}$  are beta emitters radionuclides.

4- A new separation method of  $^{137}\text{Cs}$  from solution was developed in this study to evaluate the radioactivity concentration of  $^{90}\text{Sr}$  by the evaporation process.

5-  $^{137}\text{Cs} / ^{90}\text{Sr}$  ratio of HLLWP was calculated, it was 1.0314 which is consisted with the theoretical ratio (1.0608) as the fission products of  $^{235}\text{U}$  along 45 years ago (table 2-1) with percent error is 2.77%.

6- The radioactivity of another radionuclide such as promethium-147 ( $^{147}\text{Pm}$ ) and europium-155 ( $^{155}\text{Eu}$ ) of HLLWP which expected in this waste as illustrated in the same above mentioned table (table 2-1) calculated theoretically by multiplying their percent of abundance as fission products by the total activity after 45 years. Therefore, the total activity of  $^{147}\text{Pm}$  and  $^{155}\text{Eu}$  were (8504.811 and 4101.20886) MBq respectively.

#### **4.6.2 The Results Related to the Treatment of Liquid Waste**

According to the comparison of measuring results with the international classification of radioactive liquid waste as illustrated in chapter two, the liquid of high level liquid waste pool (HLLWP) of the RCL which was used in this study considers as low-level liquid waste and the liquid of low level liquid waste pool (LLLWP) concenter as a very low-level liquid waste.

1- The natural zeolite clinoptilolite was highly efficient at all range of weight used in removing  $^{137}\text{Cs}$  and  $^{90}\text{Sr}$  ions from liquid waste.

2- The maximum removal efficiency was 98.9% and 80% for Cs and Sr respectively at 0.3 g of clinoptilolite used with 15 mL solution.

3- The treatment of HLLWP contaminated liquid reduces the total radioactivity concentration from 5.684 MBq.L<sup>-1</sup> to 0.541 MBq.L<sup>-1</sup>, that means it has converted from the low level as the liquid waste classified in this study as mentioned in previous paragraph to near to very low level.

4- The natural zeolite clinoptilolite was highly efficient at all ranges of acidity solution pH (3 - 12) for <sup>137</sup>Cs removing. It has noticed that the suitable media for removing the two radionuclides together is presented at pH range (6-9), that means the pH (6.5) of the original solution which was used in this study is suitable media.

#### **4.7 Future Works**

- 1- Study the radiological dose and risk assessment of workers in radiochemistry laboratories during decommissioning activities.
- 2- Study the radiological characterization of whole radiochemistry laboratories building.
- 3- Study other factors that affecting on the removal efficiency of Cs and Sr ions from liquid waste by natural zeolite such as wider range of pH, temperature, contact time and volume/weight ratio.
- 4- In addition to the above, for treating liquid waste containing cesium, natural Iraqi zeolite could be used to verify their validity in the removing of cesium from liquid waste due to its availability.
- 5- Study the synthesized (zeolite A) as inorganic ion exchange material, for the removal of Cs and Sr ions from aqueous solutions in both batch and fixed bed column operations.
- 6- Study the ability of clinoptilolite on the remediation and decontamination of radioactive solid waste by using a suitable method which as a result from the decommissioning of Iraqi facilities.

# **THE REFERENCES**

## *References*

---

### **REFERENCES**

- [1] J. Kenneth Shultis, Richard E. Faw, "Fundamentals of Nuclear Science and Engineering", New York, Marcel Dekker Inc. , Basel, 270 Madison Avenue, NY 10016, 2002.
- [2] United Nations Environment Programme (UNEP), "Radiation Effects and Sources", Austria, 2016.
- [3] H. Matis, "Contemporary Physics Education Project (CPEP)", Nuclear Science, Berkeley, California, third Edition – November 2003.
- [4] K. John Sutherland, "Radioactive Wastes Origins Classification and Management", Fredericton, New Brunswick, Canada, 2008.
- [5] International Atomic Energy Agency (IAEA), "Characterization of Radioactively contaminated Site for Remediation Purposes", Vienna, IAEA, 1998.
- [6] International Atomic Energy Agency (IAEA), "Terminology Used in Nuclear, Radiation, Radioactive Waste", version 2.0, Vienna, IAEA, 2006.
- [7] R. Abdel-Rahman, A. El-Kamash, H. Ali and Y. Hung, "Overview on recent trends and developments in radioactive liquid waste treatment", part 1: Sorption/Ion Exchange Technique, Int. J. Environ. Eng. Sci.2,Vo. 3, P 551-565, 2011.
- [8] International Atomic Energy Agency (IAEA), "Management of Low and Intermediate Level Radioactive Wastes with Regard to Their Chemical Toxicity", Vienna, Austria: IAEA-TECDOC-1325, 2002.
- [9] S. Al-Nasri, "Treatment of Waste water Containing Cobalt (Co-59) and Strontium (Sr-89) as a Model to Remove Radioactive Co-60 and Sr-90 Using Hierarchical Structures in Corporation Zeolites", thesis, University of Manchester, UK , 2013.
- [10] A. Osmanlioglu, International collaboration and continuous improvement AZ (United States), "On-Site Decontamination System for Liquid Low Level Radioactive Waste", Waste Management Conference , United States, 24-28 Feb 2013.
- [11] W. Pang, J. Yu, Q. Huo and J. Chen, "Chemistry of Zeolites and Related Porous Materials : Synthesis and Structure", John Wiley & Sons 129809,



## *References*

---

- 2009.
- [12] R. H. Borai, "Efficient removal of cesium from low-level radioactive liquid waste using natural and impregnated zeolite minerals", *Journal of Hazardous Materials*, p. 172 (2009) 416–422, 2009.
- [13] E. H. Borai, R. H. Harjula, "Efficient removal of cesium from low-level radioactive liquid waste using natural and impregnated zeolite minerals", *Journal of Hazardous Materials*, Vol. 172, p- 416–422, 2009.
- [14] R. Chesser, B. Rodgers, "Piecing together Iraq's nuclear legacy, *Bulletin of the Atomic Scientists*", Vols. May/June, vol. 65, No.3, p. 19–33, 2009.
- [15] R. John Copland and John R. Cochran, "Groundwater Monitoring Program Plan and Conceptual Site Model for the Al-Tuwaitha Nuclear Research Center in Iraq," *Environmental Safety and Testing Department Sandia/National Laboratories, SAND2013-4988 Unlimited R, USA*, 2013.
- [16] A. Bayati, "Determination of the Concentrations for Radioactive Elements Around Al-Tuwaitha Center Using Gamma Ray Spectroscopy and CR-39 Detectors", *Thesis: College of Education for Pure Science Ibn Al-Haitham, University of Baghdad*, 2017.
- [17] V. L. Petukhov, T. S. Gorbl, "Cs-137 and Sr-90 level in diary products", *Joulrnal of physics IV France*, no.107, P-1065, 2003.
- [18] M. Janez Križman, Sonja A., "Measurements of Sr-90 Radionuclide in Slovenian Soils before and after Chernobyl Accident", in *International Conference Nuclear Energy for New Europe, Bled, Slovenia, 5-8,120.1 September 2005*.
- [19] N. Casacuberta, P. Masque, J. Garcia-Orellana,"  $^{90}\text{Sr}$  and  $^{89}\text{Sr}$  in seawater off Japan as a consequence of the Fukushima Dai-ichi nuclear accident", *Biogeosciences*, Vols. 10, p- 3649–3659 , 2013.
- [20] L. Sousa Silva and Pecequilo B., "Gross alpha and beta activities in surface, underground and drinking waters of a high natural radioactivity region of central south Bahia state, Brazil, *Radioprotection*", Vol. 46, pp.63–67 , 2011.
- [21] J. Ferdous, Rahman M., and Begum A., "Gross Beta Activities of Tap Water Samples from Different Locations of Dhaka City", *Sri Lankan Journal of Physics*, Vol.13,N.(1), p- 01-08 , 2012.

## *References*

---

- [22] N. F., Chelishchev, "Use of natural zeolites at Chernobyl", Journal of International Committee on Natural Zeolites, Vol.13,N.(1), p- 525 – 532. , 1993.
- [23] A. Erdal. Osmanlioglu, "Treatment of radioactive liquid waste by sorption on natural zeolite in Turkey", Journal of Hazardous Materials, vol. B137 P- 332–335 , 2006.
- [24] I. Smičiklas, S. Dimovic, "Removal of Cs<sup>1+</sup>, Sr<sup>2+</sup> and Co<sup>2+</sup> from aqueous solutions by adsorption on natural clinoptilolite", Applied Clay Science/elsevier, vol. 35 P- 139–144, 2007.
- [25]
- [26] P. C. Kavi, "The preparation and characterisation of highly selective adsorbents for fission product removal from acid solutions", Ph.D thesis, University of Central Lancashire , 2016.
- [27] F. M. Radhi, "Development of Treatment Process for Radioactive-Contaminated Soil", A Thesis, College of Science / University of Baghdad, 2017.
- [28] B. Podgorsak E., "Radiation oncology physics, a handbook for teachers and students", Vienna, IAEA, Vol.657, 2005.
- [29] A. Das and T. Ferbel, "Introduction to Nuclear and Particle Physics" Second Edition, University of Rochester, World Scientific Publishing Co. Pte. Ltd. 2003.
- [30] F. L'Annunziata M., "Handbook of radioactivity analysis", (Academic Press), 2012.
- [31] United Nations Scientific Committee on the effects of Atomic Radiation (UNSCEAR), "Sources and effects of ionizing radiation sources", Vol. 1. United Nations Publications, 2000.
- [32] A. M. Huffert, R. A. Meck, and K. M. Miller, "Background as a residual radioactivity criterion for decommissioning". USNRC, Draft NUREG-1501, 1994.
- [33] National Council on Radiation Protection (NCRP), "Measurements Exposure of the population in the United States and Canada from natural background radiation", NCRP Report No. 94, 1992.

## *References*

---

- [34] National Council on Radiation Protection (NCRP), "Natural Background Radiation in the United States", NCRP Report No.45, 1975.
- [35] N. Cottingham W., D. A. Greenwood, "An introduction to nuclear physics", 2nd edition, university of Bristol, 1986.
- [36] J. C. Hansen , "Arctic Monitoring and Assessment Programme (AMAP)", p- 527, 1998.
- [37] J. Kalilainen, "Fission product transport in the primary circuit and in the containment in severe nuclear accidents", Doctoral Dissertations Aalto University publication series, 71/ 2015.
- [38] C. Patterson, "Processes going on in Nonfailed Rod during Normal Operation", California (Advanced Nuclear Technology International), September 2010.
- [39] W. Robert Mills, "Fission product yield evaluation", thesis of PhD, Faculty of Science of the University of Birmingham March 1995.
- [40] L. Thomas Rucker, "Radionuclides Related to Historical Operations at the Santa Susana Field Laboratory Area IV", Ph.D. thises, Santa Susana, March 2009.
- [41] A. L. Nichols, D. L. Aldama, M. Verpelli, "Handbook of nuclear data for safeguards:data base extention", International Nuclear Data Committee (INDC) Vienna, IAEA, August 2008.
- [42] K. Krane S., "Introductory Nuclear Physics", Chichester: John Wiley & Sons Inc 1098765432, 1988.
- [43] N. Ahmed S., "Physics and engineering of radiation detection", Academic Press, 2007.
- [44] H. Cember, Thomas E. Johnson, "Introduction to Health Physics" Fourth Edition, Wiley, McGraw-Hill Companies Inc, 2009.
- [45] G. F. Knoll, "Radiation Detection and Measurement", 3rd edition, John Wiley & Sons Inc., 2000.
- [46] N. Reguigui, "Gamma Ray Spectrometry", Canberra web site, NY University web site, September 2006.
- [47] R. Gordon Gilmore, "Practical Gamma-ray Spectrometry", (2nd edition), John Wiley & Sons., 2008.

## *References*

---

- [48] Contemporary Physics Education Project (CPEP), "Nuclear Science -A Guide to The Nuclear Science Wall Chart", Booklet of Contemporary Physics Education Project, Third Edition, 2003.
- [49] G. Croff, Allen, "Risk informed- radioactive waste classification and re classification", Helth physics, 2006.
- [50] IAEA, "Nuclear Fuel Cycle Information System - A Directory of Nuclear Fuel Cycle Facilities", Vienna, IAEA, Edition 2009.
- [51] J. Valentin, "The 2007 Recommendations of the International Commission on Radiological Protection", Elesivier, ICRP Publication 103, March 2007.
- [52] IAEA, "Extent of Environmental Contamination Natural Occurring Radioactive Material (NORM) and Technological Options for mitigation", Vienna , Austria December 2003.
- [53] IAEA, Radiation Protection and Safety of Radiation Sources: "International Basic Safety Standards" safety standadrd series No. GSR Part 3, 3, 2011.
- [54] IAEA, "Classification of Radioactive Wastefor", No. GSG-1 General Safety Guide IAEA, VIENNA: IAEA, 2009.
- [55] IAEA, "Status And Trends In Spent Fuel And Radioactive Waste Management", Vienna: IAEA- NW-T-1.14, 2018.
- [56] IAEA, "Review of the Factors Affecting the Selection and Implementation of Waste Management Technologies", IAEA-TECDOC-1096, IAEA: Vienna, Austria, 1999.
- [57] R. Abdel Rahman, H. A. Ibrahim and Yung-Tse Hung, "Liquid Radioactive Wastes Treatment, A Review", Water jornal, Vol. 3, 551-565, 2011.
- [58] IAEA, "Handling and Processing of Radioactive Waste from Nuclear Applications", Vienna, Austria: TRS No. 402; IAEA, 2001.
- [59] Ren J. S., Mu T., Zhang W., Yang S.Y., "Effect of Ingredients in waste water on property of ion exchange resin for uranium-contained waste water treatment", Atom. Ene. Sci. Technol, 2008.
- [60] D. V. Marinin, Brown N. G., "Studies Of Sorbent/ Ion Exchange Materials for The Removal of Radioactive Strontium from Liquid Radioactive Waste

## *References*

---

- and High Hardness Ground Water", *Waste Management*, p. 545-553, 2000.
- [61] G. Ozkan, "Exchanges of Strontium on Clinoptilolite Zeolite", Thesis : School Of Natural And Applied Sciences Of The Middle East Technical University, Turkey, 2000.
- [62] D.R. Lide, "Handbook of Chemistry and Physics", 75th Edition, B. R. F. I. O, CRC Press, Ed., 1995.
- [63] E. BROWNE, J. K.TULI, "Nuclear data sheets for A= 137. Nuclear Data Sheets", 108.10: 2173-2318, 2007.
- [64] Idaho, National Engineering Laboratory, "Selected Radionuclides Important to Low-Level Radioactive Waste Management", DOE/LLW-238, U.S. Department of Energy, November 1996.
- [65] A. L. Nichols, D. L. Aldama, "Handbook of Nuclear Data For Safeguards: Database Extensions", Vienna, Austria IAEA, 2008.
- [66] M. Schenk Calero, Sofia Maesen, Theo L. M., G.Martijn, Lucas L. van, "Understanding Zeolite Catalysis: Inverse Shape Selectivity Revised, *Angew*", *Angewandte Chemie International Edition, Journal of the Gesellschaft Deutscher Chemiker*, Volume 41, Issue 14, 2002.
- [67] E. M. Flanigen, J. C. Jansen, and H. Van Bekkum, *Introduction to Zeolite Science and Practice*, 2nd edition, Elsevier Science BV, Amsterdam, 2011.
- [68] N. E. Zimmermann, M. Haranczyk, "History and utility of zeolite framework-type discovery from a data-science perspective". *Crystal Growth & Design*, 16.6: 3043-3048, 2016.
- [69] Xu, R.P., W. Yu, J. Huo, Q. Chen, J. Gao, Z, "Chemistry of Zeolite and Related Porous Materials", p- 145-146, Wiley: Singapore , 2007.
- [70] B. Bogdanov, D. Georgiev, K. Angelova, K. Yaneva, "NATURAL ZEOLITES: CLINOPTILOLITE", International Science conference , Stara Zagora, BULGARIA, P-6-11, Vol. IV, June 2009.
- [71] D. L. Bish, and J. M. Boak, "Clinoptilolite-heulandite nomenclature. *Reviews in mineralogy and geochemistry*", 45(1): p. 207-216, 2001.
- [72] D. W. Breck, "Zeolite Molecular Sieves", John Wiley and Sons, New York

## *References*

---

- , 1974.
- [73] C.D.Williams, "Synthesis of pure clinoptilolite without the use of seed crystals", *Chemical Communications*, (21): p. 2113-2114., 1997.
- [74] R. John Copland and John R., "Groundwater Monitoring Program Plan and Conceptual Site Model for the Al-Tuwaittha Nuclear Research Center in Iraq", Environmental Safety and Testing Department Sandia/ National Laboratories, SAND2013-4988 Unlimited R, 2013.
- [75] J. D. Berger, "Manual for conducting radiological surveys in support of license termination", US Nuclear Regulatory Commission , 1992.
- [76] Nuclear Regulatory Commission (NRC), "Multi-agency radiation survey and site investigation manual", (MARSSIM), NUREG-1575, U.S. p. 137-139, 2000.
- [77] IAEA, "Measurement of radionuclides in food and environment guidebook", TECDOC-1092, June 1989.
- [78] S. Biswas, J. Ferdous "Study of Gross Alpha and Gross Beta Radioactivities in Environmental Samples," *Journal of scientific research*, Res. 7 (1-2), 35-44, 2015.
- [79] Laboratory National Exposure Research (LNER), "Gross Alpha and Gross Beta Radioactivity in Drinking Water", U.S.: EPA 900, US Gov. Printing Office, 1980.
- [80] Committee Standards Policy and Strategy(CSPS), "Measurement of radioactivity in the environment – Soil, Part3: Measurement of gamma-emitting radionuclides", British Standards, ISBN 978 0 580 53277 1, 2008.
- [81] G. A. Sutton, "The analysis of environmental materials using gamma spectrometry", Great Britain, Directorate of Fisheries Research, 1993.
- [82] Manual, SP3 A66-BW Software User's, Software Version 7 Gamma Vision, "Gamma-Ray Spectrum Analysis and MCA", Printed in U.S.A. ORTEC Part No. 783620 1013, 2013.
- [83] J. Peter, "Studies of nuclear fuel by means of nuclear spectroscopic methods", *Desertation*, Faculty of science and technology, Universty of Upsala, 2002.
- [84] R. Nafaa, "Gamma Ray Spectrometry Practical Information", September

## References

---

- 2006.
- [85] G. F. Knoll, "Radiation Detection and Measurement", (3rd edition), USA: John Wiley & Sons Inc., 2000.
- [86] R. Gilmore G., "Practical Gamma-ray Spectrometry.", 2nd Edition, Wiley-VCH Verlag, Weinheim, Germany, 2008.
- [87] N. Jibiri and T. Abiodun, "Effects of food diet preparation techniques on radionuclide intake and its implications for individual ingestion effective dose in Abeokuta", Southwestern Nigeria, 2012.
- [88] M. Sudarshan and R. Singh, "Effects of fast neutron damage on the performance of a high resolution high-purity germanium coaxial detector". J.Phys. D: Appl. Phys. 24, 1991.
- [89] L. A. Curie, "Limits for Qualitative Detection and Quantitative Determination, Application to Radiochemistry, Analytical Chemistry" 40(3), 586-593, 1968.
- [90] G. R. Gilmore, "Practical Gamma-ray Spectrometry", 2nd edition, Chichester: John Wiley & Sons Ltd., 2008.
- [91] E. Ehsanpour, Abdi M. R., Mostajaboddavati M. and Bagheri, H., "<sup>226</sup>Ra, <sup>232</sup>Th and <sup>40</sup>K contents in water samples in part of central deserts in Iran and their potential radiological risk to human population", Journal of Environmental Health Science and engineering, Vol. 12.1: 80 , 2014.
- [92] N. Tsoulfanidis, MacGraw Hill, "Measurement and Detection of Radiation", CRC press, 2010.
- [93] Knoll G., "Radiation Detection and Measurement", Second Edition, John Wiley & Sons, 1989.
- [94] Peter Brouwer, "Theory of XRF", Netherlands: PANalytical B.V, 2010.
- [95] Amer. A. Sakran, "Synthesis Prussian blue/reduced graphene oxide nano composite for the removal of cesium ion (Cs+) from wastewater as a model for the removal of radioactive cesium (Cs-137)", Ferdowsi University of Mashhad, Faculty of Science, 2017.

## الملخص:

الهدف من هذه الدراسة هو تخمين وتخفيض النشاط الاشعاعي الكلي لأحواض النفايات المشعة السائلة (RLWPs) في مختبرات الراديو كيمياء (RCL) في موقع التويثة. تم تحليل النماذج المجمعة من هذه الاحواض بتقنيتين، الاولى هي استخدام منظومة تحليل طيف كاما ذات كاشف الجرمانيوم عالي النقاوة (HPGe) ذي الكفاءة النسبية 65% لقياس تركيز النشاط الاشعاعي لباعثات اشعة كاما وتحديد نوع النظائر المشعة. وقد بينت النتائج أن معدل تركيز الفعالية لنظير السيزيوم-137 ( $^{137}\text{Cs}$ ) كان  $2.688 \text{ MBq.L}^{-1}$  و  $850.61 \text{ Bq.L}^{-1}$  لحوض النفايات المشعة عالية ومنخفضة المستوى (HLLWP and LLLWP) على التوالي. اما التقنية الثانية هي استعمال منظومة العد الاجمالي لجسيمات الفا وبيتا وكاما نوع S5XLB ذو الكاشف الغازي التناسبي لقياس تركيز الفعالية لبواعث جسيمات بيتا النقية الموجودة في العينة ذاتها والتي لا يمكن كشفها في التقنية الاولى.

السيزيوم-137 والسترونشيوم-90 هما النظيران المشعان الرئيسيان لنواتج الانشطار النووي لنظير اليورانيوم-235 ( $^{235}\text{U}$ ) وبأعمار نصف 30 و 29 سنة تقريباً. تم فصل نظير السيزيوم من هذه النماذج بإستحداث طريقة جديدة وهي طريقة التبخير وذلك لانه باعث لجسيمات بيتا ايضا مترافقة مع فوتونات كاما، لذلك فإن معدل النشاط المتبقي لنماذج حوض النفايات السائلة عالية المستوى هو  $2.606 \text{ MBq.L}^{-1}$  و  $0.0017 \text{ MBq.L}^{-1}$  وبالرجوع الى تأريخ عمل مختبرات الراديو كيمياء، ان هذه النفاية تتعلق بنواتج الانشطار النووي لنظير اليورانيوم ( $^{235}\text{U}$ )، لذلك فإن النشاط الاشعاعي المتبقي يعود الى نظير السترونشيوم-90 ( $^{90}\text{Sr}$ ) تبعاً لطول عمره النصفى .

تمت معالجة هذه النفايات السائلة والتي تحتوي على النظيرين المشعين السيزيوم والسترونشيوم بتقنية التبادل الايوني بواسطة استخدام مادة الزيولايت الطبيعي (clinoptilolite) والمستعمل على نطاق واسع في تطبيقات المعاملة. تم دراسة تأثير عاملي كمية الزيولات المستخدم (وزنه) وحامضية المحلول (pH) على كفاءة الازالة لنظيري السيزيوم والسترونشيوم.

النتائج كشفت بأن الزيولايت الطبيعي (clinoptilolite) كفوء جداً في ازالة ايونات السيزيوم من هذه النفايات السائلة على كل المدى المستخدم في هذه الدراسة من وزن المادة وحامضية السائل، بينما تباينت كفاءة الازالة لأيونات السترونشيوم مع هذه العوامل.





وزارة التعليم العالي والبحث العلمي  
جامعة بغداد  
كلية التربية للعلوم الصرفة-ابن الهيثم  
قسم الفيزياء

## تخمين وتقليل النشاط الاشعاعي الكلي لحوض النفايات السائلة في مختبرات الراديوكيمياء في موقع التويثة

رسالة تقدم بها

**زيدون حافظ ابراهيم**

بكالوريوس في علوم الفيزياء

كلية التربية للعلوم الصرفة- ابن الهيثم/جامعة بغداد

(1997)

مقدمة إلى مجلس كلية التربية للعلوم الصرفة- ابن الهيثم/ جامعة بغداد

وهي جزء من متطلبات نيل شهادة الماجستير

في علوم الفيزياء

بأشراف

ر.مهندسين / د. سلام خضير عبد الله

أ.م.د. احمد فاضل مخبير

محرم 1439هـ

ايلول / 2018م